

STATUS OF THESIS

Title of thesis

**WAVE-CURRENT INTERACTION ON OFFSHORE SPAR  
PLATFORMS IN MALAYSIA WATER**

**I SITI NOR ADHA BINTI TUHAJAN**

hereby allow my thesis to be placed at the Information Resource Center (IRC) of Universiti Teknologi PETRONAS (UTP) with the following conditions:

1. The thesis becomes the property of UTP
2. The IRC of UTP may make copies of the thesis for academic purposes only.
3. This thesis is classified as

Confidential

Non-confidential

If this thesis is confidential, please state the reason:

---

---

---

The contents of the thesis will remain confidential for \_\_\_\_\_ years.

Remarks on disclosure:

---

---

---

Signature of Author

Permanent address: Jalan Redan

Hujung, Kanchong Darat, 42700

Banting, Selangor Darul Ehsan

Date : 4/11/13

Endorsed by

Signature of Supervisor

Name of Supervisor

Prof. Dr Kurian V. John

Dr KURIAN V. JOHN  
PROFESSOR  
Civil Engineering Department  
Universiti Teknologi PETRONAS  
Bandar Seri Iskandar, 31750 Tronoh  
Perak Darul Ridzuan, MALAYSIA.

Date : 4/11/2013

UNIVERSITI TEKNOLOGI PETRONAS

**WAVE-CURRENT INTERACTION ON OFFSHORE SPAR PLATFORMS IN  
MALAYSIA WATER**

by

**SITI NOR ADHA BINTI TUHAIJAN**

The undersigned certify that they have read, and recommend to the Postgraduate Studies Programme for acceptance this thesis for the fulfillment of the requirements for the degree stated.

Signature:



Dr KURIAN V. JOHN  
PROFESSOR  
Civil Engineering Department  
Universiti Teknologi PETRONAS  
Bandar Seri Iskandar, 31750 Tronoh  
Perak Darul Ridzuan, MALAYSIA.

Main Supervisor:

Prof. Dr. Kurian V. John

Signature:



Co-Supervisor:

Assoc. Prof. Ir. Dr. Mohd Shahir Liew

Signature:



Assoc. Prof. Ir. Dr Mohd Shahir Liew  
Head  
Civil Engineering Department  
Universiti Teknologi PETRONAS  
Bandar Seri Iskandar, 31750 Tronoh  
Perak Darul Ridzuan, MALAYSIA

Head of Department:

Assoc. Prof. Ir. Dr. Mohd Shahir Liew

Date:

8 / 11 / 13

**WAVE-CURRENT INTERACTION ON OFFSHORE SPAR PLATFORMS IN  
MALAYSIA WATER**

by

**SITI NOR ADHA BINTI TUHAJAN**

A Thesis

Submitted to the Postgraduate Studies Programme  
as a Requirement for the Degree of

MASTER OF SCIENCE

CIVIL ENGINEERING

UNIVERSITI TEKNOLOGI PETRONAS

BANDAR SERI ISKANDAR,

PERAK

NOVEMBER 2013

DECLARATION OF THESIS

Title of thesis

**WAVE-CURRENT INTERACTION ON OFFSHORE SPAR  
PLATFORMS IN MALAYSIA WATER**

I SITI NOR ADHA BINTI TUHAJAN

hereby declare that the thesis is based on my original work except for quotations and citations which have been duly acknowledged. I also declare that it has not been previously or concurrently submitted for any other degree at UTP or other institutions.

Witnessed by



Signature of Author



Signature of Supervisor

Permanent address: Jalan Redan

Hujung, Kanchong Darat, 42700

Banting, Selangor Darul Ehsan.

Name of Supervisor

Prof. Dr. Kurian V. John

Dr KURIAN V. JOHN  
PROFESSOR  
Civil Engineering Department  
Universiti Teknologi PETRONAS  
Bandar Seri Iskandar, 31750 Tronoh  
Perak Darul Ridzuan, MALAYSIA.

Date : 4 / 11 / 13

Date : 4/11/2013

DEDICATION

*To My Beloved Late Father, Tukaijan Bin Marion*

*To My Beloved Mother, Rossilawati Binti Waqiran*

*To My Beloved Husband & His Family*

*To My Brothers & Sisters*

*To All My Friends & Colleagues*

## ACKNOWLEDGEMENTS

First of all, Alhamdulillah. I thank ALLAH for the strength that keeps me standing and for the hope that keeps me believing that this affiliation would be possible and divine.

I would like to express my genuine appreciation to my supervisor, Prof. Dr. Kurian V. John, for his excellent guidance, motivation and support throughout the course of my study at Universiti Teknologi PETRONAS. I appreciate his patience, insightful comments and for giving me the opportunity to think and learn independently and for giving me the freedom in performing the research. I am very fortunate to have a wonderful mentor and advisor guiding and assisting me. Special thanks to AP. Ir. Dr. Mohd Shahir Liew, my co-supervisor, for giving valuable suggestions and advices. In addition, special thanks to the Offshore Engineering Center UTP (OECU) members, who always share their ideas and give support to all members. I would like to thank Universiti Teknologi PETRONAS for the facilities provided in this work with a team of great staff during the model tests and for the softwares provided in the workstation for the simulation works. Not to forget, my helpful colleague, Ng Cheng Yee for guiding and helping me during this study.

I express my warmest gratitude to my husband, Muhammad Adib Bin Muhammad Arif, and my mother, Rossilawati Binti Wagiran, for their dedications, encouragements, and love during my complicated time in finishing this research. family, for their love, prayers, sincerities and unconditional support at every stage of my life. I extend my thanks and gratitude to all my friends, near and far, especially to Hazmatul Farha Binti Hamzah, who gives me friendship, prayers, and support and who shares a great and memorable time during the tenure of my research and thesis work.

## ABSTRACT

It is well known that in offshore region, wave and current coexist simultaneously that make them being the most important processes controlling the hydrodynamic behavior. The presence of current in the water body gives a significant effect to the response of the offshore structure. Many studies had been done in order to determine the behavior of the wave with the presence of the current. The studies have shown that the wave-current interaction changes the wave behavior and characteristics such as the wave length, wave forces, and slow drift motions. These changes give a significant effect to the response of the structure.

In this study, the dynamic response analysis of classic and truss spars were investigated both numerically and experimentally in random wave and regular wave combined with currents. The motion responses in surge, heave, and pitch had been evaluated. The numerical analysis included the frequency domain and time domain analysis. For the frequency domain analysis, the wave characteristics were determined by using the Linear Airy theory while the Morrison equation was used to compute the wave forces. The Morrison equation assumed the force to be composed of inertia and drag forces. In addition, the JONSWAP Spectrum was used to determine the wave spectrum while the Wave-Current Modified Spectrum was used to determine the wave-current spectrum. The Newmark Beta Method was used for the time domain analysis in order to solve the equation of motions which included the mass, damping, and stiffness of the structures.

For the model test, the spar platforms were modeled as rigid bodies connected to the sea floor by four catenary mooring lines attached at the fairleads. The wave-current force calculations were based on the Morrison equation applied at the instantaneous position of the structure. Experimentally, the classic and truss spar models fabricated to a scale of 1:100 were tested in regular and random wave combined with series of currents. The results obtained in the model tests were

processed and evaluated by using MATLAB code to get the RAO values. The results of the numerical analysis were cross-checked with the experimental model test results and commercially established simulation software results for validation.

In the simulation analysis, the SACS software was used in order to determine the dynamic response of the spars when subjected to wave and current. This software is commercially established software widely used in the industry. The model was analyzed using this software by defining the joints and the members of the structures. This software applied the linear diffraction analysis that is applicable to the structure with a diameter exceeding 0.2 times the wavelength of the incident wave. The comparisons of the results for different methods were found to be in a good agreement in predicting the dynamic response of the spar.

A parametric study was done for various current velocities and types of offshore structures to determine the effect of these parameters to the response of the structure. The wave and current conditions were taken from the Metocean data for Malaysia offshore regions, while the classic and truss spars were used for the study. This parametric study showed that there was a significant effect of the current added with wave on the spar responses for Malaysia offshore regions. Thus, the inclusion of the current in the structural response analysis is very essential for the Malaysian offshore regions. In this study, it is found that the response of the truss spar is lower compared to the classic spar. Therefore, truss spar is the most preferable structure to be installed in the offshore regions.

## ABSTRAK

Semua sedia maklum bahawa di kawasan pesisiran pantai, ombak dan arus berlaku secara serentak dan ini membuatkan kedua-duanya merupakan proses yang sangat penting yang mengawal keadaan hidrodinamik. Kewujudan arus di dalam air laut telah memberikan kesan yang ketara terhadap tindakbalas oleh struktur laut dalam. Banyak kajian telah dilakukan untuk menentukan tingkah laku ombak dengan adanya arus. Kajian-kajian ini menunjukkan bahawa interaksi ombak-arus telah merubah tingkahlaku dan ciri-ciri ombak seperti panjang ombak, daya ombak, dan pergerakan hanyutan yang perlahan. Perubahan ini memberikan kesan yang penting kepada tindakbalas sesuatu struktur.

Dalam kajian ini, analisis dinamik terhadap spar klasik dan spar rangka telah dikaji secara numerik dan eksperimen bagi keadaan ombak rawak dan ombak tetap yang berbeza bersama dengan arus. Pergerakan tindakbalas dalam pergerakan translasi pada paksi X, pergerakan translasi pada paksi Y, dan pergerakan rotasi pada paksi Z telah dikaji. Analisis numerik adalah termasuk analisis domain frekuensi dan domain masa. Untuk analisis domain frekuensi, ciri-ciri ombak ditentukan dengan menggunakan Teori Gelombang Linear. Manakala Persamaan Morrison telah digunakan untuk mengira daya ombak. Persamaan Morrison menganggap daya terdiri daripada daya inersia dan juga daya tarikan. Spektrum JONSWAP telah digunakan untuk menentukan spektrum ombak dan Spektrum Ombak-Arus Diubah digunakan untuk menentukan spektrum ombak-arus. Cara Newmark Beta telah digunakan untuk analisis domain masa untuk menyelesaikan persamaan pergerakan yang mana meliputi berat struktur, keredaman struktur, dan kekakuan struktur.

Bagi ujian model, pelantar spar telah dimodelkan sebagai jisim yang tidak bergerak yang bersambung dengan lantai laut dengan menyambungkannya bersama kabel penambat pada pencangkuk. Pengiraan daya ombak-arus adalah berdasarkan persamaan Morrison yang digunakan pada posisi struktur tersebut. Melalui

eksperimen, model spar klasik dan spar rangka yang berskala 1:100 telah diuji dalam ombak rawak tetap yang berbeza yang digabungkan bersama arus. Keputusan yang diperolehi melalui eksperimen telah diproses dan dikaji selidik dengan menggunakan kod MATLAB untuk mendapatkan nilai RAO. Keputusan yang diperolehi melalui kajian numerik telah dibandingkan dengan keputusan eksperimen dan keputusan simulasi menggunakan perisian komersial untuk mengesahkan keputusan-keputusan yang telah diperolehi.

Melalui analisis simulasi, perisian SACS telah digunakan bagi menentukan tindakbalas dinamik bagi spar-spar tersebut apabila dikenakan ombak bersama arus. Perisian ini digunakan secara meluas di dalam industri. Model tersebut telah direka di dalam perisian ini dengan menentukan sambungan dan palang bagi struktur tersebut. Input bagi maklumat alam sekitar diperlukan sebelum memulakan analisis. Perisian ini menggunakan analisis pembelauan di mana ianya boleh digunakan untuk struktur yang mempunyai diameter melebihi 0.2 daripada panjang arus daripada ombak yang mendatang datang. Perbandingan antara kaedah-kaedah yang berlainan ini menunjukkan keputusan yang amat bagus persetujuannya.

Satu kajian parametrik telah dijalankan untuk beberapa kelajuan arus dan jenis-jenis struktur laut bagi menentukan kesan parameter ini terhadap tindakbalas struktur. Kondisi ombak dan arus diambil daripada data Metocean dari perairan Malaysia manakala spar klasik dan spar rangka telah digunakan dalam kajian parametrik ini. Kajian parametrik ini menunjukkan kesan yang amat penting dengan kehadiran arus di dalam ombak terhadap reaksi struktur spar di kawasan perairan Malaysia. Kajian ini membuktikan bahawa spar rangka memberikan tindakbalas yang lebih rendah berbanding dengan spar klasik. Ini menjadikan spar rangka lebih sesuai dipasang di perairan Malaysia. Kajian ini menunjukkan kehadiran arus di dalam ombak telah menunjukkan betapa pentingnya memasukkan kedua-dua parameter tersebut pada peringkat rekabentuk struktur.

In compliance with the terms of the Copyright Act 1987 and the IP Policy of the university, the copyright of this thesis has been reassigned by the author to the legal entity of the university,

**Institute of Technology PETRONAS Sdn Bhd.**

Due acknowledgement shall always be made of the use of any material contained in, or derived from, this thesis.

**© Siti Nor Adha Binti Tuhaijan, 2013**

Institute of Technology PETRONAS Sdn Bhd

All rights reserved.

## TABLE OF CONTENT

STATUS OF THESIS .....	i
APPROVAL PAGE.....	ii
TITLE PAGE.....	iii
DECLARATION.....	iv
DEDICATION.....	v
ACKNOWLEDGEMENTS.....	vi
ABSTRACT .....	vii
ABSTRAK.....	ix
LIST OF FIGURES .....	xvi
LIST OF TABLES.....	xx
LIST OF APPENDICES .....	xxi
LIST OF ABBREVIATIONS.....	xxii

### Chapter

1. INTRODUCTION.....	1
1.1 Introduction .....	1
1.2 Problem Statement .....	2
1.3 Objectives of Study .....	3
1.4 Scopes of Study .....	4
1.5 Thesis Organization .....	5
2. LITERATURE REVIEW.....	6
2.1 Offshore Structures .....	6
2.1.1 General .....	6
2.1.2 Platforms in Malaysia.....	7
2.2 Spar Platforms.....	7
2.2.1 General .....	7
2.2.2 Spar in Malaysia.....	9
2.3 Hydrodynamic Analysis of Offshore Platform .....	10
2.3.1 Previous Studies on Offshore Platforms, Other Than Spar.....	13

2.3.2 Previous Studies on Spar Platforms .....	15
2.4 Wave-Current Interaction on Offshore Structure .....	19
2.4.1 Wave-Current Interaction.....	19
2.4.2 Previous Studies on Wave-Current Interaction .....	21
2.5 Summary of Literature .....	28
2.6 The Need for Research.....	28
3. METHODOLOGY .....	30
3.1 Chapter Overview .....	30
3.2 Six Degrees Of Freedom (6 DOF) .....	31
3.3 Frequency Domain Analysis .....	31
3.3.1 Linear Airy Theory.....	32
3.3.2 Morrison Equation.....	34
3.3.3 Wave Spectrum- JONSWAP Spectrum .....	36
3.3.4 Wave Current Modified Spectrum .....	37
3.3.5 Simulation of Wave Profile from Spectra .....	37
3.3.6 Motion Response Spectrum.....	38
3.4 Time Domain Analysis.....	38
3.4.1 Equation of Motion .....	39
3.4.2 Newmark Beta Integration Method.....	42
3.5 Model Tests.....	43
3.5.1 Modeling Law .....	43
3.5.2 Prototype Description.....	45
3.5.3 Test Facilities and Instrumentation .....	48
3.5.4 Generation of Wave and Current.....	49
3.5.5 Model Tests Setup and Procedure .....	49
3.5.6 Free Decay Test.....	50
3.5.7 Model Tests Data Processing .....	53
3.6 Diffraction Theory.....	57
3.6.1 Linear Wave Diffraction Analysis using SACS Software .....	58
3.6.2 Classic Spar Modeling .....	59
3.6.3 Truss Spar Modeling .....	61
3.7 Chapter Summary.....	63

4. RESULTS AND DISCUSSION .....	64
4.1 Chapter Overview .....	64
4.2 Regular Wave .....	64
4.2.1 Frequency Domain (FD) Analysis Results for Prototypes .....	65
4.2.1.1 Classic Spar Prototype .....	65
4.2.1.2 Truss Spar Prototype .....	67
4.2.2 Spar Model Test Results.....	68
4.2.2.1 Classic Spar Model Results .....	68
4.2.2.2 Truss Spar Model Results.....	70
4.2.3 Comparison of Results .....	72
4.2.3.1 Frequency Domain (FD) Analysis & Model Test Results.....	72
4.2.3.2 Truss Spar Prototype .....	75
4.3 Random Wave .....	77
4.3.1 Frequency Domain (FD) Analysis Results for Prototypes .....	77
4.3.1.1 Classic Spar Prototype.....	77
4.3.1.2 Truss Spar Prototype .....	79
4.3.2 Time Domain (TD) Analysis Results for Prototypes .....	81
4.3.2.1 Classic Spar Prototype.....	81
4.3.2.2 Truss Spar Prototype .....	81
4.3.3 Spar Model Test Results.....	85
4.3.3.1 Classic Spar Model Results .....	85
4.3.3.2 Truss Spar Model Results.....	87
4.3.4 Linear Wave Diffraction Analysis (LWD) using SACS Simulation	
Software .....	88
4.3.4.1 Classic Spar Prototype.....	88
4.3.4.2 Truss Spar Prototype .....	90
4.3.5 Comparison of Results .....	92
4.3.5.1 Frequency Domain (FD) Analysis & Model Test Results.....	92
4.3.5.2 Time Domain (TD) Analysis, Model Test, & Linear Wave	
Diffraction (LWD) Analysis Results .....	97
4.4 Parametric Study .....	102
4.4.1 Current Velocities .....	102
4.4.2 Type of Spars .....	104
4.5 Chapter Summary.....	106

5. CONCLUSIONS AND FURTHER STUDIES .....	107
5.1 Chapter Overview .....	107
5.2 Conclusions .....	107
5.3 Future Studies.....	109

**APPENDICES**

**A. MODEL TEST DATA**

**B. FREE DECAY TEST**

## LIST OF FIGURES

Figure 2.1: Surge RAO Comparison for Different Structures.....	9
Figure 2.2: Heave RAO Comparison for Different Structures.....	9
Figure 2.3: Pitch RAO Comparison for Different Structures.....	9
Figure 2.4: Kikeh Spar .....	10
Figure 2.5: The Current Profile .....	21
Figure 3.1: Research Activities .....	30
Figure 3.2: Definition of 6 DOF for Floating Structure .....	32
Figure 3.3: Wave Parameters .....	34
Figure 3.4: Classic Spar Model .....	44
Figure 3.5: Truss Spar Model.....	44
Figure 3.6: Classic Spar Model Dimension.....	46
Figure 3.7: Truss Spar Model Dimension .....	47
Figure 3.8: The Wave Paddles .....	48
Figure 3.9: The Model Test Setup.....	48
Figure 3.10: The On-going Model Test.....	50
Figure 3.11: Model Test Arrangement .....	51
Figure 3.12: Wave Probes and Vectrinometers Arrangement.....	52
Figure 3.13: Surge Response Subjected to Regular Wave.....	53
Figure 3.14: Heave Response Subjected to Regular Wave .....	54
Figure 3.15: Pitch Response Subjected to Regular Wave .....	54
Figure 3.16: Time Series for Surge Subjected to Random Wave (RD3) .....	55
Figure 3.17: Time Series for Heave Subjected to Random Wave (RD3) .....	55
Figure 3.18: Time Series for Pitch Subjected to Random Wave (RD3) .....	56
Figure 3.19: Time Series for Random Wave (RD3) .....	56
Figure 3.20: Spectra Density subjected to Random Wave (RD3).....	57
Figure 3.21: The Simulation Flowchart .....	59
Figure 3.22: Classic Spar Model for Simulation.....	60
Figure 3.23: Plan View of Classic Spar Simulation.....	60

Figure 3.24: Section View of Classic Spar Simulation.....	60
Figure 3.25: Truss Spar Model for Simulation .....	61
Figure 3.26: Plan View of Truss Spar Simulation .....	61
Figure 3.27: Section View of Classic Spar Simulation.....	62
Figure 4.1: FD Analysis – Classic Spar Surge Response (Regular Wave).....	65
Figure 4.2: FD Analysis – Classic Spar Heave Response (Regular Wave).....	66
Figure 4.3: FD Analysis – Classic Spar Pitch Response (Regular Wave).....	66
Figure 4.4: FD Analysis – Truss Spar Surge Response (Regular Wave) .....	67
Figure 4.5: FD Analysis – Truss Spar Heave Response (Regular Wave) .....	67
Figure 4.6: FD Analysis – Truss Spar Pitch Response (Regular Wave) .....	68
Figure 4.7: Model Test – Classic Spar Surge Response (Regular Wave) .....	69
Figure 4.8: Model Test – Classic Spar Heave Response (Regular Wave).....	69
Figure 4.9: Model Test – Classic Spar Pitch Response (Regular Wave).....	70
Figure 4.10: Model Test – Truss Spar Surge Response (Regular Wave) .....	71
Figure 4.11: Model Test – Truss Spar Heave Response (Regular Wave) .....	71
Figure 4.12: Model Test – Truss Spar Pitch Response (Regular Wave) .....	72
Figure 4.13: Comparison – Classic Spar Surge Response (Regular Wave) .....	73
Figure 4.14: Comparison – Classic Spar Heave Response (Regular Wave) .....	74
Figure 4.15: Comparison – Classic Spar Pitch Response (Regular Wave) .....	74
Figure 4.16: Comparison – Truss Spar Surge Response (Regular Wave).....	75
Figure 4.17: Comparison – Truss Spar Heave Response (Regular Wave).....	76
Figure 4.18: Comparison – Truss Spar Pitch Response (Regular Wave).....	76
Figure 4.19: FD Analysis – Classic Spar Surge Response .....	78
Figure 4.20: FD Analysis – Classic Spar Heave Response .....	78
Figure 4.21: FD Analysis – Classic Spar Pitch Response .....	79
Figure 4.22: FD Analysis – Truss Spar Surge Response .....	80
Figure 4.23: FD Analysis – Truss Spar Heave Response .....	80
Figure 4.24: FD Analysis – Truss Spar Pitch Response .....	81
Figure 4.25: TD Analysis – Classic Spar Surge Response .....	82
Figure 4.26: TD Analysis – Classic Spar Heave Response .....	82
Figure 4.27: TD Analysis – Classic Spar Pitch Response .....	83

Figure 4.28: TD Analysis – Truss Spar Surge Response .....	83
Figure 4.29: TD Analysis – Truss Spar Heave Response .....	84
Figure 4.30: TD Analysis – Truss Spar Pitch Response .....	84
Figure 4.31: Model Test – Classic Spar Surge Response.....	85
Figure 4.32: Model Test – Classic Spar Heave Response.....	86
Figure 4.33: Model Test – Classic Spar Pitch Response.....	86
Figure 4.34: Model Test – Truss Spar Surge Response .....	87
Figure 4.35: Model Test – Truss Spar Heave Response .....	87
Figure 4.36: Model Test – Truss Spar Pitch Response .....	88
Figure 4.37: LWD Analysis – Classic Spar Surge Response.....	89
Figure 4.38: LWD Analysis – Classic Spar Heave Response.....	89
Figure 4.39: LWD Analysis – Classic Spar Pitch Response.....	90
Figure 4.40: LWD Analysis – Truss Spar Surge Response .....	90
Figure 4.41: LWD Analysis – Truss Spar Heave Response.....	91
Figure 4.42: LWD Analysis – Truss Spar Pitch Response.....	91
Figure 4.43: Surge RAO Comparison for Classic Spar Subjected to Random Wave (RD3) and Current (C1) .....	93
Figure 4.44: Heave RAO Comparison for Classic Spar Subjected to Random Wave (RD3) and Current (C1) .....	93
Figure 4.45: Pitch RAO Comparison for Classic Spar Subjected to Random Wave (RD3) and Current (C1) .....	94
Figure 4.46: Surge RAO Comparison for Truss Spar Subjected to Random Wave (RD3) and Current (C1) .....	95
Figure 4.47: Heave RAO Comparison for Truss Spar Subjected to Random Wave (RD3) and Current (C1) .....	96
Figure 4.48: Pitch RAO Comparison for Truss Spar Subjected to Random Wave (RD3) and Current (C1) .....	96
Figure 4.49: Surge RAO Comparison for Classic Spar Subjected to Random Wave (RD3) and Current (C1) for Different Methods .....	98
Figure 4.50: Heave RAO Comparison for Classic Spar Subjected to Random Wave (RD3) and Current (C1) for Different Methods .....	98

Figure 4.51: Pitch RAO Comparison for Classic Spar Subjected to Random Wave (RD3) and Current (C1) for Different Methods.....	99
Figure 4.52: Surge RAO Comparison for Truss Spar Subjected to Random Wave (RD3) and Current (C1) for Different Methods.....	100
Figure 4.53: Heave RAO Comparison for Truss Spar Subjected to Random Wave (RD3) and Current (C1) for Different Methods.....	101
Figure 4.54: Pitch RAO Comparison for Truss Spar Subjected to Random Wave (RD3) and Current (C1) for Different Methods.....	101
Figure 4.55: Surge RAO Comparison for Different Currents.....	103
Figure 4.56: Heave RAO Comparison for Different Currents.....	103
Figure 4.57: Pitch RAO Comparison for Different Currents.....	104
Figure 4.58: Surge RAO Comparison for Different Spars .....	105
Figure 4.59: Heave RAO Comparison for Different Spars.....	105
Figure 4.60: Pitch RAO Comparison for Different Spars.....	106

## LIST OF TABLES

<b>Table 3.1: The Froude Scaling .....</b>	<b>45</b>
<b>Table 3.2: Specified Random Wave Conditions for Model Tests.....</b>	<b>49</b>
<b>Table 3.3: Specified Regular Wave Conditions for Model Tests.....</b>	<b>49</b>
<b>Table 3.4: Specified Current Velocity Conditions for Model Tests.....</b>	<b>49</b>
<b>Table 3.5: The Natural Period of 3 DOF .....</b>	<b>50</b>
<b>Table 3.6: Input Data for Simulation.....</b>	<b>62</b>

## LIST OF APPENDICES

A. MODEL TEST DATA .....	117
B. FREE DECAY TEST .....	127

## LIST OF ABBREVIATIONS

DFFT	Discrete Fast Fourier Transform
DOF	Degree of Freedom
FD	Frequency Domain Analysis
FPSO	Floating Production, Storage, and Offloading
LWD	Linear Wave Diffraction Analysis
MATLAB	Matrix Laboratory Software
OTS	Opti-Tracking System
PMO	Peninsular Malaysia Operation
RAO	Response Amplitude Operator
RD	Random Wave
RG	Regular Wave
SACS	Structural Analysis Computer System
SBO	Sabah Operation
SEMI	Semi-submersible
SKO	Sarawak Operation
TD	Time Domain Analysis
TDSIM	Nonlinear Time Domain Compute Code-Hydrodynamic Forces
THOBEM	Time Domain Higher Order Boundary Element Method
TLP	Tension Leg Platform
TRSPAR	Nonlinear Time Domain Compute Code-Wave Only
WAMIT	Wave Analysis Developed at MIT

# CHAPTER 1

## INTRODUCTION

### **1.1 Introduction**

Malaysia is one of the leading countries which produce oil and gas for fulfilling the global demand. The oil and gas industry in Malaysia has expanded significantly since Malaysia installed its first deepwater structure called Kikeh Spar in 2007. Kikeh Spar was installed near Sabah Sea at 1,300 m water depth. The intense competition with other countries has made Malaysia realize the importance of the deepwater exploration development. Many studies have to be done in order to support this development. The understanding of the hydrodynamic behavior of structures in Malaysian offshore regions is very important because it will provide information that can be used during the preliminary design stage of the deepwater structures [1, 2, 3]. Therefore, it is important for us to develop our own technology so that we can design, analyze, and maintain the structures.

The understanding of the hydrodynamic behavior in Malaysian offshore regions, enable us to determine the responses of deepwater structures. It is known that Malaysia's offshore regions are subjected to significant water current simultaneously with the wave. Wave and current are normally the major environmental forces in the offshore region [1, 4]. The existence of the current in the water body alters the wave profile [5]. A study on the wave-current interaction has to be done in order to understand the characteristics of these interactions at Malaysian offshore regions.

For the last few decades, various studies on wave-current interaction characteristics had been done due to the major effects on the design of the offshore platforms [1, 3]. In these studies, time domain analysis [3, 6, 7, 8] and frequency domain analysis [6, 7, 9] had been carried out in order to determine the dynamic behavior of all types of offshore structures.

For the spar, several studies had been done in order to determine the dynamic behavior of the structure. For the estimation of the forces, Linear Airy Theory and Morrison equation have been used [10]. Based on the potential flow theory, numerical approach for wave-current interaction around a large structure had been investigated. In other studies, the time domain method had been used to determine the effects of current on the radiation and the diffraction of regular waves around two-dimensional body [3]. The results showed significant structural responses due to the existence of current in the water waves.

There are some possible interaction mechanisms between waves and currents [11, 12, 13]. The mechanisms might include surface wind stress, bottom friction, wave climate, wave field, depth and current refraction, and modulation of the absolute and relative wave period. Besides, the combined current and wave may lead to changes of wave forces, wave run-up, and slow drift motions [14]. Therefore, it is important to predict the responses of the structures towards the subjected wave and current which may involve very large horizontal excursions. The existence of the current in the water body changes the pattern of the wave diffraction and radiation by floating structures. It is a different pattern compared with that from the pure wave action.

## **1.2 Problem Statement**

Due to the high global demand, the oil and gas exploration has expanded since the first installation of the fixed offshore platform in 6 m water depth in Gulf of Mexico in 1947. There are more than 10,000 units of platforms that had been installed worldwide for the last six decades. At the early stage of the oil and gas industry, it was only focused on the shallow water exploration until the amounts of the natural sources in this region were facing depletion. As a result, the oil exploration in the deepwater region is investigated and new deepwater technology is implemented.

Spar is a type of deepwater floating platform used in the water of depth more than 1,500 m. There are few types of spar that available and widely used recently which are classic spar, truss spar, and cell spar. In Malaysia, there is a spar platform called Kikeh Spar which is the only spar platform that had been installed outside the Gulf of Mexico. It was installed at more than 1,300 m water depth at Sabah's sea.

Further study on the design and construction of spar platform is very important for the future deepwater development in Malaysia. For this, the consultants use very costly commercial software and charge huge consultancy fees. It is necessary for us to develop our technology so that we can analyze, design, and maintain the spar and associated mooring components. It is important to mention here that Malaysian offshore regions have been identified as subjected to significant water current also. Hence wave-current interaction is an important technology to be developed for our Malaysian locations. This involves deriving the required theoretical formulations and generating the strategic data for the locations in Malaysia. As many oil and gas companies are operating in our locations, we will be able to use these strategic data for consultancy purposes also.

### **1.3 Objectives of Study**

The objectives of this study include:

1. To determine the dynamic responses of classic and truss spar subjected to wave and current using both frequency and time domain numerical methods.
2. To validate the results of numerical analysis by comparing with experimental model test results and commercially established simulation software using linear diffraction analysis.
3. To arrive at definite conclusions on the effect of current added with wave on the spar responses for Malaysian offshore regions, and also to compare the response between the two types of spar.

The purpose of this study is to determine the motion responses of classic and truss spars subjected to both wave and current. In this study, the numerical dynamic response analysis of these spars has been done using frequency domain and time domain analyses. The frequency domain dynamic analysis is simpler and less time consuming as compared to time domain because the estimation of the response can be

calculated by using the wave spectrum method. Besides, the results are simpler to interpret and apply for further analysis. However, there is a limitation for the frequency domain analysis where all nonlinearities in the equation of motion are replaced by the linear approximations which will lead to low accuracy and error in response prediction. The nonlinearities include fluid drag force, mooring line force, viscous damping and stiffness of the system for different motions consideration. This analysis was done by using a mathematical coding in MATLAB by applying the Newmark Beta Method in order to solve the equation of motion. Model tests were done to validate the numerical analysis results. Two fabricated models with a scale of 1:100 were tested in the Offshore Laboratory, Universiti Teknologi PETRONAS. In addition, a simulation work applying the linear diffraction analysis using commercial software called SACS was done. These results were compared for validation. Parametric study was done for different current velocities to study the effects of the existence of current in the water body. In addition, two different types of spars were compared to determine the structure dynamic responses and stability. The wave and current conditions were taken from the Metocean data of Malaysian offshore regions. This parametric study will show the effect of the current added with wave on the spar responses for Malaysian offshore regions.

#### **1.4 Scopes of study**

The scope of the research was confined within the following scopes.

1. Type of Platforms
  - a. Truss Spar
  - b. Classic Spar
  
2. Wave Criteria
  - a. Combination of wave and current
  - b. Malaysian metocean data
  
3. Mooring line
  - a. Four mooring lines

The research was aimed to focus particularly on the model tests and optimization of theoretical formulations in comparison with the model tests. It is believed that the results will be useful in facilitating the present state of the study and in providing the strategic data for the preliminary design used in Malaysian offshore regions.

### **1.5 Thesis organization**

In this section, the organization of the thesis presented herein.

Chapter 2 presents a general summary of the literature pertaining to the objectives of the study. It covers the offshore structures, spar platforms, wave-current interaction, and the hydrodynamic analysis of offshore platforms. The reported researches are classified into four categories and a general description of each category is given.

In Chapter 3, the research methodology is discussed in details. The numerical analyses which include frequency domain and time domain are explained. This includes the governing equation and the boundary conditions for the water particles. The sequence of the model test for both classic and truss spar is explained in this second part of this chapter. Lastly, a detailed explanation of the simulation work using SACS software is presented.

To verify the accuracy of the numerical program, the results will be compared to a comprehensive detailed model test and presented in Chapter 4 for both classic and truss spars. For further validation, the simulation results are compared to numerical and model test results. In addition, the parametric study for the different current velocities and type of spars are also presented at the end of this chapter. Finally, the trend of the results will be discussed.

Chapter 5 summarizes the findings of this study. The conclusions addressing each objective are mentioned. Finally, recommendations for further improvements and research are proposed.

## CHAPTER 2

### LITERATURE REVIEW

#### **2.1 Offshore Structures**

##### **2.1.1 General**

Offshore structure is a structure that consists of several facilities including the drilling wells, oil and gas extracting and processing, and also a facility to export the products to the onshore. There are two main categories of offshore structure which are fixed and floating structures. The fixed structure installed in the offshore region by fixing it to the seafloor while the floating structure installed by attaching it to the mooring line.

A wooden wharf outfitted with a rig for drilling vertical wells into the sea floor was the earliest offshore structure that had been installed at the coast of southern California near Santa Barbara in 1887 [15]. In order to support the structure, some improvement on the design had been done which was the installation of the timber piers of the structures. But, after a certain period, it was found that the lifetime of the timber piers was limited due to the marine organisms. Later, the timber was replaced by the reinforced concrete as the supporting structures for many platforms up to the late 1940s.

Since the first oil recovery until today, there are several types of offshore platforms that had been design namely as conventional fixed platforms, compliant tower, tension leg platform, spar, semi-submersibles, and FPSO (Floating production, storage, and offloading facility). For the water depth up to 500 m, the jack-up rig, gravity platform, and jacket platforms are designed and installed in this region, while compliant tower, tension leg platform, and semisubmersible are designed for depths up to 2,000 m.

## **2.1.2 Platforms in Malaysia**

Malaysia water is divided into three basins which are Sabah basin, Sarawak basin and West Malaysia of Terengganu basin [16]. Malaysia's first oil discovery was in 1910 on Canada Hill in Miri. Oil and gas are the most widely used forms of energy that the world has ever known. With the continuing demand of petroleum, the need arises to explore the oil and gas reserves from deep water depths far off the continental shelf. Today, more than 400 offshore structures are installed in the Malaysian offshore regions.

## **2.2 Spar Platforms**

### **2.2.1 General**

Spar is a floating structure stabilized by mooring lines and attached to the seafloor. There are three types of spars which are classic spar, truss spar, and cell spar. The difference among these spars is on the structure design. For the classic spar, it consists of one-piece cylindrical hull and for the truss spar, it has a midsection composed of truss elements connecting to the upper buoyant hull, also known as a hard tank with the bottom soft tank containing a permanent ballast. The cell spar is built using multiple vertical cylinders. The spar has a capability to be installed in ultra deepwater which is up to 3,000 m of water depth [17]. Spars have proved to be very stable floating structures.

Generally, the spars consist of several elements such as topside, hull shell, buoyancy tank, centerwell, risers, and mooring lines [18]. The spar has inherent stability since it has a large counterweight at the bottom and does not depend on the mooring to hold it upright. It also has the ability to move horizontally and to position itself over wells at some distance from the main platform location by adjusting the mooring line tensions. In the late 1990s, the first three draft caisson vessels, or spars, were installed for use in 180 m water depth. Spars are designed as floating vertical cylinders that can support production decks above storm waves. During drilling and

production operations, these structures are kept in place by mooring lines and thrusters.

The motions and loads of spars are controlled by two parts [19]. The primary part is controlled by the hull configurations which consists of draft and heave plates. The secondary part is controlled by the mooring system which consists of taut and synthetic cables. Thus, the design of the spar is very important for the stability when it is installed in the water. The effect of the hydrodynamic forces may be critical on the connection of the offshore structures. For both classic and truss spars, the connections between the topsides and spar hull are critical locations for fatigue design because of the motion characteristics of a spar platform [20]. A truss spar will experience both wave-frequency motion and low-frequency motion. The wave-frequency motion is peaked around the wave-frequency, while the low-frequency motion corresponds to the natural periods of the truss spar rigid-body motions. The wave frequency motions can be estimated reasonably well with potential and diffraction theory, but the low-frequency motions will not be accounted. It has been found that for topsides-to-hull connections, spectral method can accurately predict the fatigue damage.

Spar is more economical compared to the other deep water offshore structures [21]. The spar is having long periods in heave, pitch and rolls which makes it insensitive to the wave frequencies and their height harmonics. In addition, the spar does not undergo any type of springing and ringing response in severe storms as tension leg platforms may undergo. The spar is also insensitive with the water depth since it is mainly a floating cylinder, thus, the spar can be relocated to another spot in the ocean regardless of the water depth or the deck load. Although the spar is a large diameter cylinder with respect to the wave lengths, the use of Morrison equation with modifications has proved to be capable of capturing the trend of the responses as well as most of the nonlinearities associated with it, such as the slowly varying drift motion. The effect of wave drift damping is small. However, it improves slightly the response amplitude at the natural frequencies of the structure particularly at the early stages of the analysis.

In the spar design, there is some information that has to be included [22]. In this review, the comparison of the different offshore structures which are tension leg platform (TLP), semi-submersible (SEMI), and spar for the surge, heave, and pitch response were shown. Figures 2.1 to 2.3 show the surge, heave, and pitch responses respectively.

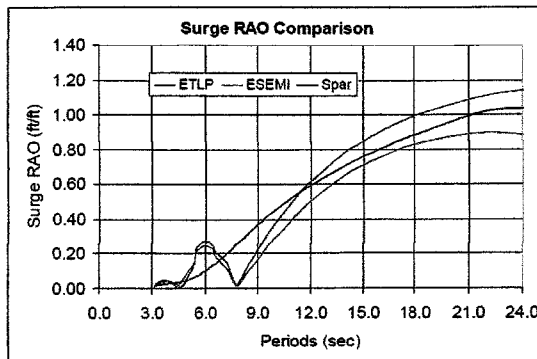


Figure 2.1: Surge RAO Comparison for Different Structures

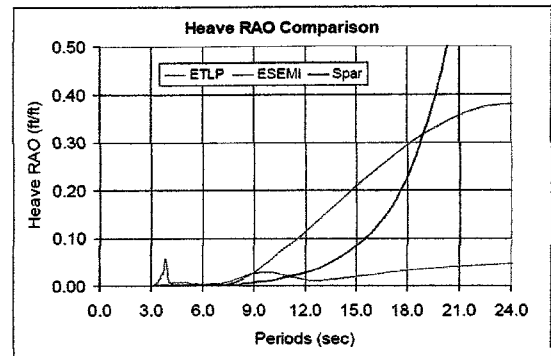


Figure 2.2: Heave RAO Comparison for Different Structures

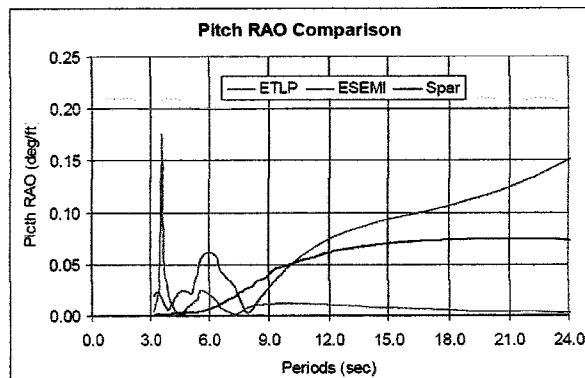


Figure 2.3: Pitch RAO Comparison for Different Structures

### 2.2.2 Spar in Malaysia

In line with the global development, Malaysia had constructed and installed its first deepwater floating platform which was the Kikeh spar. It was installed completely with topsides facilities, hull, mooring system, riser, and wellhead systems. It was located in 1,330 m water depth of offshore Sabah, Malaysia. This spar platform was the first spar ever installed outside the Gulf of Mexico and the first application of tender-assisted drilling on a spar platform [23]. The Spar hull for Kikeh was 142 m long, with a diameter of 32 m and had a steel weight of 12,000 metric tons. The

weight of topsides facilities was about 3,000 metric tons and it was provided with a 25-slot wellbay for dry tree wellheads. Figure 2.4 shows the Kikeh Spar that had been installed in Malaysia.

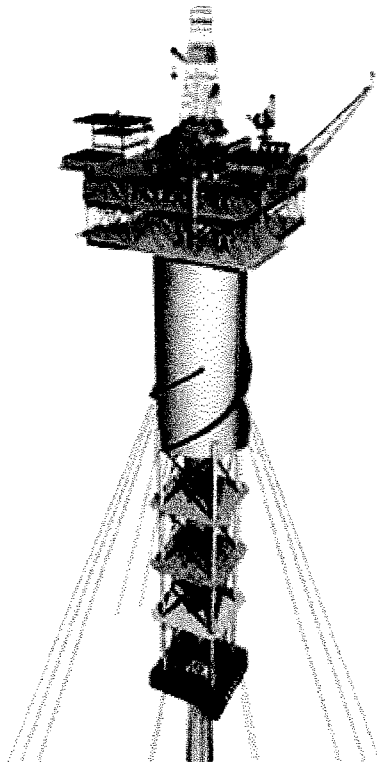


Figure 2.4: Kikeh Spar

### **2.3 Hydrodynamic Analysis of Offshore Platform**

For the deepwater, the influence of the ocean bottom topology on the water particle kinematics is considered negligible [5]. A number of regular wave theories have been developed to describe the water particle kinematics associated with ocean waves of varying degrees of complexity and levels of acceptance by the offshore engineering community. The wave theories include the Airy wave theory, Stokes second and higher order theories, stream function, and Cnoidal wave theories. The dynamic behavior of the structure can be determined by using either frequency domain or time domain analysis. Frequency domain analysis is performed for the simplified solution and it is useful for long term response prediction. It is simpler to interpret and always being used for the preliminary design stage. Moreover, it can estimate responses due to a random wave input through spectral formulations. Still, the limitation of this

analysis is that all nonlinearities in the equation of motion must be replaced by linear approximations. Time domain analysis utilizes the direct numerical integration of the equations of motion allowing the inclusion of all system nonlinearities which are nonlinear fluid drag force, nonlinear mooring line force and nonlinear viscous damping. However, this analysis increases computer time and difficult to interpret and apply.

In the open sea, a floating, moored structure may respond to wind, waves and current with motions on three different time scales, wave frequency motions, low frequency motions and high frequency motions [24]. The largest wave loads on offshore structures take place at the same frequencies as the waves, causing wave frequency motions of the structure. To avoid large resonant effects, offshore structures and their mooring systems are often designed in such a way that the resonant frequencies are shifted well outside the wave frequency range.

Offshore structures have the added complication of being placed in an ocean environment where hydrodynamic interaction effects and dynamic response become major considerations in their design [25]. Nonlinearities in the description of the hydrodynamic loading characteristics of the structure fluid interaction and in the associated structural response can assume importance and need be addressed. These subject areas would include the hydrodynamics, the structural dynamics, and the advance structural techniques.

There are several methods in order to calculate the hydrodynamic forces. A review on the Morrison equation had been done by Merz [26]. In this paper, it was stated that it was convenient to think about the hydrodynamic loading in terms of flow processes. Multiple processes such as wind-generated waves, remote swell, current, and structural motion were active simultaneously, and their nonlinear interaction resulted in the fluid force on the structure. The Morrison equation stated that the fluid force was a superposition of a term in phase with the acceleration of the flow which was inertia, and a term whose dominant component was in phase with the velocity of the flow which was drag. It was accounted for some flow nonlinearity, by way of the drag term.

Another explanation on the wave force on offshore drilling structure was done by Aagaard *et al.* [27]. This paper presented a method for calculating ocean wave forces on offshore drilling structures. The method was based upon data from two full-scale wave force measurement installations in the ocean and a mathematical model representing hydrodynamic forces on submerged bodies in unsteady flow and the kinematic flow field of highly nonlinear waves. The method was considered applicable to a broad range of wave conditions commonly encountered in the offshore structure design. Several comparisons showed that the method represented measured forces satisfactorily for engineering design.

There are a large number of different incremental solution methods for the dynamic analysis of structures and one of them is a step-by-step method [28]. In general, they involve a solution of the complete set of equilibrium equations at each time increment. In the case of nonlinear analysis, it may be necessary to reform the stiffness matrix for the complete structural system for each time step. Also, iteration may be required within each time increment to satisfy equilibrium. As a result of the large computational requirements, it can take a significant amount of time to solve structural systems with just a few hundred degrees-of-freedom.

The most general approach for the solution of the dynamic response of structural systems is the direct numerical integration of the dynamic equilibrium equations [29]. This involves, after the solution is defined at time zero, the attempt to satisfy dynamic equilibrium at discrete points in time. Many different numerical techniques have previously been presented. However, all approaches can fundamentally be classified as either explicit or implicit integration methods. Explicit methods do not involve the solution of a set of linear equations at each step. For most real structures, which contain stiff elements, a very small time step is required in order to obtain a stable solution. Therefore, all explicit methods are conditionally stable with respect to the size of the time step.

There were various studies on the analysis of spars and other platforms such as tension leg platform and semi-submersible had been done. In these studies, frequency domain analysis [6, 7, 9] and time domain analysis [3, 6, 7, 8] had been carried out in order to determine the dynamic behavior of the structures. For the estimation of the

forces, Linear Airy wave theory and Morrison Equation were used. The responses due to random waves known as Response Amplitude Operator (RAO) in surge, heave and pitch were determined [10].

### **2.3.1 Previous Studies on Offshore Platforms, Other Than Spar**

Burke *et al.* [30] had done a study on a time series model for dynamic behavior of fixed jacket offshore structure. An analytical model was presented for evaluating the dynamic behavior of offshore structures subject to earthquake and storm wave forces. A mathematical model was formulated as a system of nonlinear, differential equations that were solved by direct numerical integration on a digital computer. The offshore structure was represented in the model by a lump mass system with linear stiffness and damping characteristics. Nonlinearities arose from the representation of hydrodynamic forces on the structure by the Morrison equation, with velocities and accelerations based on the relative motion between structure and water. Random wave forces were obtained from wave velocities and accelerations simulated from a Pierson- Moskowitz wave spectrum while earthquake excitation consisted of a time history of horizontal base accelerations obtained from actual or simulated earthquake accelerograms.

A mathematical model for computation of wind, wave and current loads was briefly presented by Popescu *et al.* [2]. This paper presented approaches to the problem of wave, current and wind loads acting on the structure of the fixed platforms, using experimental and theoretical methods. A scale model 1:40 was used for measurement of wind while scale of 1:20 was used for wave force tests. The result was for the design, in safe and optimal condition of the offshore platforms. The concerning on the design and construction of offshore platforms were necessary. In addition, adequate designing should be done in order to obtain a workable and economical offshore platform to perform the given function. Besides, the accurate evaluation of hydrodynamic forces on the structures of platforms was very important for a proper design of these platforms.

Huse [31] had done a study on a TLP. In this study, the response of a TLP to waves could be loosely categorized into three frequency ranges which were mean and

slow drift frequencies, wave frequency, and high frequency. For the mean drift frequency, the hydrodynamic that affect the slow drift forces on a TLP were viscous forces, wave drift damping and wave drift excitation forces. The high frequencies were affected by first order wave components and higher second-order components occurring at sum-frequencies that correspond to resonant conditions.

Another study on the dynamic analysis of the TLP as a rigid body had been carried out using both frequency and time domain methods by Kurian *et al.* [6]. In this study, the Linear Airy Theory and Morrison equation were used for the estimation of forces while Newmark Beta Method was used for the time domain analysis. The frequency domain results were found to be much approximate as it could not take into account much nonlinearity. However, this method had potential to be used for preliminary design as it gave a good pattern of the motion responses.

In addition, a comparison with the experimental results was done by Roitman *et al.* [7]. Some effects of fluid-structure interaction were briefly discussed in the light of results from both impact and wave loading tests. At this stage of the test program, a few important conceptual characteristics of a TLP were checked. For this, a number of impact tests in still water were carried out to determine. The results of the natural periods and the related motion modes were determined in order to compare with the theoretical results.

A case study on the motion characteristics of a Trimaran hull form for both theoretical and experimental analysis was done by Hebblewhite *et al.* [32]. For the last two decades, many researches on the prediction of heave and pitch motion were done. The investigation was performed to reduce the heave and pitch motion of the structures in the open sea. This was due to the high consideration for passenger comfort. The comparison had shown that there was significant validity in using appropriate theoretical methods in order to reduce resources spent in design. In addition, the wave induced motion characteristics were found to correlate well over the range of Froude numbers tested. This correlation was particularly evident for the heave motions, while those for pitch were generally underestimates near resonance.

### 2.3.2 Previous Studies on Spar Platforms

A study on the effects of second order diffraction forces on the global response of spars had been done by Mekha *et al.* [21]. The spar was modeled as a rigid body with three degrees of freedom, connected to the sea floor by mooring lines which attached to the spar structure at the fairleads. The inertia forces were calculated using Morrison equation with frequency dependent ( $Cm$ ) coefficient based on diffraction theory while the drag force were computed using nonlinear term of Morrison equation. In this study, the analyses were performed in time domain where the different nonlinear modifications to Morrison equation were included to account for diffraction effects.

The coupling effects of mooring lines and risers on the motion responses of the structures became increasingly significant. A comparison of the coupling effects for the cell truss spar platform in frequency and time domain analyses with model test had been done by Zhang *et al.* [33]. Viscous damping, inertia mass, current loading and restoring from this slender structures should be carefully handled to accurately predict the motion responses and line tensions. For spars, coupling the mooring system and riser with the vessel motion typically resulted in a reduction in extreme motion responses. The comparison was to find the applicability of different approaches. The low frequency parts of motion responses were commonly affected by the nonlinear effects.

An innovative configuration of floating platform was required for the exploration of the hydrocarbon reservoir under the seabed in the very deepwater. The understanding on the hydrodynamic interactions between the structure and the wave and the quantification of the nonlinear component of this interaction had been a subject of continuing research. The nonlinear interaction component of deepwater spar was presented by Ma *et al.* [34]. In addition, this paper was done to investigate a formulation for two nonlinear force components called the axial divergence force and the centrifugal force. It was shown that the magnitude of these two forces components was strongly dependent on wave conditions and might be small in some circumstances but could not be neglected. As a result, the nonlinear equations for wave loading and motion were developed and solved.

Kurian *et al.* [35] had done a study on the response of the truss spar that subjected to wave only. The numerical analysis by using time domain had been done and the results were agreed well with the model test results. In this study, A MATLAB program named 'TRSPAR' was developed to determine the responses by numerical method. The nonlinear time domain numerical model performed step-by-step numerical integration of the exact large amplitude equation of motion, producing time histories of motions. The fluid forces on individual members were computed by the modified Morrison equation in which the integration of the forces was performed over the instantaneous wetted length. The total force at each time step was obtained by summing the forces on the individual members. Incident wave kinematics were calculated by using Wheeler stretching formula. This program was then applied to a prototype spar, named Marlin truss spar. The simulated results were compared with the corresponding numerical results and test measurements.

Under the same study, the effect of slowly varying drift forces on the motion characteristics of truss spar platforms was investigated. The spar was designed to have natural periods of vibration much higher than the dominant wave periods, so that there were hardly any linear forces at the natural frequencies. Due to the nature of nonlinear surface water waves, the difference frequency interactions among ocean wave components might result in low frequency wave excitation forces. Although the nonlinear low frequency wave forces were small in magnitude, the structure might experience large low frequency motions, known as slow drift motions, because the exciting frequency was closed to the natural frequency. A separate MATLAB program using quasi-static analysis was developed to predict the stiffness of mooring lines. From the results, the mooring line system showed nonlinear behavior. It was shown that the restoring force caused by positive horizontal excursion was higher than those due to negative surge motion particularly in relatively high surge motion.

A numerical investigation damping effects on coupled heave and pitch motion of an innovative deep draft multi-spar was done by Li *et al.* [36]. In this simulation, the damping was determined through the free decay tests based on a rigorous coupled hull and mooring model. The nonlinear motion equations of coupled heave and pitch considering the time-varying restoring forces was established and solved with six damping cases by using the fourth order Runge-Kutta method. The results indicated

that the heave damping significantly influences the occurrence of pitch instability, meanwhile the damping contribution of heave plates and mooring lines also played an important role. In common and even extreme weather conditions, the heave and pitch responses of the spar platform were considered small. This treatment ordinarily gave satisfied results, but seriously underestimated the pitch response when large heave motion was induced by the wave whose exciting period was near to the heave natural period. This issue was described as a Mathieu instability, which was probably triggered when pitch natural period was twice the heave natural period. In order to decrease the heave motion, two heave plates directly integrated with the hard tank were expected to excite viscous damping vertically and to attract more heave added mass to keep the heave natural period away from the wave frequency controlled area.

The dynamic analysis of a typical truss spar in frequency domain had been conducted and the motion responses in surge, heave and pitch had been evaluated by Kurian *et al.* [37]. The truss spar had been modeled as a rigid body with three degrees of freedom at its center of gravity, connected to the sea floor by ten component catenary mooring lines attached to the spar at the fairleads. The analysis had been done by choosing the suitable wave spectrum model to represent an appropriate density distribution of the sea water at the site under consideration. The prediction using frequency domain was not very accurate as it could not take the nonlinearities into account. The results of this frequency domain analysis could be useful for the preliminary design of spar and its component.

Another study of a spar using time domain analysis was done by Mekha *et al.* [38]. The inertia forces were calculated using a constant inertia coefficient ( $C_m$ ) as in the standard form of Morrison equation or using a frequency dependent  $C_m$  coefficient based on diffraction theory. The drag forces were computed using the nonlinear term of Morrison equation in both cases.

Hydrodynamic analyses of a geometric spar were performed by Wang *et al.* [39]. The analyses were done both in frequency- and time domains by considering the coupling effects of the vessel and its riser and mooring system. Based on the boundary element method, the three-dimensional panel model of the geometric spar and the related free water surface model were established, and the first-order and

second-order difference-frequency wave loads and other hydrodynamic coefficients were calculated. Frequency domain analysis of the motion Response Amplitude Operators and Quadratic Transfer Functions and time domain analysis of the response series and spectra in an extreme wave condition were conducted for the coupled system with the mooring lines and risers involved. These analyses were further validated by the physical model test results. In the frequency domain analysis, linear diffraction theory in potential flow was used to calculate the inertia force and diffraction force acting on the main body of the geometric spar, and the wave drag forces on the mooring lines and risers were solved by using the Morrison equation. The coupled motion equation of the system was discretized into the systems of algebraic equations and solved using boundary element method, thus the added mass, damping coefficients and Response Amplitude Operators (RAO) was gained. In the time domain analysis with irregular wave excitation, the excitation time series were regenerated by means of the Fast Fourier Transform, and the motion equations were solved directly by numerical integration to obtain the six degrees of freedom motions and wave force series.

TDSIM was a nonlinear time domain computer code developed for modeling the hydrodynamic responses of truss spar platforms. This code was developed by Datta *et al.* [40]. The program was based on the modified Morrison equation formulation and assumed the spar diameter to be small with respect to the wavelengths. It was designed to predict not only the six degrees of freedom large amplitude motions, velocities and accelerations, but also the hydrodynamic loads on structural members in the presence of random waves, wind and current. The comparison to the experimental results showed the accurate prediction on the motions and loads.

Another study on the dynamic behavior of spar under regular sea waves had been done by Agarwal *et al.* [41]. The hydrostatic provided the restoring force in heave, roll and pitch. The mooring lines also provided the restoring force which was represented by nonlinear horizontal springs. The wave force of the unidirectional regular wave was calculated by using Linear Airy Theory and Morrison equation. The response analysis in time domain was done in order to solve the dynamic behavior using iterative incremental Newmark Beta approach.

The dynamic response and the wave loads of a spar in unidirectional and directional seas were determined by Anam *et al.* [42]. The effects of wave directionality on the structures were very important in the design stage. The wave loads on a slender spar of slack mooring lines were computed using modified Morrison equation and the corresponding responses using the Newmark Beta method numerical scheme in the time domain. The difference in wave kinematics resulted in the differences in computed wave loads and responses of the spar, which indicated that the wave directionality might play an important role in the design of offshore structures.

A numerical investigation on the hydrodynamic performance of a new spar concept was done by Zhang *et al.* [43]. The hydrodynamic behavior both in operating and survival conditions was studied by means of numerical simulation. Basic model tests were also conducted to calibrate the numerical approach and a few aspects were highlighted which includes global performance and mooring line analysis. In this investigation, the calculation showed the long motion natural periods, which was one of the great advantages of the spar concept. This period was sufficiently outside the prevailing wave frequency range and thus heave motion was generally insignificant. Because there were resonant frequencies in the low frequency region, it was essential to filter the responses to further explore the coupled effects in different frequency regions.

## **2.4 Wave-Current Interaction on Offshore Structure**

### **2.4.1 Wave-Current Interaction**

Wave and current coexist simultaneously in the coastal region that makes them being the most important processes controlling the hydrodynamic behavior [1]. In addition, both wave and currents are normally the major environmental forces in this region [4]. Thus, the determination of the hydrodynamic loads is very important for the design stage of offshore platform [2, 3]. The existence of current in the water body causes vortex induced motions and the effect of turbulence excites the surge and sway

motions [17]. Since the last few decades, various studies on wave and current have been done due to the major effects on the design of the offshore platform [1, 3].

The occurrence of the steady current is due to the ocean circulation in the open sea [44]. While the cyclic change in lunar and solar system has caused the tidal current. Although surface currents will be the governing ones for floating structures, the current distribution as a function of depth below the surface may also be of importance for the design of a mooring system of a floating structure, the designer is especially interested in the probability that a particular extreme current velocity will be exceeded during a certain period of time. The variation in the velocity and direction of the current is very slow, and current may therefore be considered as a steady phenomenon. The contribution to the load on offshore structures from the design current is very significant [13]. Therefore, the research related to the determination of wave-current interaction is important.

The current profile observed in pure current flows is modified due to the presence of waves [1]. When waves propagate opposite the current, an increase in the current intensity is achieved near the mean water level, while a reduction is obtained from following waves and currents. The nonlinear interaction between these two processes is still not well understood and as several studies have demonstrated, can play an important role in wave dynamics, in hydrodynamics and also in sediment transport processes. In addition, when waves and currents coexist simultaneously, the steady current profile loses the algorithmic shape observed in pure conditions.

Current profile can be defined as a specified speed-depth profile [44]. The current speed is added vectorially to the wave particle speed for calculation of drag force according to Morrison equation. A possible depth profile for current is shown in Figure 2.5. The depth is specified according to a negative Z coordinate system, pointing upwards and with an origin at the mean sea surface level. It is because the wave elevation is taken into account the current speed factor should be given up to the maximum wave crest. The current is assumed to be uni-directional and the direction are specified in the same format as the wave direction.

However, there has been very little investigation of the forces that are exerted when the current presented in addition to the water [11]. Ideally, wave and current

must always be measured simultaneously since the existence of the current has changed the behavior of the current itself. From the studies, the mechanisms that may involve in the wave-current interaction includes the surface wind stress, bottom friction, wave climate, wave field, depth and current refraction, and modulation of the absolute and relative wave period [11, 12, 13].

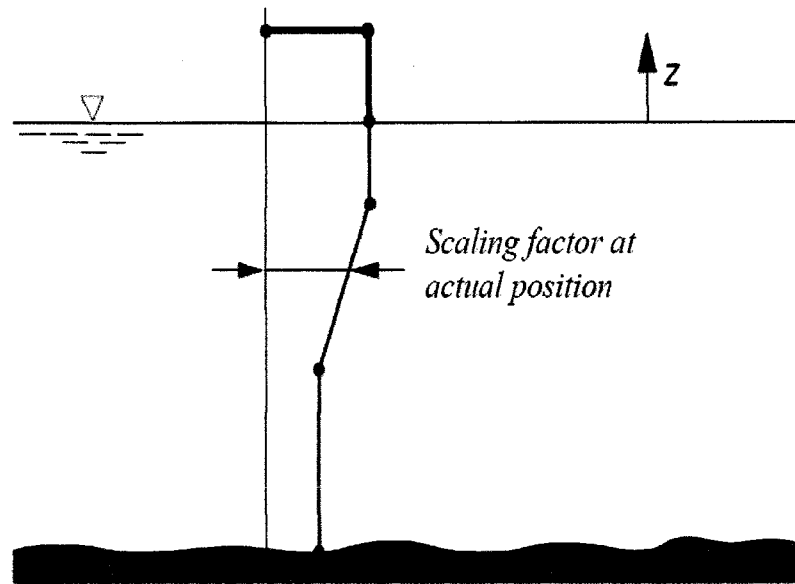


Figure 2.5: The Current Profile

#### 2.4.2 Previous Studies on Wave-Current Interaction

A study on the wave-current interaction based on different conditions according to the angle of propagation between waves and currents had been done in order to observe the effect of wave-current interaction on the mean steady current profile by Olabarrieta *et al.* [1]. The conditions were the following waves and current, the opposing waves and currents, and the perpendicular waves and currents. In the perpendicular cases, a reduction of the flow velocity was observed. While for the following cases reduction of the velocity was observed just below the wave trough level, and the intensification occurred in the opposing one. These changes became more evident as the wave height increased and as the wave period decreased.

In the different study done by Isaacson *et al.* [3], the time domain method had been used to observe the effects of a current on the radiation and the diffraction of regular waves around a two dimensional body. The result showed the importance of current or forward speed effects on a large offshore structure in waves. In general, a weak nonlinear relation with the current had been observed for the first and second order results.

The time domain and frequency domain analyses of the spar platform had been done in the presence of currents by Anam *et al.* [8]. Current might increase the static offset significantly so that the structure behavior might become nonlinear. In the presence of the current, drag force caused second order response, which could result in significantly different response from the wave case only. Moreover, current load increased the first order response slightly and decreased the third harmonic responses of the wave only case. This was because the existence of the current added to the current velocity in the drag force in Morrison equation, resulting in substantially static load as well as an added damping due to current. The change in offset from the wave-current case was noticeable. The wave-velocity appeared only in the drag force in Morrison equation, where the average current velocity is added to the horizontal wave velocity in the drag term. Therefore, the dynamic force due to drag in the presence of current was greater than for the wave-only case but still not very important for this inertia dominated nonlinear problem.

Tayfun *et al.* [12] studied the refraction of incoherent random gravity waves with currents and bottom topography resulted in spatial variations in the spectral characteristics of the free surface. A radiation transfer equation was in a simple analytic form for the case of one dimensional inhomogeneities in currents and topography. The analytic form was examined in terms of two dimensional wave numbers, polar frequency direction spectra along the associated dynamic and kinematic constraint relevant to wave breaking and reflection. The refraction of surface wave interacting with currents and underwater topography was resulting in spatial variations in their kinematic and dynamic properties.

The regular and focused wave combined with current interacting with a truss spar platform was investigated by Liu *et al.* [14]. A Time Domain Higher Order Boundary

Element Method (THOBEM) code was developed for simulating wave-current interactions with three-dimensional floating bodies. One of the important problems in offshore engineering was the slow drift motions of floating marine structures. The combined current and wave might lead to changes of wave forces, wave run-up, and slow drift motions. Therefore, it was a great importance to predict the slow drift motions generated by the resonance between the wave current and the floating structures, which might involve very large horizontal excursions. Wave-body interaction problems were solved by frequency and time domain methods, numerical results were compared with experimental results and other numerical results to validate the numerical methods. It was well known that the overall patterns of the wave-current diffraction and radiation by a three-dimensional floating structure were different from those of the pure wave action. The result of this study stated that the numerical results of wave force, wave run-up and body response were all in a close agreement with those obtained by frequency domain methods.

The wave force on a slender structure was explained by Journee *et al.* [45]. A slender cylinder in this discussion implied that its diameter was small relative to the wave length. The cylinder diameter should be much less than the wave length. Derivations were done for a unit length of cylinder. Force relationships would yield the force per unit length. This relationship should then be integrated over the cylinder length to yield a total force. The determination of  $Cd$  and  $Cm$  could be done by using Morrison Method, Fourier Series Approach, Least Squares Method, Weighted Least Squares Method and Alternative approach. It was generally accepted practice to vectorially superpose the current velocity on the velocity resulting from the waves before calculating the drag force. The current had no effect at all on the accelerations so that the inertia force is unchanged by the current.

Based on the potential flow theory, linear waves and small current velocity approximation, a numerical approach for wave-current interaction around a large structure was investigated by Lin *et al.* [46]. The velocity potential in a wave current coexisting field was separated into two parts which were steady current potential and an unsteady wave potential. The water surface elevation around a large structure in a wave-current coexisting field could then be obtained by substituting both unsteady wave potential and current velocity into the first-order dynamic surface boundary

condition. Changes of wave height in the down-wave behind a large structure were more significant than those in the up-wave region due to the effect of current. In the down-wave region, the wave height in the outflow side was larger than the case of zero current and increased with increasing current magnitude, whereas, the opposite was true in the inflow side. For a fixed current velocity, in the down-wave region behind a cylinder, the wave height decreased with an increase in the angle between wave and current, whereas an opposite trend could be detected in the up-wave region.

Noorzaei *et al.* [47] described the analytical and numerical methods adopted in developing a program for modeling wave and current forces on slender offshore structural members. Two common wave theories had been implemented in the present study, namely Linear Airy Theory and Stokes' fifth order theory, based on their attractiveness for engineering use. The program was able to consider wind drift and tidal currents by simply adding the current velocity to the water velocity caused by the waves. Morrison equation was used for converting the velocity and acceleration terms into resultant forces and was extended to consider arbitrary orientations of the structural members. Furthermore, this program had been coupled to a three-dimensional finite element code, which could analyze any offshore structure consisting of slender members. For calibration and for comparison purposes, the developed programs were checked against a commercial software package called Structural Analysis Computer System (SACS).

Another study had been done by Chandler *et al.* [48] for combined wave and current on a horizontal cylinder. The purposes of the present study were to investigate the interaction that occurs between known wave pattern and current, to determine the effects that this interaction had upon the hydrodynamic loading on a submerged, horizontal circular cylinder and to relate the changes in loading to the detected flow pattern around the cylinder. Comparisons with measured data showed that linear theory and the stream function theory satisfactorily described the wave motion for the conditions investigated, and that velocity superposition could be used with either of these theories to describe conditions involving waves plus currents, with reasonable accuracy.

Arena *et al.* [49] investigated the Morrison force on a slender vertical cylinder, produced by random wave groups with large waves, either in an undisturbed wave field or for waves superimposed on a uniform current. For this purpose Boccotti's Quasi-Determinism theory was extended to wave-current interaction. Thus, assuming that a very large wave occurred at some fixed time and location for a fixed value of current velocity, the analytical expressions of the free-surface displacement and of the velocity potential were obtained. Finally, it was found that the maximum wave force given by the New Wave model, which was suggested by the API recommendations for the calculation of wave forces of sea waves on a structure, tend to underestimate the maximum total force given by the Quasi-Determinism theory.

In the study on the effects of the wave-current interaction on large volume structure by Zhao *et al.* [50], the fluid motion was incompressible and the effect of flow separation was neglected. The structure was free to oscillate harmonically in six degrees of freedom. It was not easy to consider the effect of current only. In addition, Doppler shift would not be sufficient to explain the results as the local and steady flow around a cylinder was taken into account. This study indicated that the flow would not separate around bodies without sharp edges if the  $KC$  number was low and the current velocity was smaller than the amplitude of the horizontal wave velocity component at the free surface. If the flow was not separating in combined wave and current, it would be incorrect to add current forces in still water to predict mean second-order forces.

The current effects on extreme response value statistics of offshore structures subjected to wave and current had been studied by Taniguchi *et al.* [51]. This study considered the nonlinearities arising from hydrodynamic drag forces and wave-current-structure interaction. Some analytical results showed that the presence of current had great influence on the structural response statistics comparing with those statistics in the absence of current. Therefore, incorporating wave-current-structure response was essential. The contribution of current velocity to the structural response statistics was examined by reliability analysis approach. The interests in these effects on the response properties of offshore structures had been highlighted. The positive current lowered the wave spectrum amplitude. This was because positive current tend to lengthen the waves and to gentle the wave amplitude thus reducing the energy level

of the waves. Therefore, the high frequency waves were eliminated as compared with that in the absence of current. On the contrary, adverse current shortened the waves, steepened the wave forms and feed energy into the wave system, therefore the surface wave spectrum increased in magnitude. During gathering high frequency waves, some waves dissipated due to cutoff frequency during energy feeding. The inclusion of wave-current-structure interaction was essential to evaluate them.

A study on the interaction between steady non-uniform currents and gravity waves with applications for current measurement had been done by Huang *et al.* [52]. This study showed that the magnitude and the location of the energy peak in the spectrum were altered. The influence of current would be predominant at the higher wave number range. The current conditions changed the surface slope pattern drastically. This phenomenon was studied by use of Philips' equilibrium range spectrum in wave number space. When the waves propagated into a region with current, the energy contained in that particular frequency band would change through interchange of energy between waves and current. Explanation on the energy spectra and cutoff frequency of the negative current equation was due to the wave breaking phenomenon. In addition, the energy density at a frequency higher than this cutoff point was much lower than would be the case without current.

In general, waves did not propagate on quiescent water but travel on currents driven by the tidal forces of the sun and moon, by earth's gravity or by the wind. If the current was positive then the transformations experienced by random waves as they encounter the current were relatively straight forward to predict. However, for negative current, one which opposed the waves, the effects were more complex, owing to the enhanced level of wave breaking induced by the current as stated by Hedges *et al.* [53]. In general, as waves propagated onto an opposing current they tend to shorten and increase in height. Frequency cutoff spectral density of free surface displacement would become infinity, the energy of the particular component waves could not propagate onto the current and wave breaking would occur at the current boundary. Halkyard [18] stated that the existence of the opposing current might affected the heave and pitch response greatly.

A mathematical modeling of wave-current interaction in a hydrodynamic laboratory basin was studied by Margaretha [54]. In this study, the surface wave on a layer of fluid when a current existing in the layer was investigated. A low dimensional model using clearly interpretable variables was studied. The natural variables to describe the wave were the wave frequency, the wave length, the wave amplitude and the mean-free surface elevation.

The studies on the wave-current interaction were not limited for the deepwater only. Some studies on wave-current interaction also had been done in the Southern North Sea by Osuna *et al.* [55] and in the River Pearl Estuary by Wang *et al.* [4]. At the Southern North Sea, it was observed that along the Belgian coast, the current induced by the radiation stress was as same as the excess current obtained by a wave-dependant sea surface stress and highly controlled by bathymetric features. At the River Pearl Estuary, the study found that waves propagating from the open sea would be attenuated significantly when they enter into the estuary, with their energy dissipating due to the sheltering by islands and the shallow water depth in it. The tidal flow increased the wave heights generally. In addition to that, the effect of the ebbing flow on waves was also significant. The incoming wave from the south had a great influence on the flow and mass transport in the estuary.

Instead of deepwater structure, some studies had been done on the wave-current interaction on the shore structures by Johnson *et al.* [56]. A proper understanding of the effect of submerged breakwaters on near shore waves and currents was necessary for the calculation of sediment transport and morphological evolution in the vicinity of such structures. This was important in order to achieve a good functional design of the submerged structure for coastal protection. These structures resulted primarily in wave energy dissipation through the physical mechanisms of wave breaking and friction. The energy dissipation resulted in gradients in wave radiation stresses, which drove the mean flow pattern and wave setup.

## **2.5 Summary of Literature**

1. In line with the global development, the oil and gas industry has expanded in Malaysia. Malaysia has more than 400 offshore structures, and today Malaysia has successfully installed its first deepwater floating structure which is Kikeh Spar. Kikeh Spar is located at Sabah Sea with 1,300 m water depth. The deepwater development is growing rapidly in Malaysia as the oil exploration is now more focusing in deepwater region.
2. The hydrodynamic analysis was studied by many researchers. Many methods were implemented in order to predict and determine the dynamic responses of the offshore structures. The frequency domain and time domain analysis were widely used by many researchers. However, for a special case, a diffraction analysis was done for a structure which having diameter exceeds 0.2 of the wave length of the incident wave. The wave particle characteristics can be determined by using Linear Airy Theory while the wave forces can be calculated by using Morrison equation. Besides, many model tests were done in order to understand the behavior of the structure in a small scale. However, the information on the behavior of the spar structure is still limited.
3. The wave and current coexisted simultaneously in the open sea. The existence of the current had changed the behavior of the wave. There was not much study on the wave-current interaction especially in Malaysian offshore regions. Thus, this showed that the study on the wave-current interaction is very essential. The prediction of this interaction is very important especially in the design stage of the structures. The understanding on this interaction can highly contribute to the development of this industry in Malaysia.

## **2.6 The Need for Research**

Nowadays, the deepwater development is growing rapidly in Malaysia water. It is believed that this research study will establish the following:

1. The understanding of wave-current interaction in Malaysian offshore regions.

2. The understanding of the offshore spar platform responses when subjected to wave and current.
3. The importance of doing model tests in order to get accurate results.
4. The importance of doing simulation analysis in order to validate the numerical analysis and model test results.
5. The use of the model tests data for consultancy purpose as a primary information for the design stage of the spar platforms in Malaysian offshore regions.
6. The need to develop our technology so that we can analyze, design, and maintain spar and other deepwater structures.
7. The need for the development of wave-current interaction as an essential technology to be developed for our Malaysian offshore regions.

CHAPTER 3  
METHODOLOGY

**3.1 Chapter Overview**

The methodology is briefly explained below and the research activity flow chart is shown in Figure 3.1:

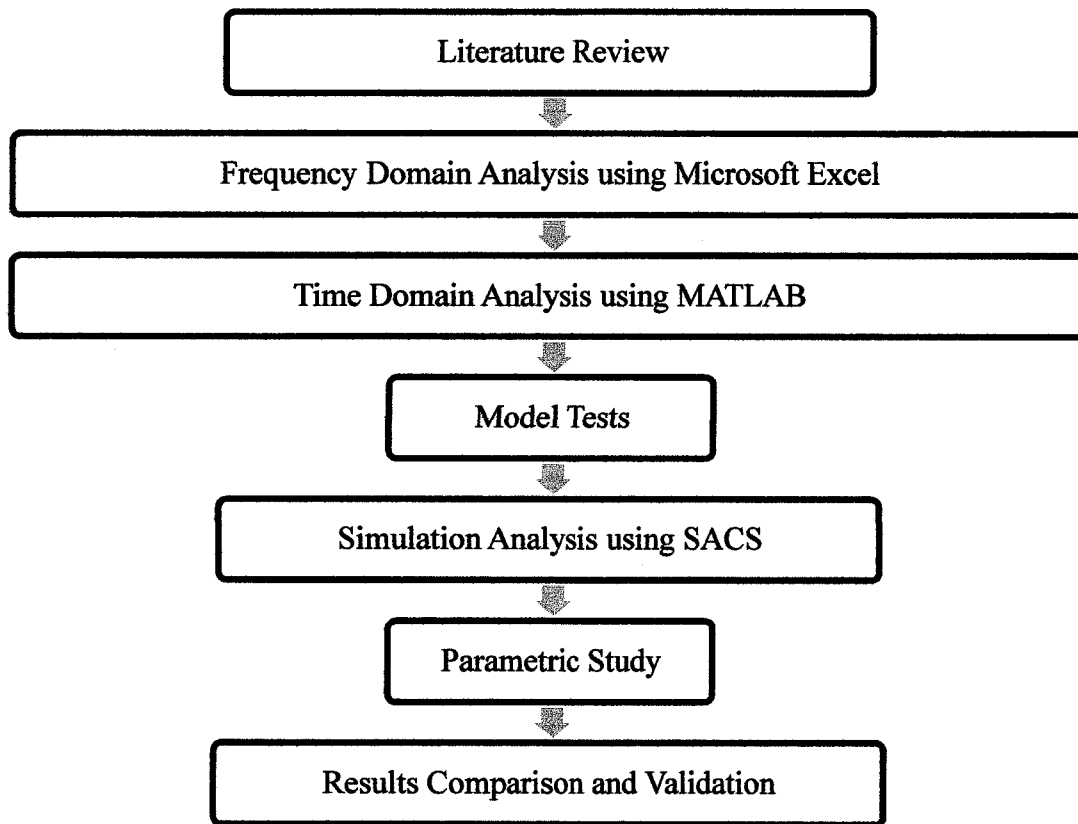


Figure 3.1: Research Activities

As mentioned in the previous chapter, the purpose of this study is to investigate the dynamic behavior of classic and truss spars subjected to wave and current. This study focused on two typical types of spar platforms which are classic spar and truss spar. There are three steps that had been implemented in this study which were numerical

analysis, model tests, and simulation analysis using commercial software. The numerical dynamic analysis including the frequency domain and time domain analyses on both spars were conducted and the motion responses in surge, heave, and pitch had been evaluated. The model tests had been done for both spar models. In this model test, the dynamic responses of the models had been observed and evaluated. The environmental data were taken from the Metocean data for Malaysian offshore regions. There were series of regular wave, random wave, and currents for the model test. For validation, a linear wave diffraction analysis using commercial software called SACS had been done in order to determine the dynamic responses of both structures. All of the results were compared and evaluated for validation. A parametric study was done for current velocities and types of spars to determine the effect of these parameters to the structural responses.

### **3.2 Six Degrees of Freedom (6 DOF)**

A structure which free to move in wave is assumed rigid and experience six independent degrees of motion consists of three translational and three rotational motions. Often, the structure is strictly to move and has fewer degrees of freedom due to the moving constraint caused by the mooring line or other mechanical connection that attached to the seafloor. Assuming a suitable coordinate system, OXYZ, at the center of gravity of the structure the translational motions are described as motions along the axes. The longitudinal motion along X is termed as surge, the transverse motion along Z is sway, and the vertical motion along Y is heave. The angular motion is defined as motions about three axes X, Y, and Z. The angular motion about Z is pitch, about X is roll, and about vertical axis Y is yaw. These motions are schematically shown in Figure 3.2.

### **3.3 Frequency Domain Analysis**

Frequency domain analysis is performed for the simplified solution and it is useful for long term response prediction. It is simpler to interpret and always been used in the preliminary design stage. Moreover, it can estimate responses due to a random wave

input through spectral formulations. Still, the limitation of this analysis is all nonlinearities in the equation of motion must be replaced by linear approximations.

Frequency domain analysis is inherently linear, and in order to apply the approach to a nonlinear problem, all nonlinearities must be linearized [5]. Due to the approximations made, the linearized frequency domain approach cannot be expected to match the nonlinear time domain method exactly, and the expected degree of accuracy is not as well established due to the limited literature on the topic.

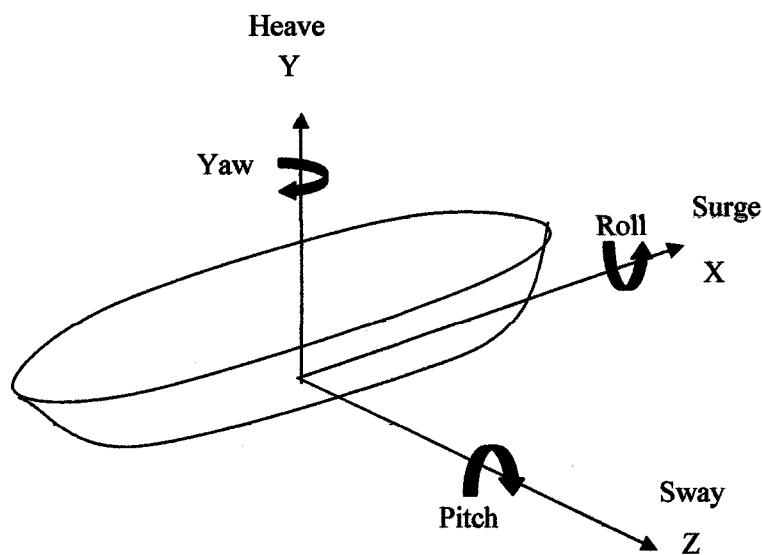


Figure 3.2: Definition of 6 DOF for Floating Structure

### 3.3.1 Linear Airy Theory

In this study, the corresponding horizontal and vertical components of wave particle velocity and acceleration could be determined by using linear wave theory, with the inclusion of the wave height and wave period chosen according to the location of the structure. The waves were propagating in the direction of the positive X axis. The kinematics of the wave water was determined by Equations 3.1 – 3.4:

Horizontal water particle velocity:

$$u = \frac{\pi H \cosh ks}{T \sinh kd} \cos \theta \quad (3.1)$$

Vertical water particle velocity:

$$v = \frac{\pi H \sinh ks}{T \sinh kd} \sin \theta \quad (3.2)$$

Horizontal water particle acceleration:

$$\dot{u} = \frac{2\pi^2 H \cosh ks}{T^2 \sinh kd} \sin \theta \quad (3.3)$$

Vertical water particle acceleration:

$$\dot{v} = -\frac{2\pi^2 H \sinh ks}{T^2 \sinh kd} \cos \theta \quad (3.4)$$

In which  $s = y + d$ ,  $\theta = kx - \omega t$ , wave number  $k = \frac{2\pi}{L}$ , natural frequency  $\omega = \frac{2\pi}{T}$ ,  $T$  was wave period,  $y$  was height of the point of evaluation of water particle kinematics,  $x$  was point of evaluation of water particle kinematics from the origin in the horizontal direction,  $t$  was time instant at which water particle kinematics was evaluated,  $L$  was wave length,  $H$  was wave height, and  $d$  was water depth. Figure 3.3 shows the definitions of wave parameters.

In the study of the offshore hydromechanics, the computation of the wave and current has to be done at the same time and not separately [44]. Otherwise, the quadratic drag force will be underestimated. The calculation of the drag force is done after the current and the wave velocities are vectorially superposed. Consequently, the current do not contribute to the inertia force. In addition, all the hydrodynamic velocity components have to be superposed before force computation.

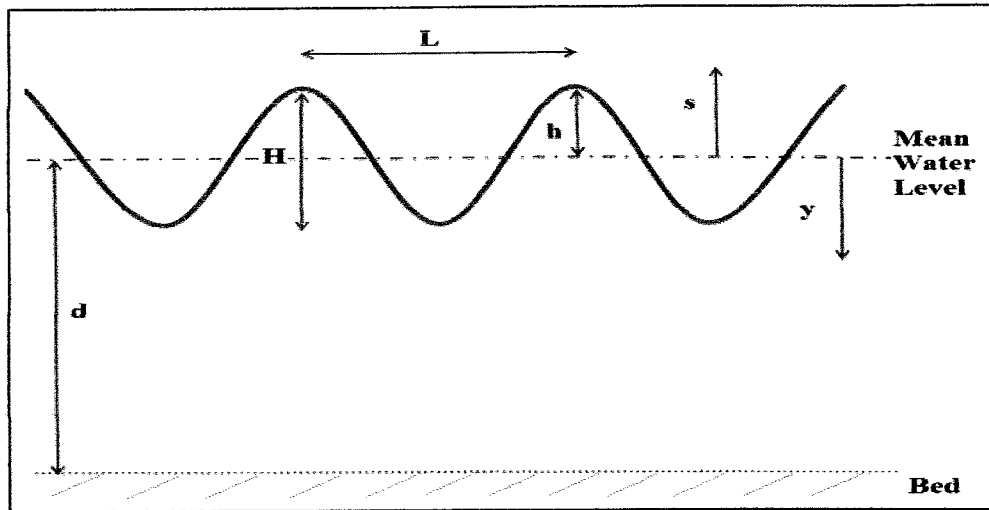


Figure 3.3: Wave Parameters

### 3.3.2 Morrison Equation

One of the primary tasks in the design of the structure includes the computation of the water wave forces on an offshore structure. It is also one of the difficult tasks since it involves the complexity of the interaction waves with the structure. There is a large variety of offshore structures such as the piled jacket type of platform, large volume gravity platforms, tension-legged platform, semisubmersibles, and arctic structures. Different formulations for wave forces are applicable and it is based on the type and size of the members of offshore structure.

Offshore structures may be exposed to various kinds of loads, such as gravity and hydrostatic pressure, and environmental loads caused by waves, currents, wind, and finally some accidental loads such as earthquake, collision or fire [57]. For most offshore structures, the combination of wave and current will constitute the most important part of the total loading. When water moves relatively to a submerged body, there will be created forces on the body. These may be of several types. Some of those may be simple to envision and analyze, but others may be elusive. One of the formulations for wave forces that can be used is Morrison equation. The Morrison equation assumes the force to be composed of inertia and drag forces. It is applicable when the drag force is significant. This is usually the case when a structure is small compared to the water wave length.

The Morrison equation states that the fluid force is a superposition of a term in phase with the acceleration of the flow which is inertia, and a term whose dominant component is in phase with the velocity of the flow which is drag [58]. It accounts for some flow nonlinearity, by way of the drag term. There are several important outstanding issues that are not considered which are free surface effects, run-up, drawdown, impact of slamming, negative damping, the interaction of vortex shedding and structural vibration, and also forces on members at an angle to the oncoming flow parallel to the free surface. It is convenient to think about the hydrodynamic loading in terms of flow processes. Multiple processes such as wind-generated waves, remote swell, current, and structural motion are active simultaneously, and their nonlinear interaction results in the fluid force on the structure.

In ocean engineering, the flow that past a circular cylinder is a canonical problem. For purely inviscid steady flow, the force on a body is zero while for the unsteady inviscid flow, the added mass effects must be considered [59]. For unsteady viscous flow, the resulting force can be determined using Morrison equation. In order to estimate the wave forces on a fixed structure, the appropriate wave theory has to be selected. Then, the mass coefficient ( $C_m$ ) and drag coefficient ( $C_d$ ) based on the Reynold's number and other factor have to be selected. Lastly, the Morrison equation can be applied to get the total forces exerted on the structures. For a vertical cylinder subjected to a current with horizontal velocity, the total force is calculated by integrating the force acting on a small section of the cylinder at each depth.

In this study, by combining the inertia and drag component of force, the Morrison equation was written as Equation 3.5.

$$f = f_D + f_I \quad (3.5)$$

In which  $f$  was total force per unit length,  $f_D$  was drag force per unit length, and  $f_I$  was inertia forces per unit length.

The principle involved in the concept of the inertia force was that a water particle moving in a wave carries a momentum with it. As the water particle passed around the circular cylinder, it accelerated and then decelerated. This required that work to

be done through the application of a force on the cylinder to increase this momentum. The incremental force on a small segment of a cylinder,  $\partial s$ , needed to accomplish this was proportional to the water particle acceleration at the center of the cylinder. The inertia force was written as Equation 3.6.

$$\partial f_I = \rho C_M \frac{\pi D^2}{4} \dot{U} \partial s \quad (3.6)$$

In which  $\partial f_I$  was inertia force on the segment  $\partial s$  of the vertical cylinder,  $\rho$  was a mass density of sea water,  $D$  was cylinder diameter,  $\dot{U}$  was local water particle acceleration at the center line of the cylinder, and  $C_M$  was inertia coefficient.

The principle cause of the drag force component was the existence of a wake region on the downstream side of the cylinder. A pressure differential was created by the wake between the upstream and downstream of the cylinder at the given instant of time due to the low pressure at the wake region compared to the pressure on the upstream side. The downstream side of the cylinder reversed every half cycle and a mirror image was created after half a cycle. This was due to the water particle motion under a wave was oscillatory within a given wave period. The pressure differential caused a force to be exerted in the direction of the instantaneous water particle velocity. The drag force was written as Equation 3.7.

$$\partial f_D = \rho C_D \frac{D}{2} |U| U \partial s \quad (3.7)$$

In which  $\partial f_D$  was drag force on the segment  $\partial s$  of the vertical cylinder,  $U$  was local water particle acceleration at the center line of the cylinder, and  $C_D$  was drag coefficient.

### 3.3.3 Wave Spectrum- JONSWAP Spectrum

The mathematical spectrum models are generally based on one or more parameters such as significant wave height, wave period, and shape factors. In this study, the

JONSWAP spectrum was implemented and the approximate expression for the JONSWAP spectrum in terms of  $H_s$  and  $\omega_0$  was written as Equation 3.8:

$$S(f) = \alpha^* H_s^2 f_0^4 f^{-5} \exp \left[ -1.25 \left( \frac{f}{f_0} \right)^{-4} \right] * \gamma^{\exp [-(f-f_0)^2(2\tau^2 f_0^2)]} \quad (3.8)$$

In which  $f_0 = \omega_0 / 2\pi$ , and  $\omega_0^2 = 0.161 g / H_s$ .

### 3.3.4 Wave Current Modified Spectrum

In deep water, the presence of current alters the form of the wave profile and also the wave spectrum. The new form of the wave-current modified spectrum were used and could be obtained as Equation 3.9:

$$S^*(\omega) = \frac{S(\omega)}{[1 + (1 + \frac{U\omega}{g})^{1/2}][1 + (\frac{U\omega}{g})^{1/2} + (1 + \frac{U\omega}{g})]} \quad (3.9)$$

In which  $S(\omega)$  was the wave spectrum without the current.

When the current was superimposed on waves and drag was not negligible compared to inertia, then the relationship between the wave force and wave profile was further complicated by the presence of current,  $Uc$ . If the current was considered uniform and in the direction of the wave, then the drag force per unit length of a vertical cylinder might be written in terms of the relative velocity between current and wave-particle velocity as:

$$f_D(t) = \rho C_D \frac{D}{2} [|U(t) + Uc|][U(t) + Uc] \quad (3.10)$$

### 3.3.5 Simulation of Wave Profile from Spectra

In this study, the height of the wave was calculated at a particular frequency from an energy density spectrum curve. At frequency,  $f_1$ , the energy density was  $S(f_1)$ . The wave height at this frequency was obtained as Equation 3.11.

$$H(f_1) = 2\sqrt{2S(f_1)\Delta f} \quad (3.11)$$

Then, for a given horizontal coordinate,  $x$ , which was the location at which the wave profile was desired, and time,  $t$ , which was incremented, the wave profile was computed from of Equation 3.12.

$$n(x, t) = \sum_{n=1}^N \frac{H(n)}{2} \cos[k(n)x - 2\pi f(n)t - \varepsilon(n)] \quad (3.12)$$

In which  $k(n) = 2\pi/L(n)$  and  $L(n)$  corresponds to the wave length for the  $n$ th frequency,  $f(n)$ . The quantity,  $N$ , was the total number of frequency bands of width,  $\Delta f$ , dividing the total energy density. Sometimes,  $f(n)$  was chosen randomly within each  $\Delta f$  for more randomness.

### 3.3.6 Motion Response Spectrum

The Response Amplitude Operator (RAO) values were based on the forces acting on the structures, the total mass, the stiffness and the damping coefficient. The RAO was calculated for both random and regular wave which could be expressed as Equation 3.13.

$$RAO = \frac{\left(\frac{F_I}{H/2}\right)}{\sqrt{(k-m\omega^2)^2 + (C\omega)^2}} \quad (3.13)$$

in which  $F$  was the inertia forces acting on the body,  $H$  was the wave height,  $K$  was the stiffness of the structures,  $m$  was the total mass of the submerged body and  $C$  was the damping coefficient.

### 3.4 Time Domain Analysis

To assess the structural integrity of offshore installation at the design stage, the environment loads and structural responses must be calculated and evaluated. Both

the static and dynamic response of a structure can be reasonably predicted at the design stage. To determine the dynamic behavior of an offshore structure, it is important to acquire realistic data on environmental conditions such as wave, wind, current, and earthquake to properly account for them in the calculations. Time domain analysis utilizes the direct numerical integration of the equations of motion allowing the inclusion of all system nonlinearities which are nonlinear fluid drag force, nonlinear mooring line force, and nonlinear viscous damping. The time domain analysis is inherently more stable than the frequency domain and it takes the nonlinear factor into consideration [5]. It is the most efficient dynamic analysis for solving the equation of motion by integrating in time the Newmark Beta Method. However, this analysis increases computer time and difficult to interpret and apply. The MATLAB software was used to solve the time domain analysis. The results were directly obtained in the output of the analysis.

### 3.4.1 Equation of Motion

The dynamic approach took into account the dynamic effects of inertia force and wave force, the force components of incoming and diffraction waves, and those due to the motion of the structure. The dynamic responses of an offshore platform might be determined by using a lumped mass mathematical model with viscous damping, linearized soil spring, and a hydrodynamic force function. The nonlinear equation of motion in matrix form for multi-degree of freedom was expressed as Equation 3.14.

$$[M]\{\ddot{x}\} + [C]\{\dot{x}\} + [K]\{x\} = \{F(t, x, \dot{x}, \ddot{x})\} \quad (3.14)$$

where,  $M$  was the total mass matrix of the platform,  $C$  was the total damping matrix of the platform,  $K$  was the stiffness matrix and the  $x$ ,  $\dot{x}$ , and  $\ddot{x}$  were the displacement, velocity and acceleration of the platform respectively. The triangular consistent mass matrix (5), diagonal in nature, was given by Equation 3.15.

$$[M] = \begin{bmatrix} M_{11} + M_{11} & 0 & 0 & 0 & 0 & 0 \\ 0 & M_{22} & 0 & 0 & 0 & 0 \\ 0 & 0 & M_{33} + M_{33} & 0 & 0 & 0 \\ 0 & 0 & 0 & M_{44} & 0 & 0 \\ M_{a51} & 0 & M_{a53} & 0 & M_{55} & 0 \\ 0 & 0 & 0 & 0 & 0 & M_{66} \end{bmatrix} \quad (3.15)$$

where,  $M_{11} = M_{22} = M_{33} = M$

$M$  was the total mass of the entire structure

$M_{44}$  was the total mass moment of inertia about x-axis =  $M_{r_x^2}$

$M_{55}$  was the total mass moment of inertia about y-axis =  $M_{r_y^2}$

$M_{66}$  was the total mass moment of inertia about z-axis =  $M_{r_z^2}$

$r_x$  was the radius of gyration about x-axis,

$r_y$  was the radius of gyration about y-axis, and

$r_z$  was the radius of gyration about z-axis,

The added mass terms of Equation 3.14 were given by Equations 3.16 and 3.17.

$$M_{a11} = 0.25\pi D^2 [C_m - 1] \rho a_{surge} \quad (3.16)$$

$$M_{a33} = 0.25\pi D^2 [C_m - 1] \rho a_{heave} \quad (3.17)$$

where  $D$  was the column diameter,  $\rho$  was the water density,  $M_{a51}$  was the added mass moment of inertia in the pitch degree of freedom due to hydrodynamic force in the surge direction and  $M_{a51}$  was the added mass moment of inertia in the pitch degree of freedom due to hydrodynamic force in the heave direction. The presence of off-diagonal terms in the mass matrix indicated a contribution in the added mass due to the hydrodynamic loading. The loading was effective only in the surge, heave, and pitch degrees of freedom due to the unidirectional wave and current acting in the surge direction on a symmetric configuration of the platform about the X and Z axes.

The damping matrix  $C$  was derived using the Equation 3.18.

$$\phi^T [C] \phi = [2\vartheta m_i \omega_i] \quad (3.18)$$

where, damping ratio  $\vartheta$  was taken as 0.1 and  $\omega_i$  represented the natural frequency. The stiffness matrix  $K$  was given by Equation 3.19.

$$[K] = \begin{bmatrix} K_{11} & 0 & 0 & 0 & 0 & 0 \\ 0 & K_{22} & 0 & 0 & 0 & 0 \\ K_{31} & K_{32} & K_{33} & K_{34} & K_{35} & K_{36} \\ 0 & K_{42} & 0 & K_{44} & 0 & 0 \\ K_{51} & 0 & 0 & 0 & K_{55} & 0 \\ 0 & 0 & 0 & 0 & 0 & K_{66} \end{bmatrix} \quad (3.19)$$

The sources of dynamic loading considered in this study consisted of hydrodynamic loading due to random wave. This hydrodynamic loading was generated by assuming JONSWAP spectrum for a given significant wave height and average zero-crossing wave period. The method involved generation of time histories of sea surface elevation, water particle velocity and acceleration. With the help of these time histories, drag and inertia forces on spar hull were determined. The force per unit length at the  $i$ th location of the cylinders was given by Equation 3.20.

$$F(t)_i = C_{mi}A_I(a_{wi} - a_s) + A_I a_s + C_{Di}A_D|u_{wi} - u_s|u_{wi} - u_s \quad (3.20)$$

where  $F(t)_i$  was the wave force per unit length of the cylinder,  $u_{wi}$  and  $a_{wi}$  were the wave particle velocity and acceleration at the particular position respectively given in Equations 3.21 and 3.22, while  $u_s$  and  $a_s$  were the structure velocity and acceleration respectively. Inertia and drag coefficient were given by  $C_{mi}$  and  $C_{Di}$ , where  $i$  term represented the specific element of the cylinder.

$$u_{wi} = \frac{\pi H \cosh ks}{T \sinh kd} \cos(kx - \omega_f t) \quad (3.21)$$

$$a_{wi} = \frac{2\pi^2 H \cosh ks}{T^2 \sinh kd} \sin(kx - \omega_f t) \quad (3.22)$$

where  $T$  was the period,  $H$  was the wave height,  $k$  was the wave number,  $\omega_f$  was wave frequency, and  $d$  was the water depth. The symbol  $s$  represented the distance

from seabed that varied in the column elements while  $x$  was X coordinate with respect to center of gravity.  $A_I = \rho\pi D^2/4$  and  $A_D = \rho D/2$ .

### 3.4.2 Newmark Beta Integration Method

In order to solve the nonlinear equation of motion, the Newmark Beta Integration Method was used. During the past 40 years, the Newmark's method had been applied to the dynamic analysis of many practical engineering structures. The numerical integration methods considered the solution of the linear dynamic equilibrium written in the following form:

$$[M]\{\ddot{x}\} + [C]\{\dot{x}\} + [K]\{x\} = \{F(t, x, \dot{x}, \ddot{x})\} \quad (3.23)$$

The direct use of Taylor's Series provides a rigorous approach to obtain the following two additional equations:

$$u_t = u_{t-\Delta t} + \Delta t \dot{u}_{t-\Delta t} + \frac{\Delta t^2}{2} \ddot{u}_{t-\Delta t} + \frac{\Delta t^3}{6} \dddot{u}_{t-\Delta t} + \dots \quad (3.24)$$

$$\dot{u}_t = \dot{u}_{t-\Delta t} + \Delta t \ddot{u}_{t-\Delta t} + \frac{\Delta t^2}{2} \dddot{u}_{t-\Delta t} + \dots \quad (3.25)$$

These equations were truncated and expressed them in the following form:

$$u_t = u_{t-\Delta t} + \Delta t \dot{u}_{t-\Delta t} + \frac{\Delta t^2}{2} \ddot{u}_{t-\Delta t} + \beta \Delta t^3 \ddot{u} \quad (3.26)$$

$$\dot{u}_t = \dot{u}_{t-\Delta t} + \Delta t \ddot{u}_{t-\Delta t} + \gamma \Delta t^2 \ddot{u} \quad (3.27)$$

The acceleration was assumed to be linear within the time step, the following equation could be written:

$$\ddot{u} = \frac{(\ddot{u}_t - \ddot{u}_{t-\Delta t})}{\Delta t} \quad (3.28)$$

The substitution of the Equation 3.28 into Equations 3.26 and 3.27 produced Newmark's equations in standard form:

$$u_t = u_{t-\Delta t} + \Delta t \dot{u}_{t-\Delta t} + \left(\frac{1}{2} - \beta\right) \Delta t^2 \ddot{u}_{t-\Delta t} + \beta \Delta t^2 \ddot{u}_t \quad (3.29)$$

$$\dot{u}_t = \dot{u}_{t-\Delta t} + (1 - \gamma) \Delta t \ddot{u}_{t-\Delta t} + \gamma \Delta t^2 \ddot{u}_t \quad (3.30)$$

Equations 3.29, 3.30, and 3.23 was used iteratively, for each time step, for each displacement DOF of the structural system. The term  $\ddot{u}_t$  was obtained from Equation 3.23 by dividing the equation by the mass associated with the DOF.

### 3.5 Model Tests

The models had been designed as rigid bodies connected to the sea floor by multi-component catenaries mooring lines. Both regular wave and random wave model spectrum were used for computing the incident wave kinematics and for computing the wave forces. The metocean data in Malaysia were used to determine the model test environmental data. Two typical classic and truss spars were selected and analyzed. Figures 3.4 and 3.5 show the classic and truss spar models respectively. The purpose of this study was to gain general understanding of classic and truss spars responses subjected to random and regular waves combined with current using dynamic analysis approach.

#### 3.5.1 Modeling Law

The geometry of the floating structure was scaled dimensionally according to the scale factor. In this study, both classic and truss spars models were designed and fabricated by using 1:100 scale factor. All the dynamic properties, such as displacement, moment of inertia, and natural periods were properly scaled using Froude's law. The structural properties such as elasticity were not necessary to scale. Even at a small scale, this scaling could provide reasonable results. Many of the details which include appendages and small members, however, were often omitted. The Froude scaling of structure and hydrodynamic parameters used for the spars seakeeping tests are included in Table 3.1 and a correction factor for the density of seawater,  $S=1.01\text{kg/m}^3$  had been applied in the scale factor when needed.

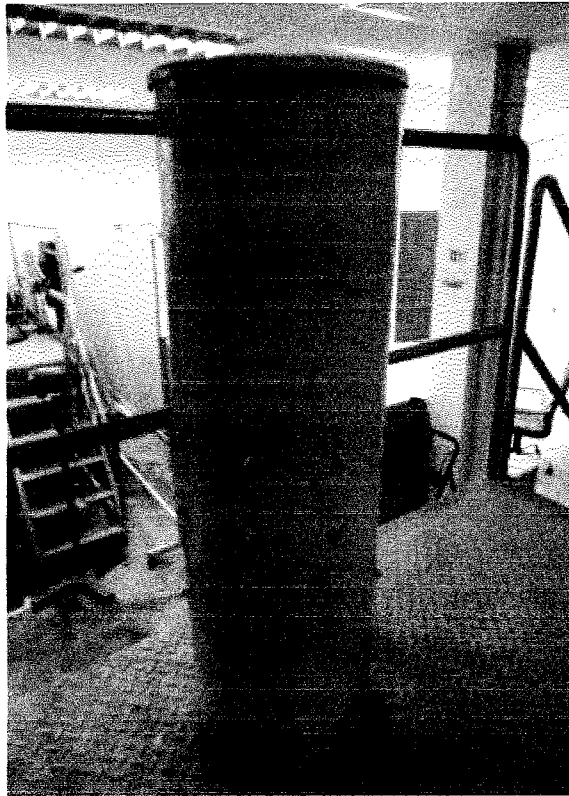


Figure 3.4: Classic Spar Model

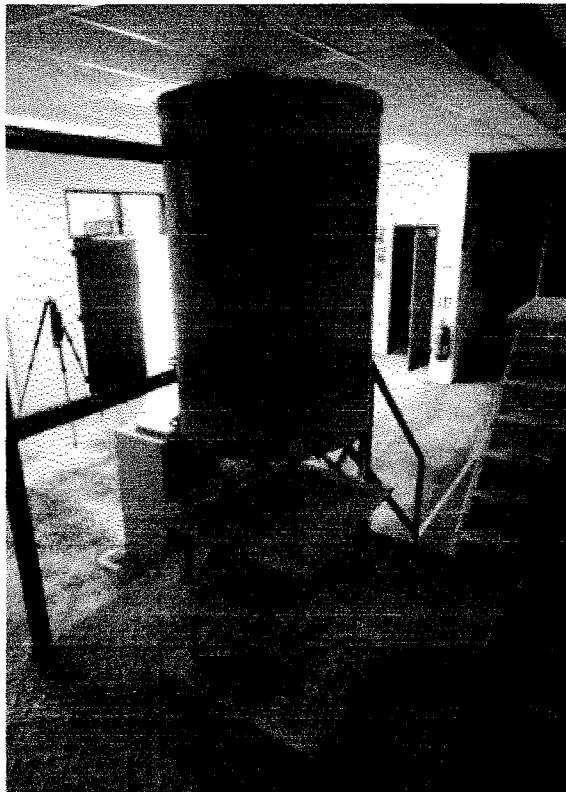


Figure 3.5: Truss Spar Model

Table 3.1: The Froude Scaling

Parameters	Scale Factor	Scaling Ratio for Scale Factor of 100
Length	$\lambda$	100
Time	$\lambda^{1/2}$	10
Velocity	$\lambda^{1/2}$	10
Acceleration	$\lambda^0$	1
Area	$\lambda^2$	10000
Volume	$\lambda^3$	1000000
Force	$S\lambda^3$	1010000
Mass	$S\lambda^3$	1010000
Angular Acceleration	$\lambda^0$	1
Spring Constant	$\lambda^2$	10000
Spectral Density	$\lambda^{5/2}$	100000

### 3.5.2 Prototype Description

The classic and truss spars model dimensions are shown in Figures 3.6 and 3.7 respectively. Both models were used for this study. The models were designed by adopting a scale ratio of 1:100 and were fabricated by using galvanized steel. The lower part of the spar was ballasted with water. The hull diameter was 300 mm for the classic spar while for the truss spar the hull diameter and length were 300 mm and 420 mm respectively. The total lengths for both spars were 900 mm.

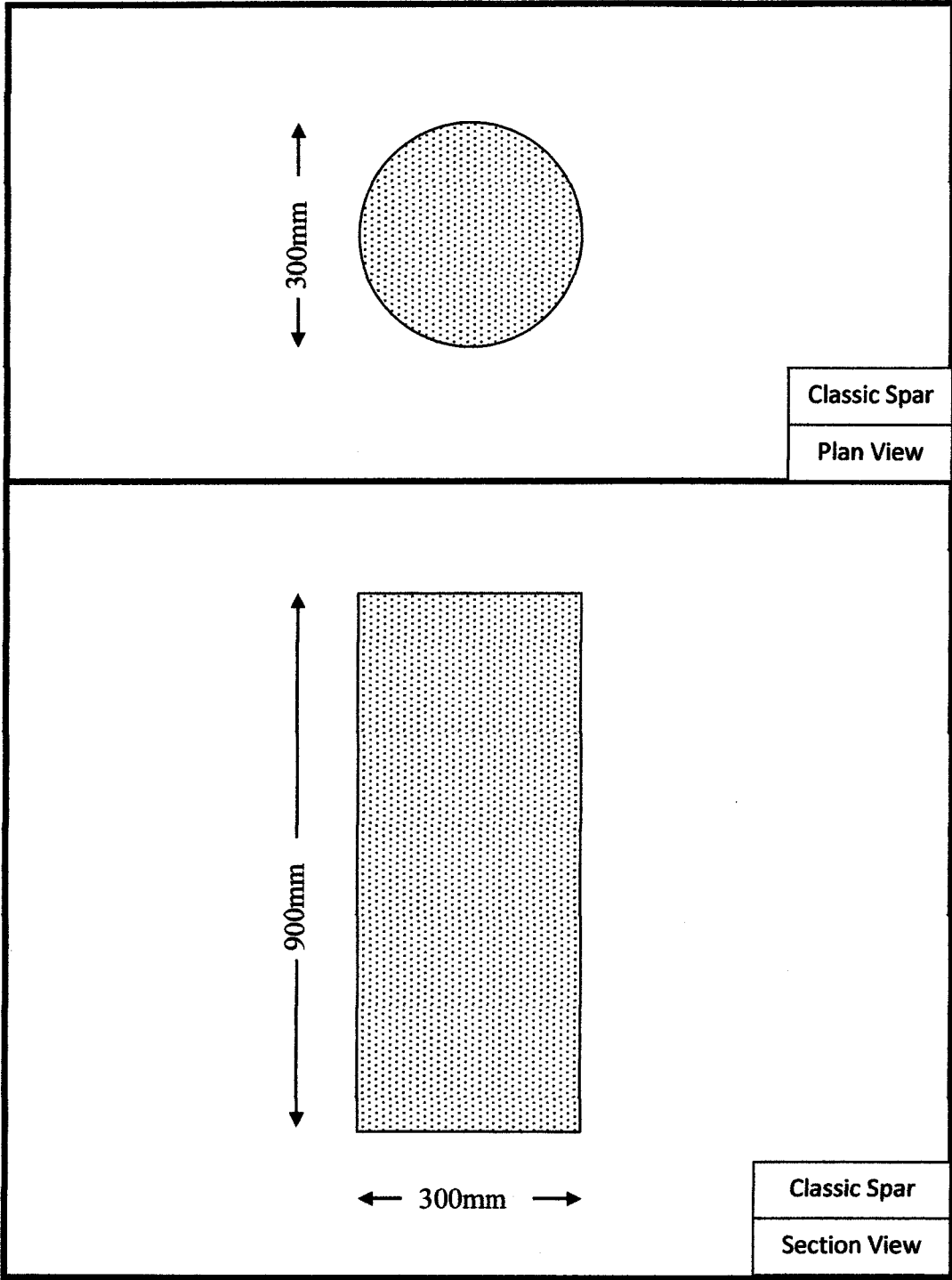


Figure 3.6: Classic Spar Model Dimension

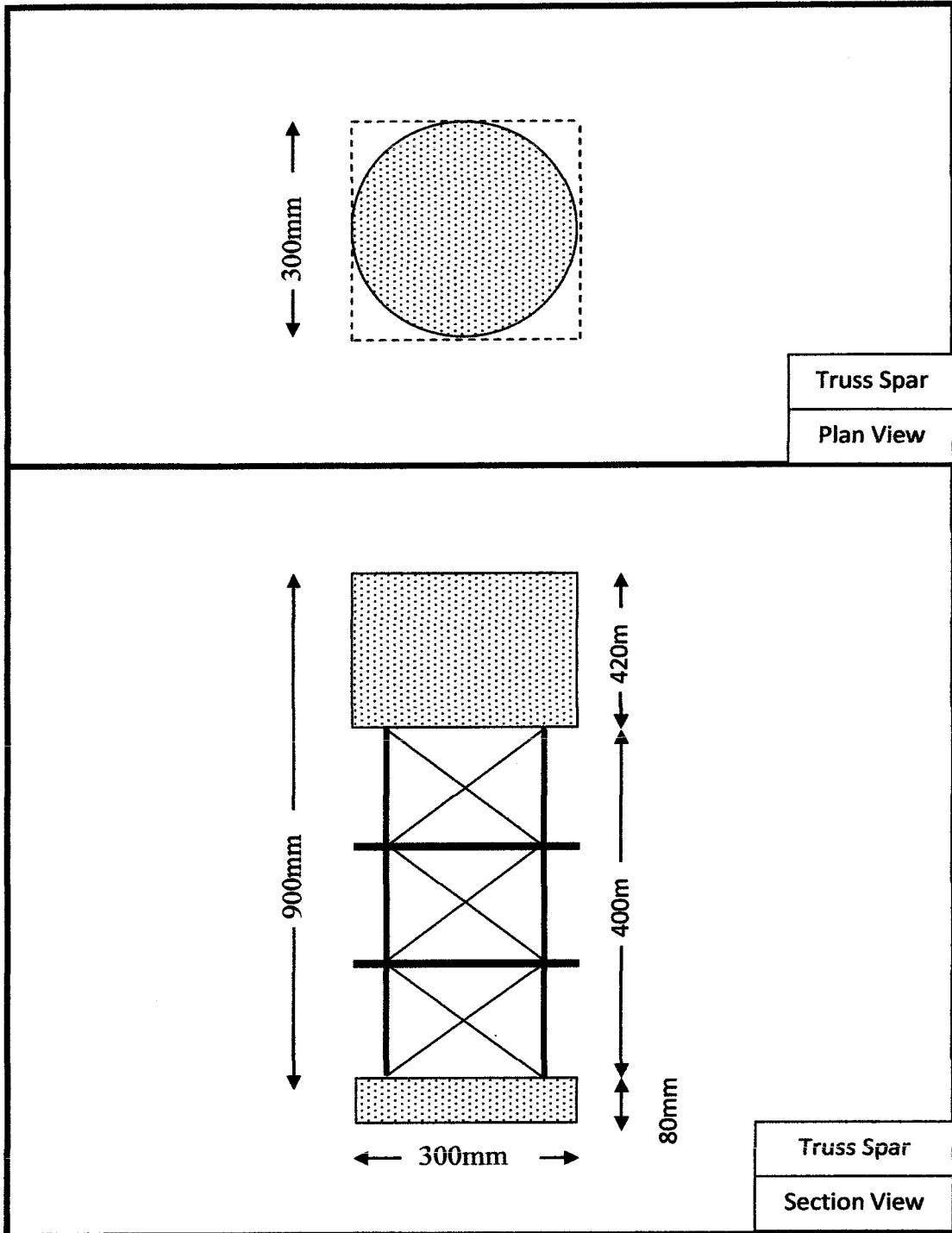


Figure 3.7: Truss Spar Model Dimension

### 3.5.3 Test Facilities and Instrumentation

The physical modeling study had been conducted in the Offshore Laboratory of Universiti Teknologi PETRONAS, Malaysia. The model testing facility consisted of 23 m long, 12 m wide, and 1.5 m deep wave tank equipped with instruments such as wave probes and pressure transducers. The accelerometers and the optical tracking system were used to measure the translational and rotational motions of the model while the vectrino velocimeters were used to measure the current velocities. The wave generator was capable of generating regular and irregular waves and currents. It was also equipped with an overhead crane of capacity 5,000 kg, six glass windows and two movable remote control bridge platforms to support the testing personnel and equipment.

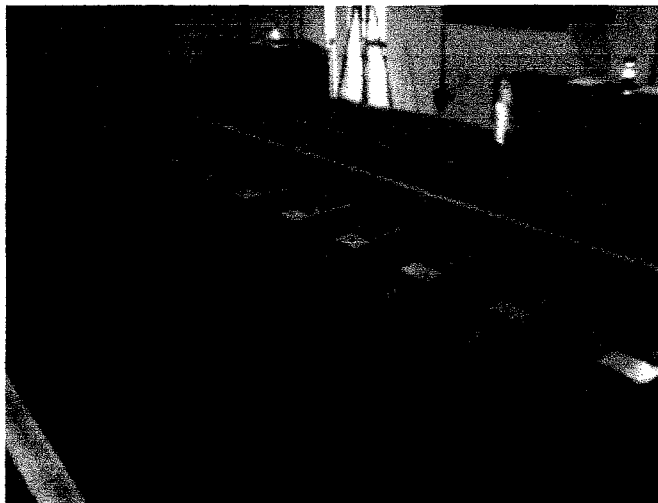


Figure 3.8: The Wave Paddles

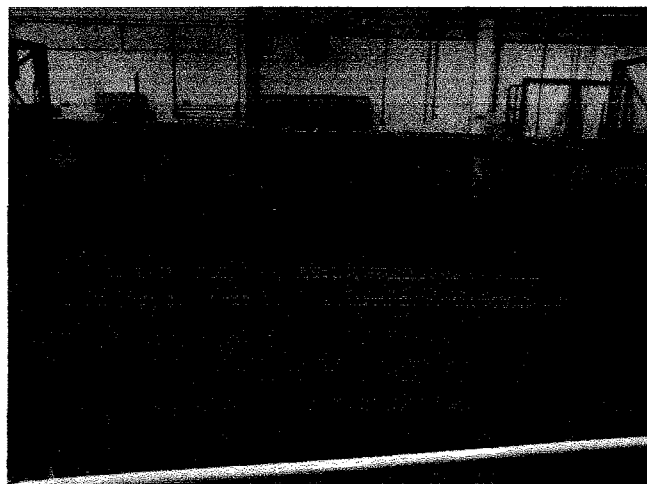


Figure 3.9: The Model Test Setup

### 3.5.4 Generation of Wave and Current

The spar model was subjected to eight values of currents and each current was combined with two sets of random waves and ten sets of regular waves. The current reading was taken by using the vectrino velocimeters that were installed in the water tank. For random wave, the test was done for 300 s while for regular wave the test was done for 180 s. The JONSWAP spectrum was used to generate the random wave. The specified random wave, regular wave, and current conditions for the wave test are shown in Tables 3.2, 3.3, and 3.4 respectively. These data were arrived based on metocean data tabulated for the three Malaysian offshore regions including Peninsular Malaysia (PMO), Sabah (SBO), and Sarawak (SKO) [60].

Table 3.2: Specified Random Wave Conditions for Model Tests

Test No	Wave Height (m)	Wave Period (s)
RD3	0.05	1.0
RD4	0.07	1.2

Table 3.3: Specified Regular Wave Conditions for Model Tests

Test No	RG1	RG2	RG3	RG4	RG5	RG6	RG7	RG8	RG9	RG10
Wave Height (m)	0.04	0.04	0.04	0.05	0.05	0.05	0.04	0.04	0.07	0.07
Wave Period (s)	0.6	0.7	0.8	0.9	1.0	1.2	1.4	1.6	1.8	2.0

Table 3.4: Specified Current Velocity Conditions for Model Tests

Test No	C1	C2	C3	C4	C5	C6	C7	C8
Current (m/s)	0.1317	0.1293	0.1050	0.0986	0.0855	0.0727	0.0590	0.0347

### 3.5.5 Model Tests Setup and Procedure

The model test arrangement consisted of the horizontal mooring system comprising of four wires attached to linear springs connecting the model to the seafloor. Within the constraints of the mooring system, the model was free to respond to the wave loading

in all six degrees of freedom. Figure 3.10 shows the equipments and model setup during the model tests were running. A data post-processing program called MATLAB was used to convert the measured responses to the response spectra by using Discrete Fast Fourier Transform (DFFT). The Response Amplitude Operators (RAOs) were obtained from the response spectra by assuming a linearly damped dynamic system. Figure 3.11 shows the model test arrangement for the plan view and Figure 3.12 shows the position of the wave probes and the vectrinometers during the model test.



Figure 3.10: The On-going Model Test

### 3.5.6 Free Decay Test

The free decay tests were conducted to calculate the natural periods of the system in heave, surge, and pitch for classic and truss spars. The models were given an initial displacement and the subsequent motions were recorded. The results are tabulated in Table 3.5.

Table 3.5: The Natural Period of 3 DOF

Degree of Freedom	Natural Period, $T_n$ (s)	
	Classic Spar	Truss Spar
Surge	127	86.5
Heave	27	26.8
Pitch	39.7	43.4

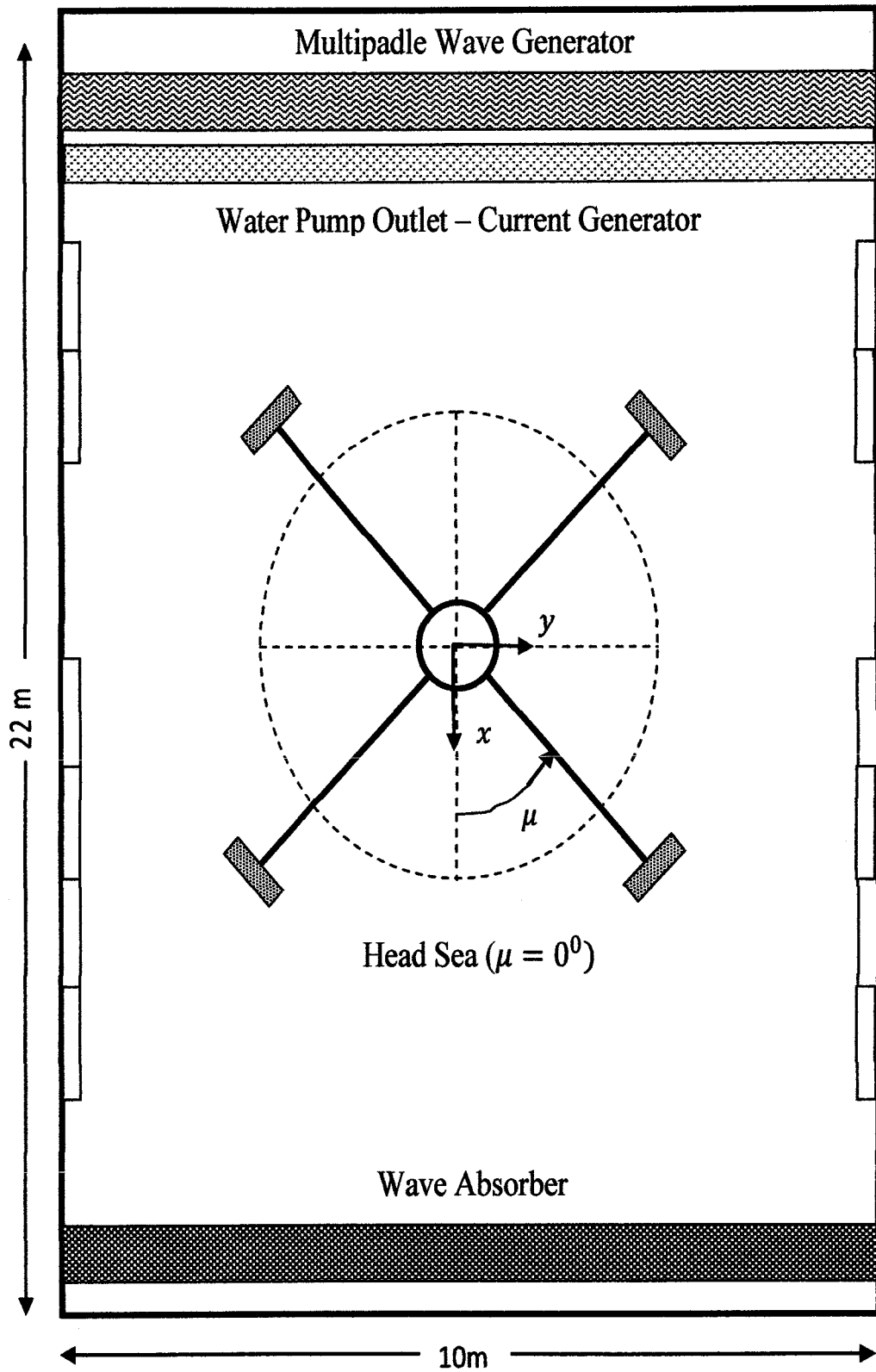


Figure 3.11: Model Test Arrangement

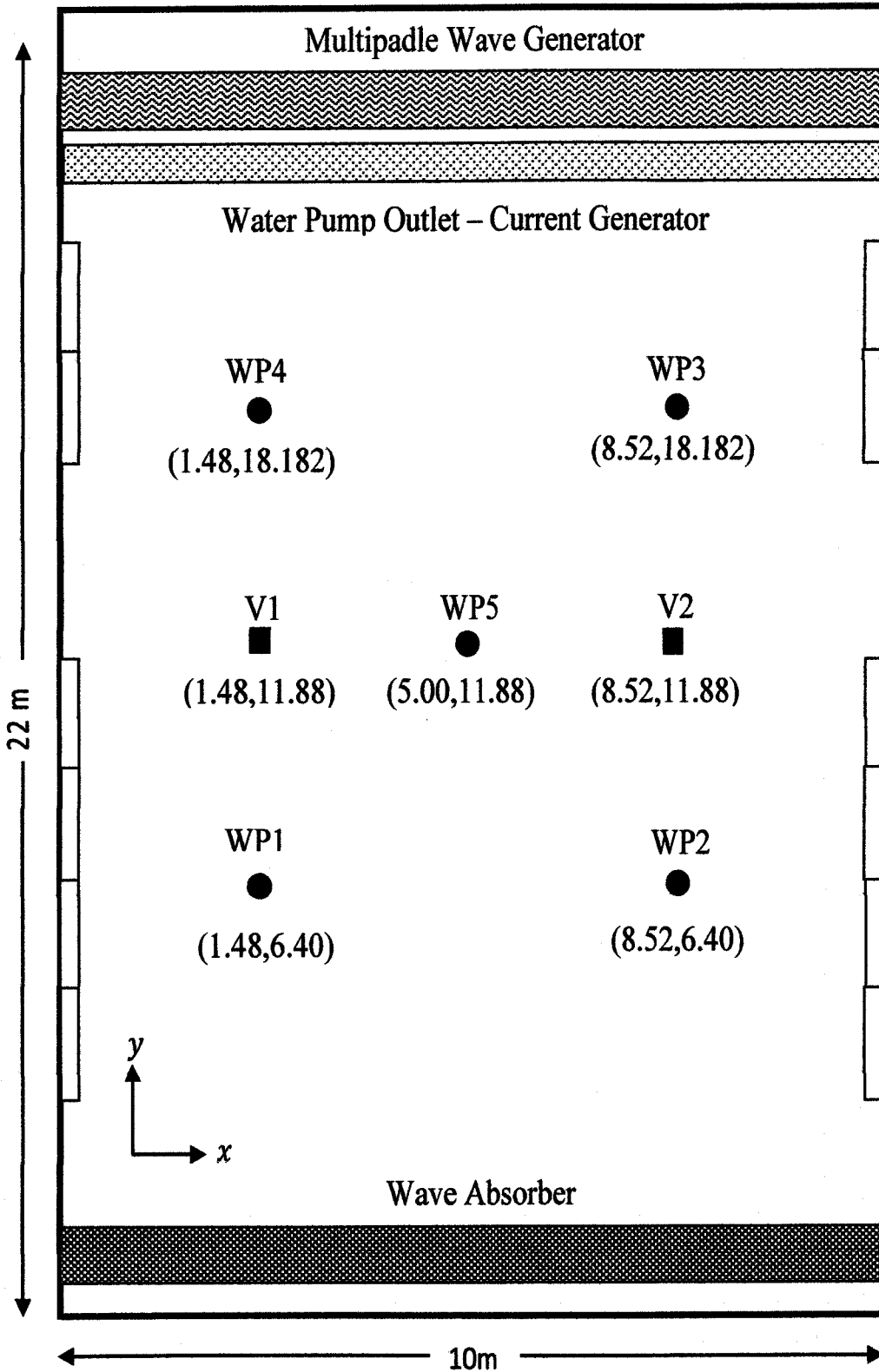


Figure 3.12: Wave Probes and Vectrinometers Arrangement

### 3.5.7 Model Tests Data Processing

The physical model testing had been done for classic and truss spars. The Opti-Tracking System (OTS) was used to record the responses of the models in surge, heave, and pitch when subjected to wave and current while the wave probe was used to obtain the wave height. The RAO values for regular wave were obtained by dividing the structure responses in surge, heave, and pitch to the specific wave height for a certain wave period. Figures 3.13 – 3.15 show the responses of the model in three degrees of freedom subjected to regular wave.

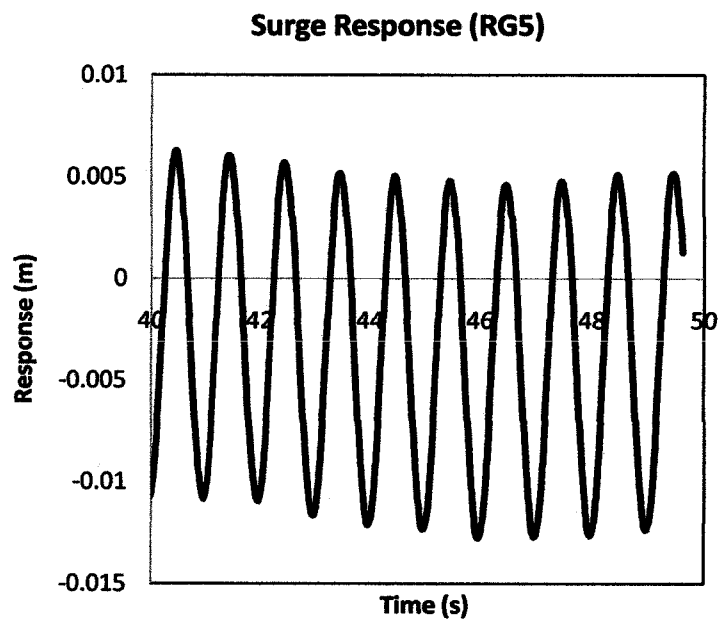


Figure 3.13: Surge Response Subjected to Regular Wave

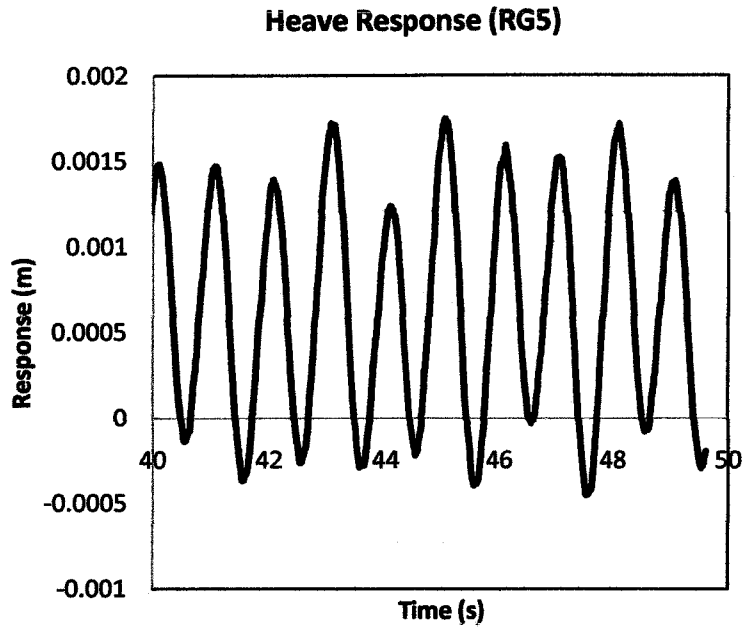


Figure 3.14: Heave Response Subjected to Regular Wave

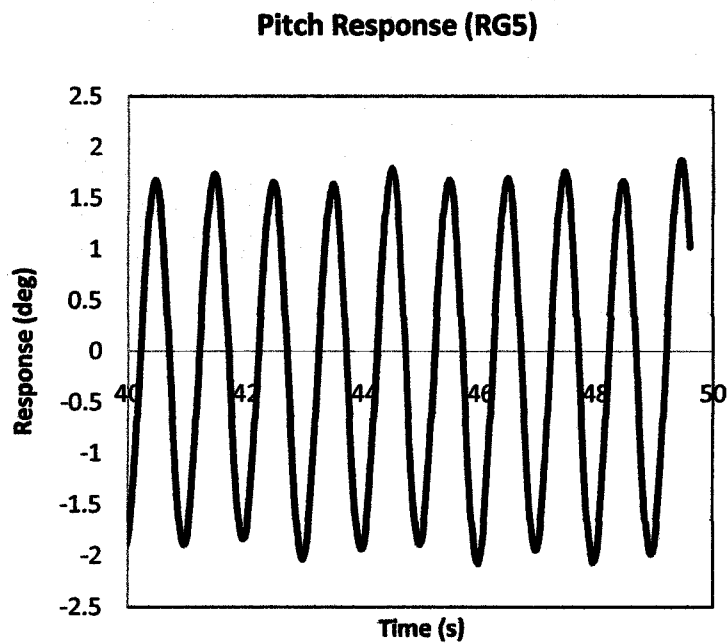


Figure 3.15: Pitch Response Subjected to Regular Wave

Different methods were applied to evaluate the random wave results. A data post-processing program which is MATLAB was used to convert the recorded response time series to the response spectra by using Discrete Fast Fourier Transform (DFFT). The RAO values were obtained by dividing the response spectrum to the wave

spectrum. Figure 3.16 – 3.19 show the time series of the structural responses in three degrees of freedom and the wave height obtained during the model tests. Figure 3.2 shows the converted spectral density for surge, heave, pitch and wave.

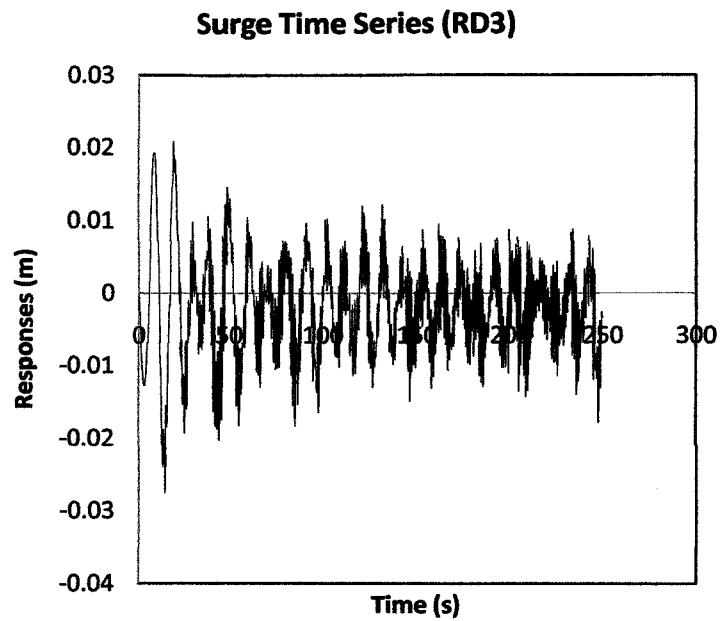


Figure 3.16: Time Series for Surge Subjected to Random Wave (RD3)

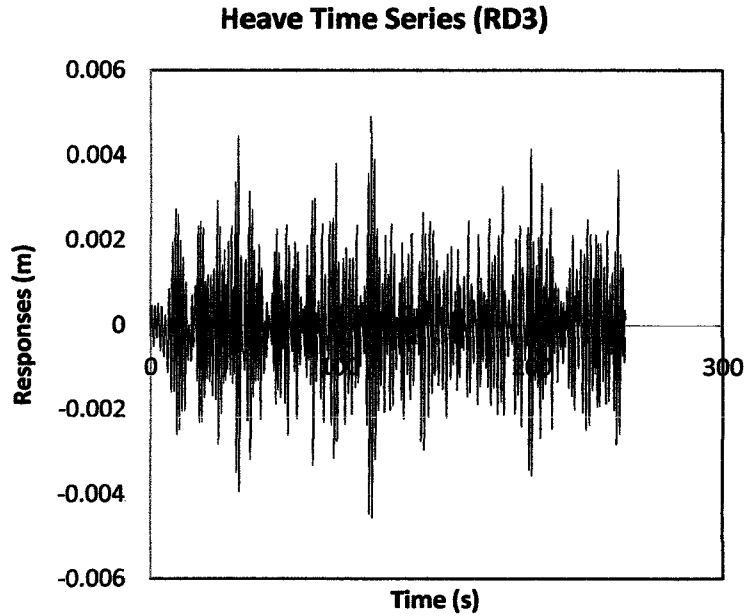


Figure 3.17: Time Series for Heave Subjected to Random Wave (RD3)

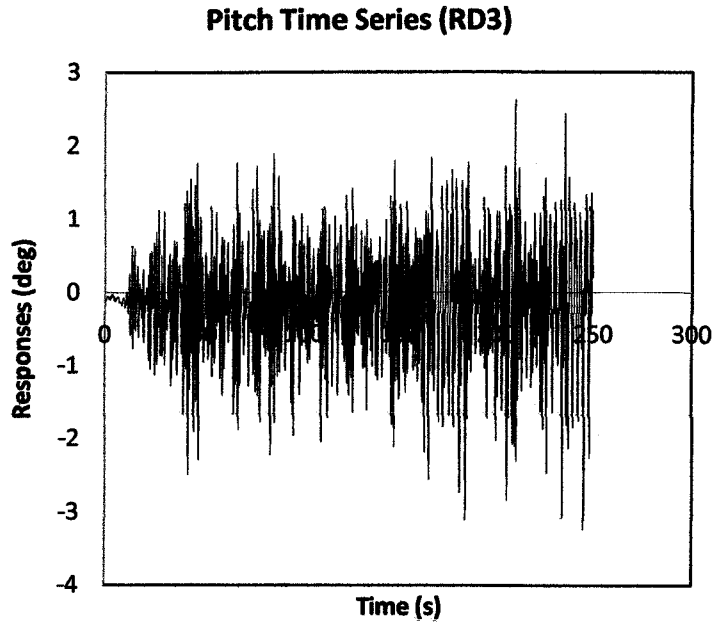


Figure 3.18: Time Series for Pitch Subjected to Random Wave (RD3)

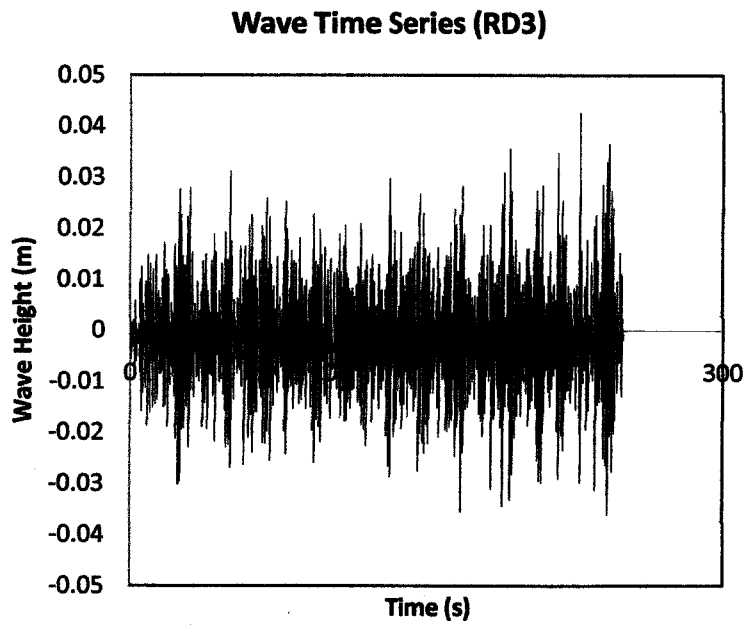


Figure 3.19: Time Series for Random Wave (RD3)

### Response Spectra Density

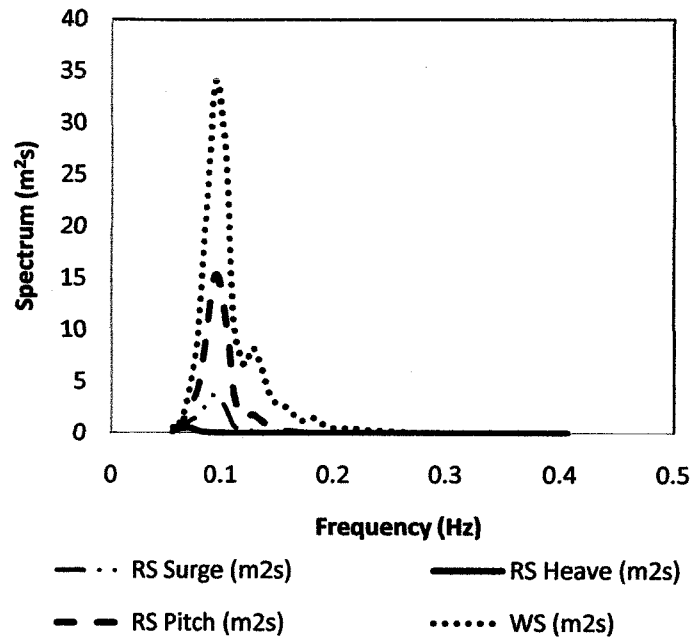


Figure 3.20: Spectra Density subjected to Random Wave (RD3)

### 3.6 Diffraction Theory

For the diameter of a structure exceeds 0.2 of the wave length of the incident wave, the linear wave diffraction analysis is applicable. The diffraction theory stated that this condition caused the localization of the flow separation. The flow separation is then confined to the small region boundary layer around the member surface. In this condition, the incident wave is scattered and the effect of the scatted wave potential is required to be considered.

In this study, the total velocity potential,  $\Phi_o$  and scattered waves,  $\Phi_s$  was given by Equation 3.31.

$$\Phi = \Phi_o + \Phi_s \quad (3.31)$$

Each of these potentials had to satisfy the Laplace equation given in a rectangular Cartesian coordinate system 0XYZ defined by Equation 3.31 and the boundary conditions were defined by Equations 3.32 to 3.36 as:

$$\Delta^2 \phi = \frac{\partial^2 \phi}{\partial x^2} + \frac{\partial^2 \phi}{\partial y^2} + \frac{\partial^2 \phi}{\partial z^2} = 0 \quad (3.32)$$

Dynamic boundary condition:

$$\frac{\partial \Phi}{\partial t} + g\eta + \frac{1}{2} \left[ \left( \frac{\partial \Phi}{\partial x} \right)^2 + \left( \frac{\partial \Phi}{\partial y} \right)^2 + \left( \frac{\partial \Phi}{\partial z} \right)^2 \right] = 0 \text{ on } y = \eta \quad (3.33)$$

Where  $\eta$  = free surface elevation and  $g$  = acceleration due to gravity.

Kinematic boundary condition:

$$\frac{\partial \eta}{\partial t} + \frac{\partial \Phi}{\partial x} \frac{\partial \eta}{\partial x} + \frac{\partial \Phi}{\partial z} \frac{\partial \eta}{\partial z} - \frac{\partial \Phi}{\partial y} = 0 \text{ on } y = \eta \quad (3.34)$$

Where,  $u = \frac{\partial \Phi}{\partial x}$ ;  $v = \frac{\partial \Phi}{\partial y}$ ;  $w = \frac{\partial \Phi}{\partial z}$ ;

Bottom boundary condition:

$$\frac{\partial \Phi}{\partial y} = 0 \text{ at } y = -d \quad (3.35)$$

Body surface-boundary condition:

$$\frac{\partial \Phi}{\partial n} = 0 \quad -d \leq y \leq \eta \quad (3.36)$$

Where,  $\frac{\partial \Phi_0}{\partial n} = -\frac{\partial \Phi_s}{\partial n} \quad -d \leq y \leq \eta$

### 3.6.1 Linear Wave Diffraction Analysis using SACS Software

The simulation of the diffraction analysis for both classic and truss spar platforms was carried out by using licensed commercial software called Structural Analysis Computer System (SACS). The results were directly obtained in the output of the analysis. In this simulation, the SACS to WAMIT (Wave Analysis developed at MIT) analysis interface program was used to determine the dynamic response of the spar platforms. This program converted the SACS model and wave information into WAMIT diffraction model. Besides, this program also created all input required for wave diffraction analysis. The benefits of using this software were it could analyse the multi-body problems with connecting stiffnesses,

it could include the mooring line analyse, and it could also perform the workability analyses. Consequently, the diffraction wave analysis interface converted the frequency and wave direction dependent coefficient into SACS transfer function. Figure 3.21 shows the flowchart of the simulation work by using SACS software.

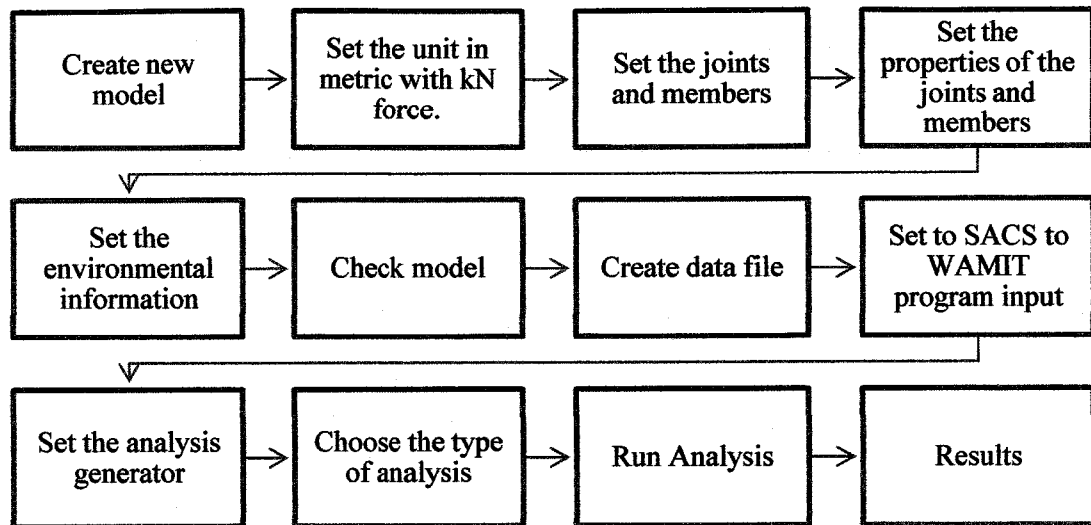
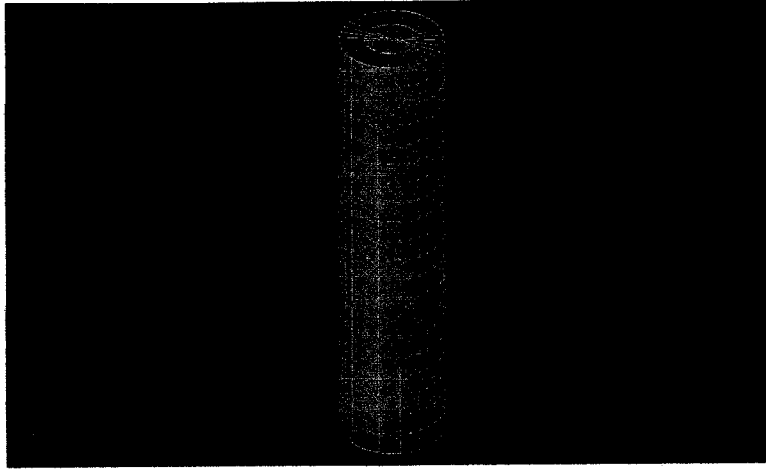


Figure 3.21: The Simulation Flowchart

### 3.6.2 Classic Spar Modeling

In order to design the classic spar model, the cylindrical mesh was used for the mesh type. For creating the mesh, the origin of the cylinder was determined by stating the X, Y, and Z coordinate. Besides, the information on the angle about the cylinder axis, the radius of the cylinder, and the length along the cylinder axis was also stated in the meshing information. After creating the cylindrical mesh, the properties of the members and plates were defined. Lastly, the simulated model was checked by using “Check Model” option in order to find any mistakes in the meshing process. Figure 3.22 shows the simulated model of classic spar. Figures 3.23 and 3.24 show the plan and section view of the classic spar during the simulation process.



**Figure 3.22: Classic Spar Model for Simulation**

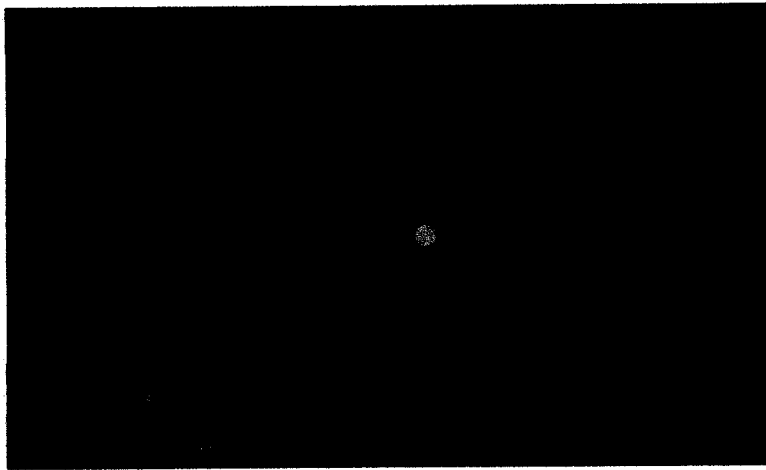


**Figure 3.23: Plan View of Classic Spar Simulation**

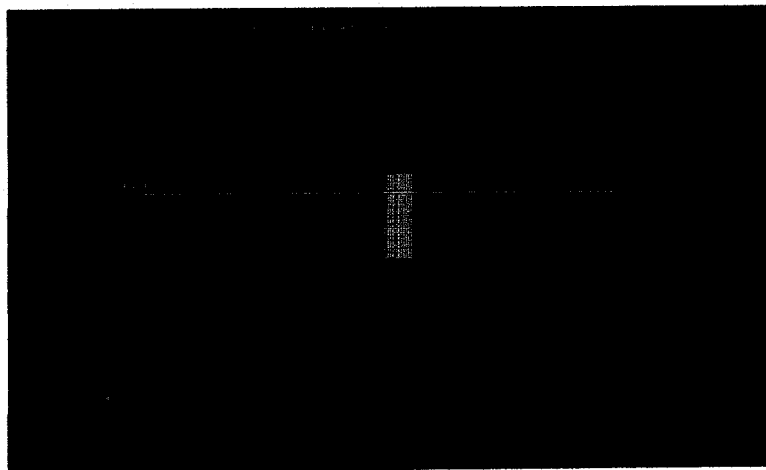


**Figure 3.24: Section View of Classic Spar Simulation**

### 3.6.3 Truss Spar Modeling

For the truss spar model, the cylindrical mesh was used for the hard tank mesh design type. While for the soft tank model design, the rectangular mesh was used for the heave plates and the trusses were designed by using circular members. For creating the mesh, the origin of the cylinder was determined by stating the X, Y, and Z coordinate. Besides, the information of the total number of joints and coordinate increment was also stated in the meshing information. After creating the mesh, the properties of the members and plates were defined. Lastly, the simulated model was checked by using “Check Model” option in order to find any mistakes in the meshing process. Figure 3.25 shows the simulated model of truss spar. Figures 3.26 and 3.27 show the plan and section view of the truss spar during the simulation process.

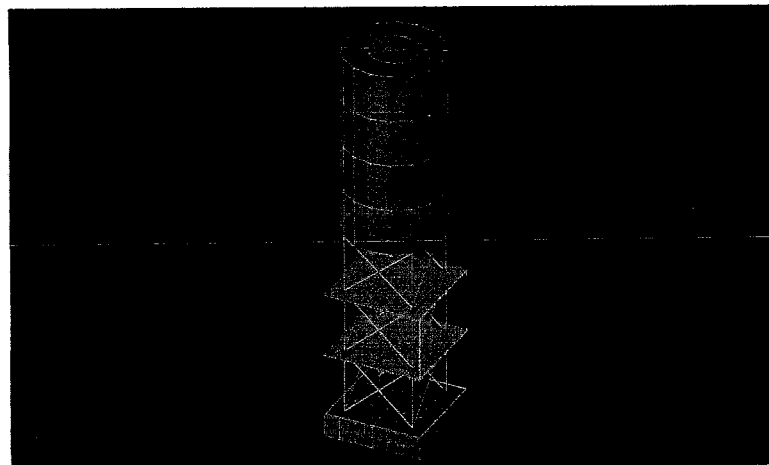


Figure 3.25: Truss Spar Model for Simulation

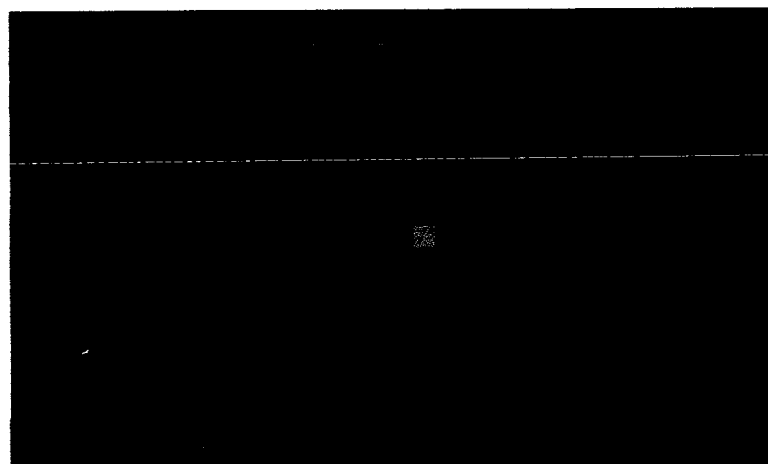


Figure 3.26: Plan View of Truss Spar Simulation

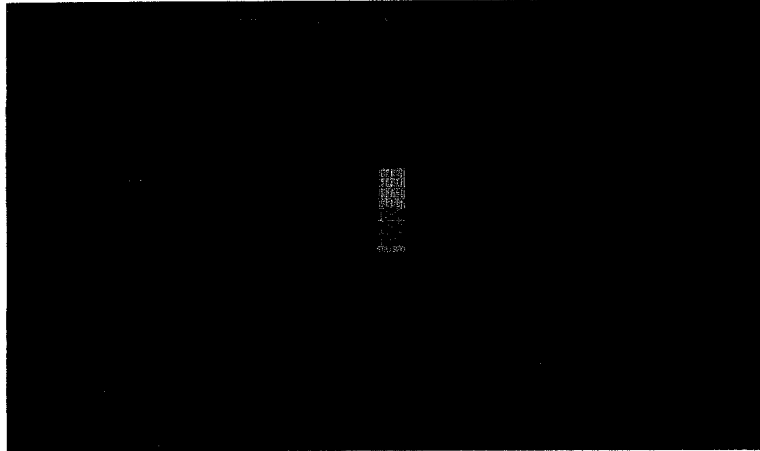


Figure 3.27: Section View of Classic Spar Simulation

Table 3.6 shows the typical input data for linear wave diffraction module for both classic and truss spars. In addition, the linear wave diffraction analysis was conducted for selected wave. The results of the simulation were used for validation.

Table 3.6: Input Data for Simulation

Description		Value
Water Depth (m)		110
Wave Height (m)		1
Sea Water Density (MT/m <sup>3</sup> )		1.030
Origin Orientation (vertical axis)		+z
Frequency Range (Hz)		0.05 – 0.20
Mooring Line	Cross section area (cm <sup>2</sup> )	30.20
	Elastic Modulus (1000kN/cm <sup>2</sup> )	14.40

### **3.7 Chapter Summary**

This chapter summarized all the methods of analysis in this study. The purpose of this study is to determine the dynamic response of offshore spar platforms in three degrees of freedom which include surge, heave, and pitch.

The numerical analysis explained in detail. For numerical analysis, the frequency domain and time domain analysis were executed in order to predict the structure responses. For Frequency domain analysis, the particle wave characteristics were determined by using Linear Airy Theory and the wave forces are calculated by using Morrison Equation. While for time domain analysis, the Newmark Beta Integration Method was used in order to solve the equation of motion which consists of the mass matrix, damping matrix and stiffness matrix of the structures.

A model test was done in The Offshore Laboratory, Universiti Teknologi Petronas for two types of spars which are classic and truss spar. In this model tests, all the dynamic responses were obtained and recorded by using an accurate instrumentation called Opti-Track System. Other instruments such as vectrinometer and wave probes were used for measuring the wave and current conditions. The obtained data in this model tests were processed by using MATLAB code to obtain the structure response RAOs.

In addition, a simulation analysis using commercial software called SACS was done for validation. In this analysis, the linear diffraction analysis method was applied. The diffraction analysis was applicable for a structure having a diameter exceeds 0.2 of the wave length of the incident wave. The flow of the simulation processes was explained briefly.

## CHAPTER 4

### RESULTS AND DISCUSSION

#### **4.1 Chapter Overview**

This chapter discusses the results obtained from the methods that had been explained in Chapter 3. The dynamic response for both classic and truss spar are presented and discussed. The RAO values for regular and random wave are presented for both spars. The numerical analysis which includes frequency domain and time domain analysis was performed in order to determine the response of the structures. The wave tank test was done in order to determine the dynamic response of the classic and truss spars. In addition, the simulation analysis by using commercial software had been done in order to validate the results. This simulation used the linear wave diffraction analysis for both classic and truss spars. Those results are compared between different methods for validation. The results showed good agreement with small differences. In this discussion, the RAO values are presented between 0.05 Hz to 0.25 Hz. The significant frequency band of the ocean wave for the offshore structure lies between 5 to 24 seconds. However, the maximum energy of the wave is between 10 to 16 seconds where the significant responses are observed.

#### **4.2 Regular Wave**

In this study, the response of classic and truss spars subjected to regular wave were evaluated by using frequency domain analysis and model tests. The results are presented below.

### 4.2.1 Frequency Domain (FD) Analysis Results for Prototypes

The frequency domain analysis was done by using the Linear Airy Theory and Morrison Equation in order to determine the wave forces. The responses of the structures subjected to regular wave are presented below.

#### 4.2.1.1 Classic Spar Prototype

The surge, heave and pitch responses for classic spar are shown in Figures 4.1 to 4.3 respectively. The maximum RAOs were found to be at 0.05 Hz for both surge and pitch responses where 3.90 m/m for surge and 0.118 deg/m for pitch response, while for the heave response, the maximum RAO was 1.42 m/m at 0.06 Hz.

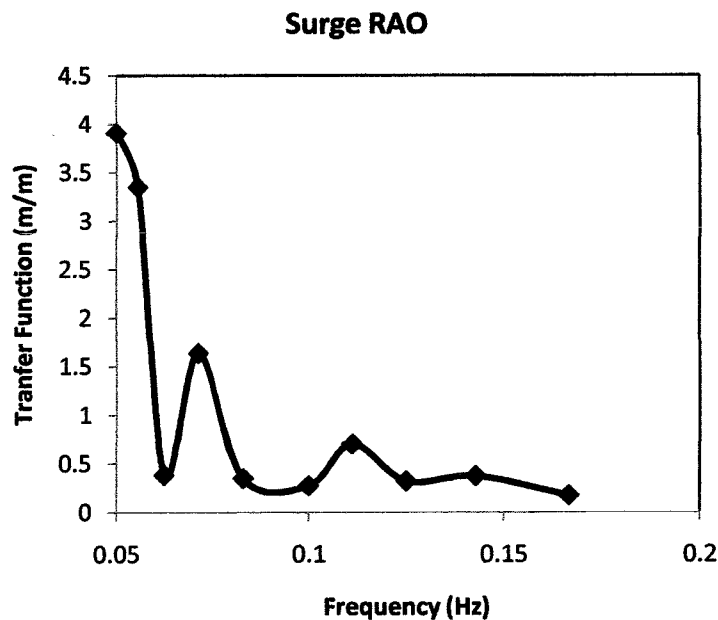


Figure 4.1: FD Analysis – Classic Spar Surge Response (Regular Wave)

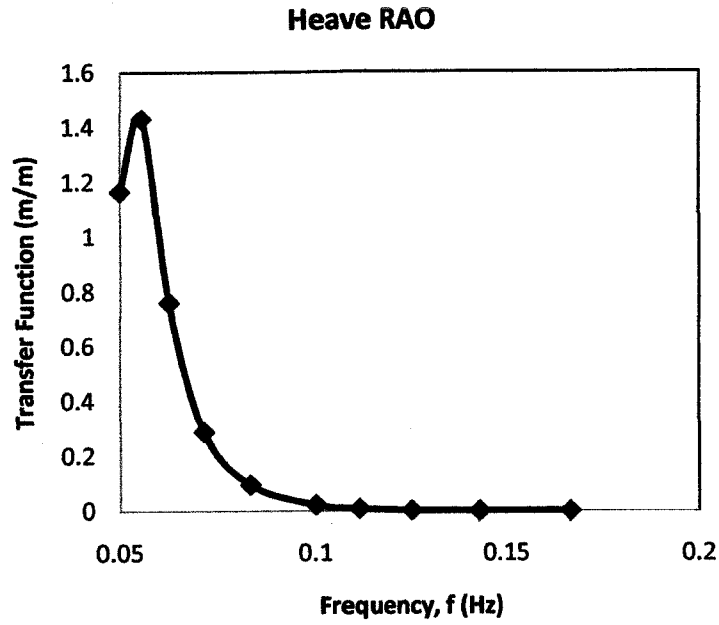


Figure 4.2: FD Analysis – Classic Spar Heave Response (Regular Wave)

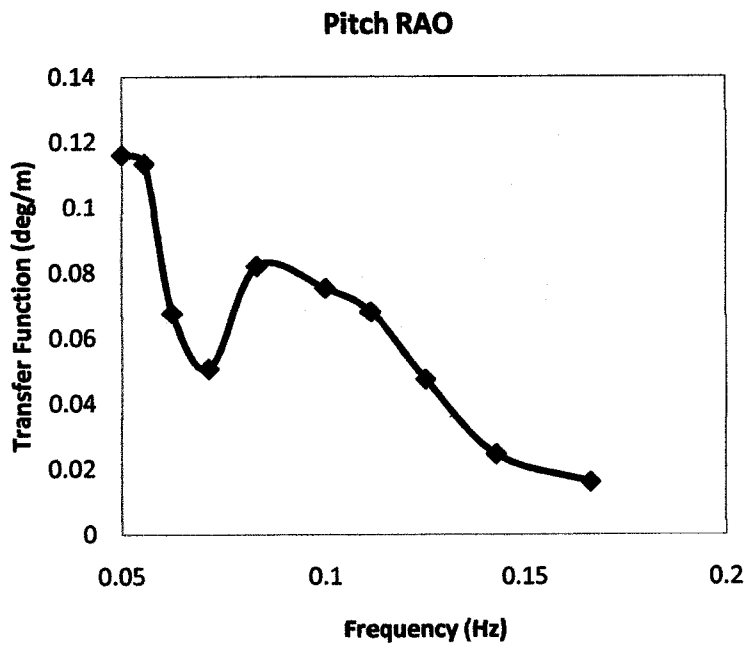


Figure 4.3: FD Analysis – Classic Spar Pitch Response (Regular Wave)

#### 4.2.1.2 Truss Spar Prototype

The surge, heave and pitch responses for truss spar are shown in Figures 4.4 to 4.6. The maximum RAOs were 2.86 m/m for surge response and 1.30 deg/m for pitch response at 0.050 Hz, while it was 1.78 m/m at 0.08 Hz for heave response.

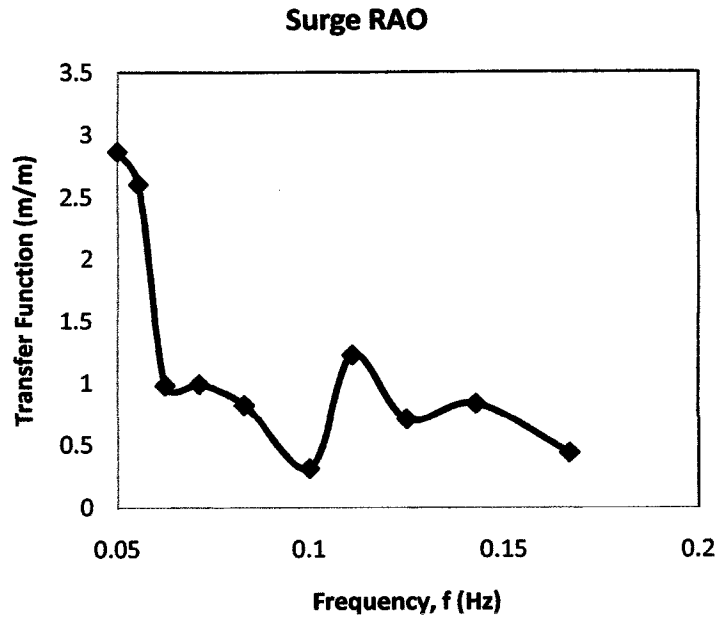


Figure 4.4: FD Analysis – Truss Spar Surge Response (Regular Wave)

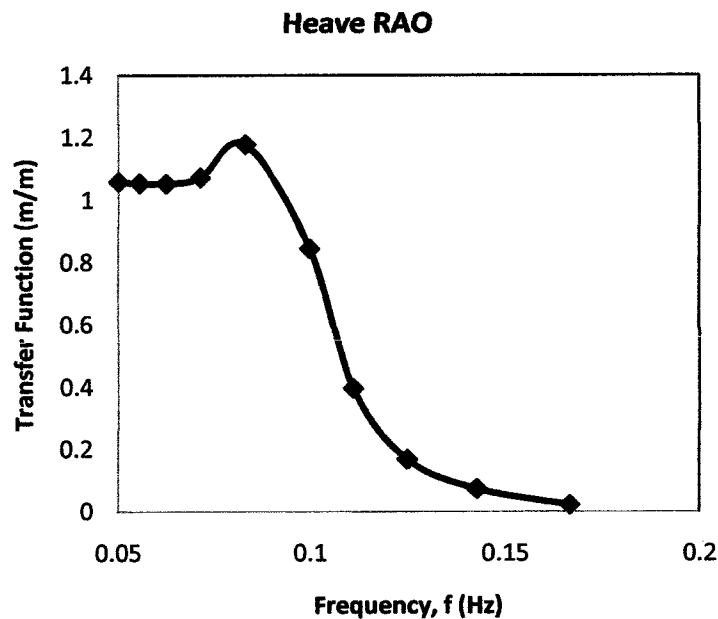


Figure 4.5: FD Analysis – Truss Spar Heave Response (Regular Wave)

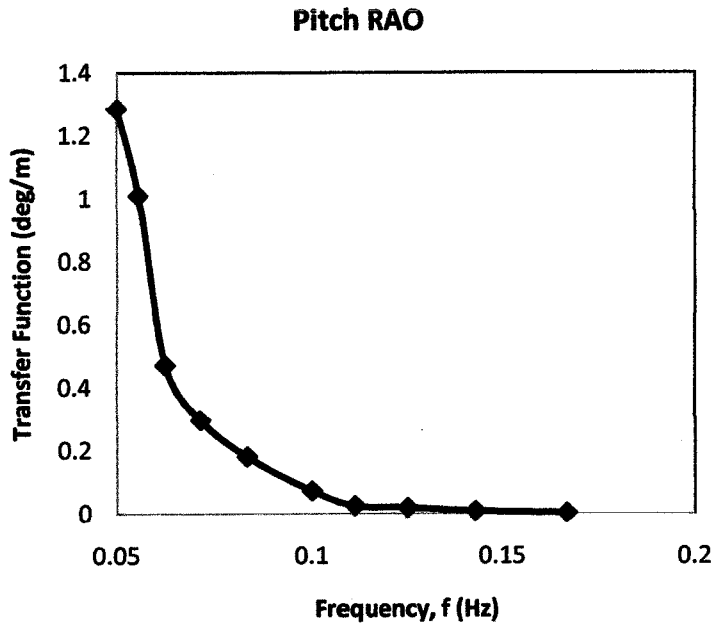


Figure 4.6: FD Analysis – Truss Spar Pitch Response (Regular Wave)

#### 4.2.2 Spar Model Test Results

The model tests were performed for both classic and truss spar models. Both models were subjected to regular wave. The results are presented below.

##### 4.2.2.1 Classic Spar Model Results

The surge, heave and pitch responses for classic spar are shown in Figures 4.7 to 4.9. The maximum RAOs were found to be at 0.05 Hz where 1.03 m/m for surge response and 2.53 m/m for heave response, while for the pitch response, the maximum RAO was 0.28 deg/m at 0.056 Hz..

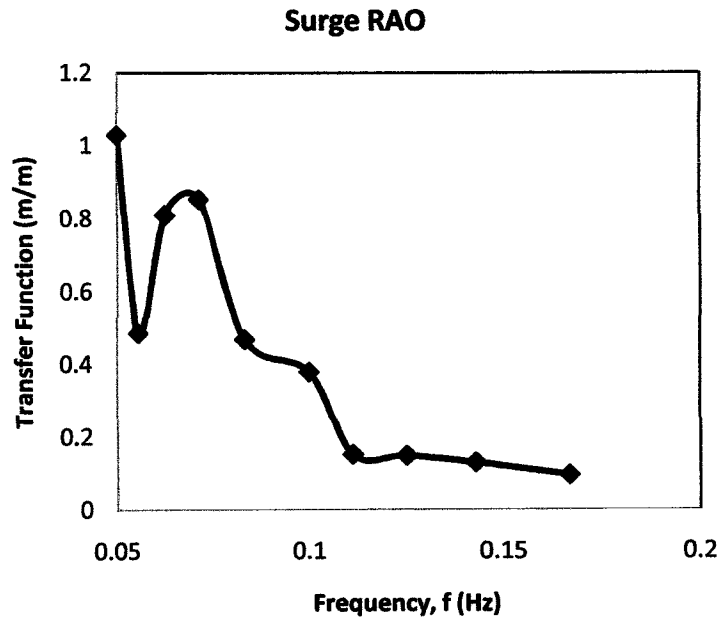


Figure 4.7: Model Test – Classic Spar Surge Response (Regular Wave)

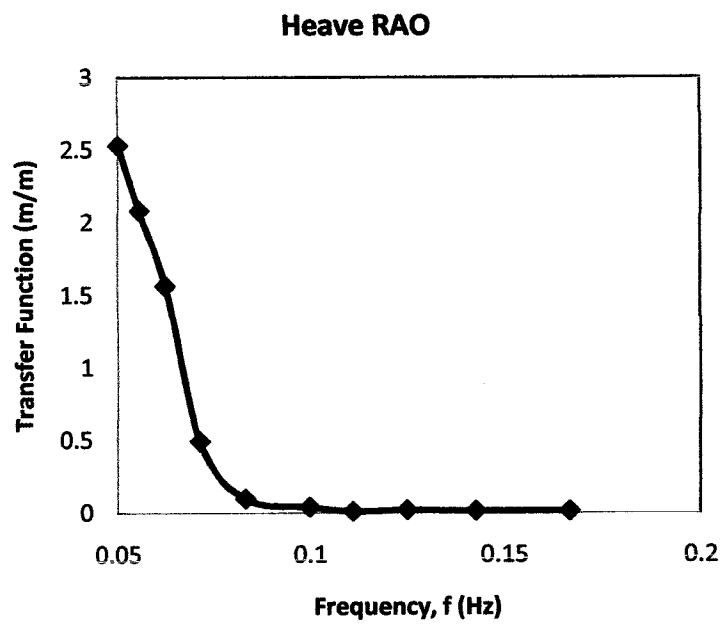


Figure 4.8: Model Test – Classic Spar Heave Response (Regular Wave)

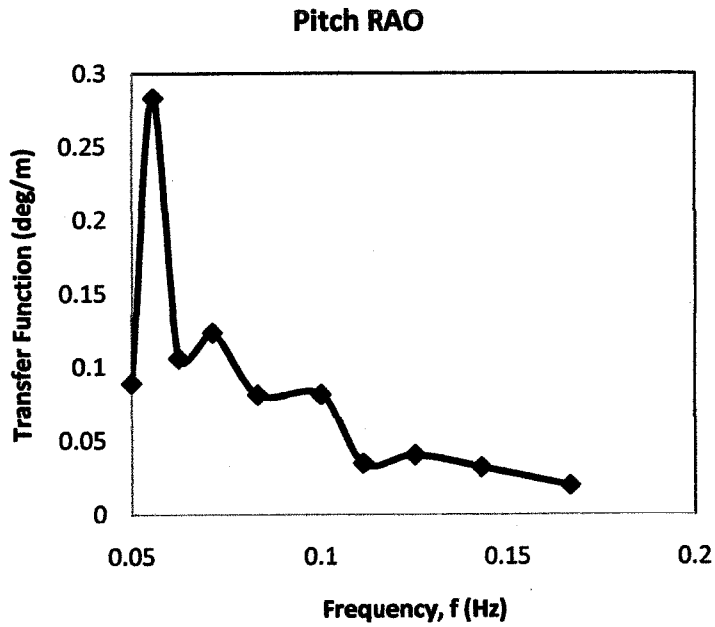


Figure 4.9: Model Test – Classic Spar Pitch Response (Regular Wave)

#### 4.2.2.2 Truss Spar Model Results

The surge, heave and pitch responses for truss spar are shown in Figures 4.10 to 4.12. The maximum RAOs for surge and pitch were found to be at 0.065 Hz where 1.16 m/m for surge response and 0.073 deg/m for pitch response, while for heave response, the maximum RAO of 1.61 m/m was found to be at 0.05 Hz

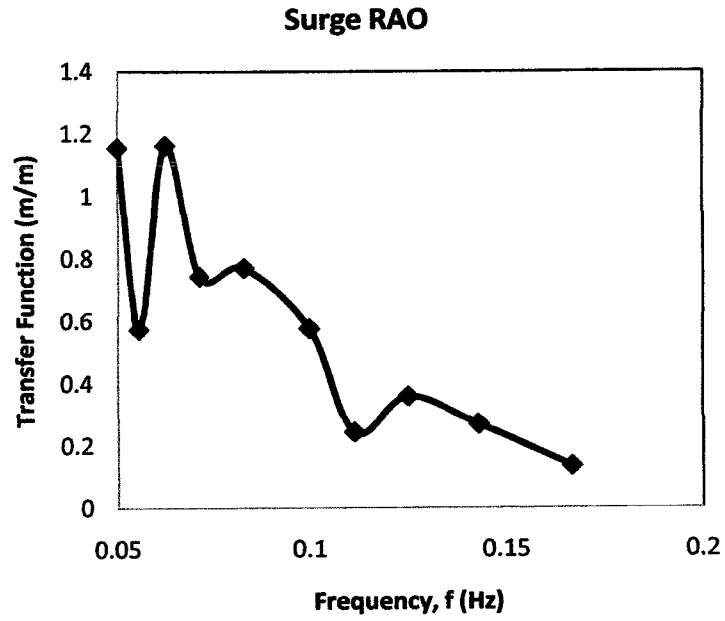


Figure 4.10: Model Test – Truss Spar Surge Response (Regular Wave)

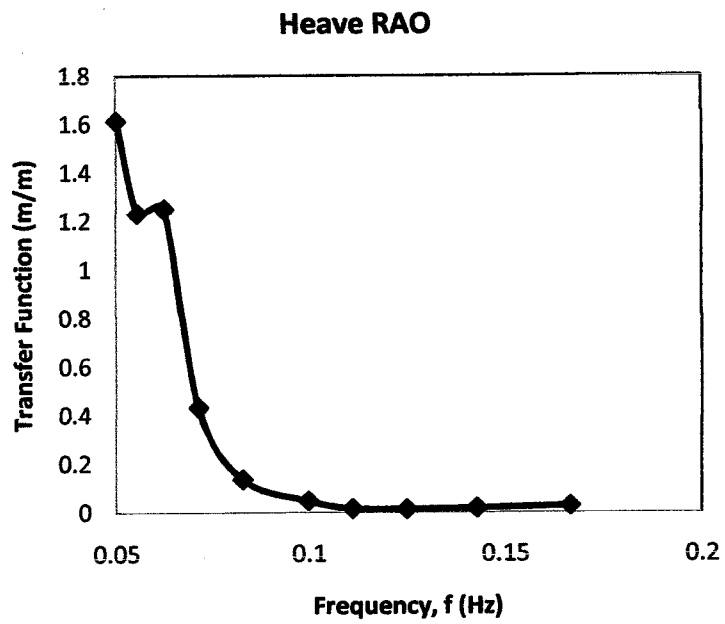


Figure 4.11: Model Test – Truss Spar Heave Response (Regular Wave)

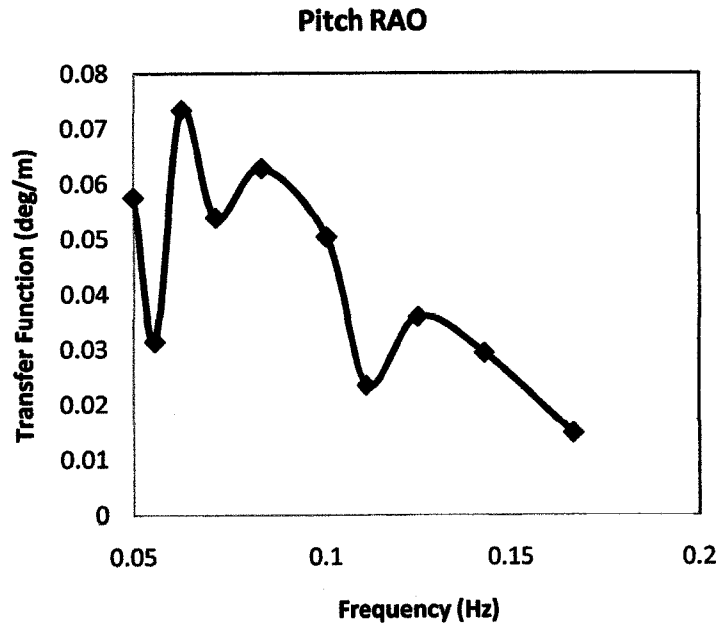


Figure 4.12: Model Test – Truss Spar Pitch Response (Regular Wave)

### 4.2.3 Comparison of Results

#### 4.2.3.1 Frequency Domain (FD) Analysis & Model Test Results

The responses of the classic and truss spars physical model were determined numerically by using the model dimensions, properties, draft and the generated wave characteristics as inputs. Some of the results are presented. The results are compared with the corresponding model test results.

##### 4.2.3.1.1 Classic Spar-Comparison of Results

The classic spar RAOs for surge, heave, and pitch of the model test processed results are compared to the FD analysis for regular wave in Figures 4.13, 4.14, and 4.15 respectively. For the surge RAO, although the trends of surge RAO were same for the frequencies above 0.083 Hz, the value of surge RAO computed by FD analysis shows significant variation when compared to the model test at the lower frequencies. The FD analysis results were higher in magnitude compared with the model test results. This might be due to the limitation in the numerical analysis which the nonlinearities

were excluded in the calculation. For the heave RAO, it could be observed that both methods are in excellent agreement except at the lower frequencies with some differences in magnitude. For the pitch RAO, the comparison shows distinct differences between these two methods in terms of magnitude of RAO. The comparison between simplified FD analysis and model test marked significant difference at frequency 0.056 Hz. However, the trend of the model test results agreed with the numerical results of FD analysis for all frequencies above 0.085 Hz. These discrepancies were due to the limitations such as neglect of diffraction effects as well as that could not be included in the analysis thereby underestimating the responses. However, the results of FD analysis can still be used during the preliminary design stage.

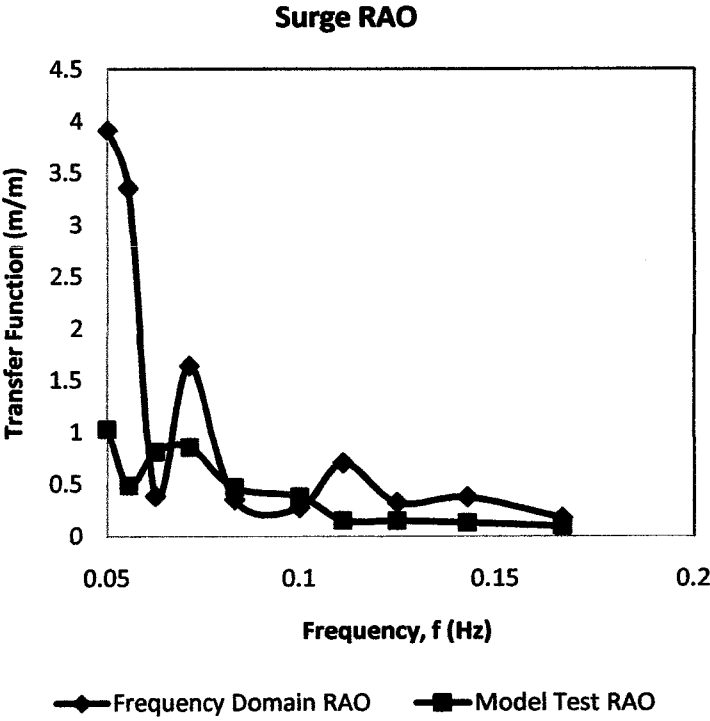


Figure 4.13: Comparison – Classic Spar Surge Response (Regular Wave)

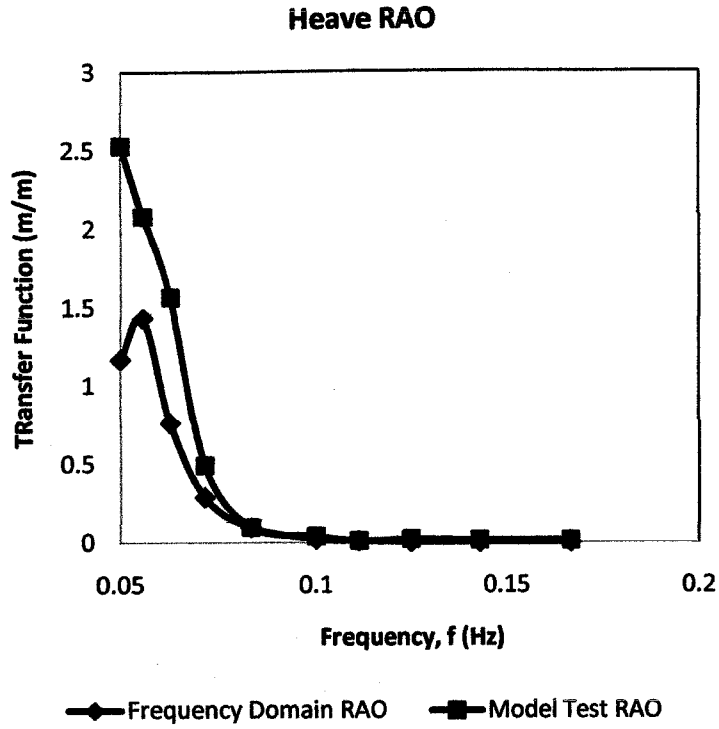


Figure 4.14: Comparison – Classic Spar Heave Response (Regular Wave)

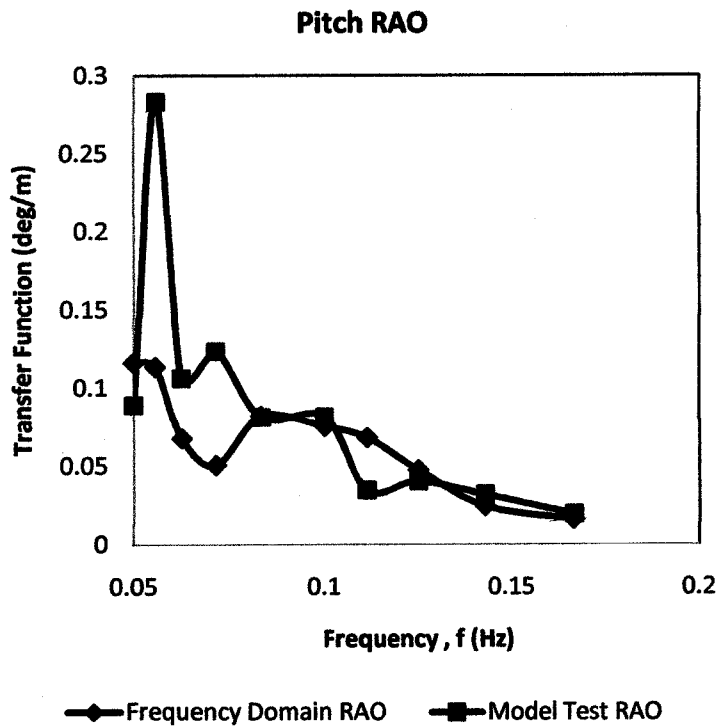


Figure 4.15: Comparison – Classic Spar Pitch Response (Regular Wave)

#### 4.2.3.2 Truss Spar Prototype

Figures 4.16 to 4.18 show the comparison of the truss spar RAOs for surge, heave, and pitch between the experimental model test processed results and the FD analysis for regular wave respectively. For the surge RAO, although the trends of surge RAO were same, the value of surge RAO computed by FD analysis shows some variation at frequency 0.11 Hz when compared with model test results. The FD domain analysis results were higher compared to the experimental results in lower and higher frequencies. For the heave RAO, the model test RAO and FD analysis RAO showed wide variations in the frequency range 0.065 – 0.140Hz. This discrepancy was probably due to optical camera resolution and the reflected wave during the model test, thus underestimating the structural responses. For the pitch RAO, although the trends of pitch RAO were same for frequency above 0.1 Hz, the value of pitch RAO computed by FD analysis shows significant variation when compared with model test results at frequency 0.05 Hz. This might be because the FD analysis did not consider the nonlinearities in the analysis. However, the results of FD analysis can still be used during the preliminary design stage.

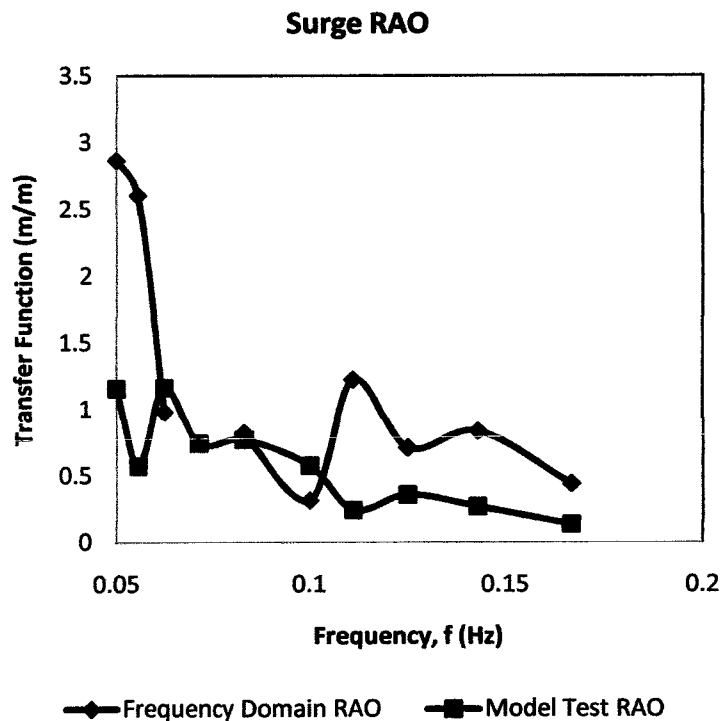


Figure 4.16: Comparison – Truss Spar Surge Response (Regular Wave)

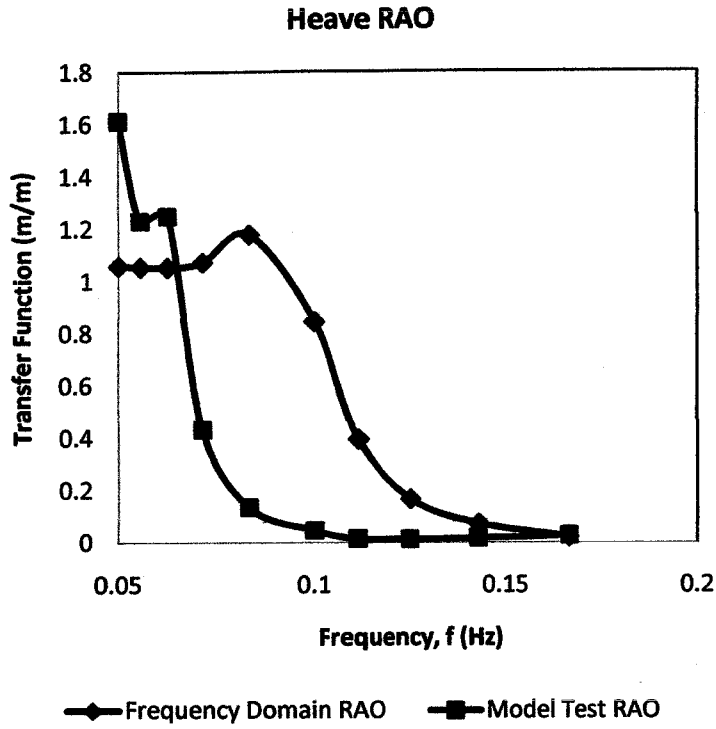


Figure 4.17: Comparison – Truss Spar Heave Response (Regular Wave)

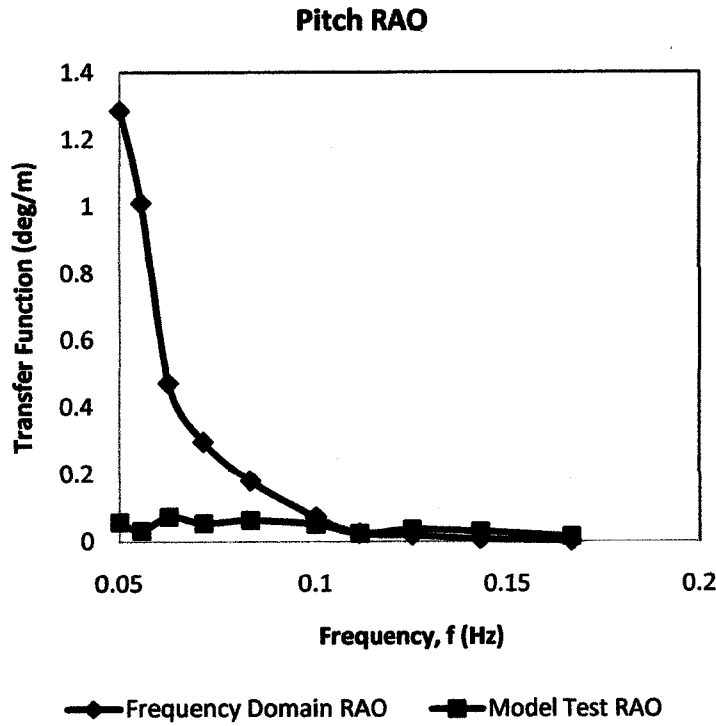


Figure 4.18: Comparison – Truss Spar Pitch Response (Regular Wave)

### **4.3 Random Wave**

The dynamic responses of offshore structure subjected random wave are difficult to interpret and evaluate. In this study, there are four methods to determine the response of the classic and truss spars which are frequency domain analysis, time domain analysis, model tests, and simulation analysis using commercial software called SACS. The results are presented below.

#### **4.3.1 Frequency Domain (FD) Analysis Results for Prototypes**

The frequency domain analysis was done by using the Linear Airy Theory and Morrison Equation in order to determine the wave forces. The responses of the structures are presented below.

##### *4.3.1.1 Classic Spar Prototype*

The surge, heave and pitch responses for classic spar are shown in Figures 4.19 to 4.21. The maximum RAOs were found to be at 0.055 Hz for both surge and heave responses where 0.68 m/m for surge response and 1.70 m/m for heave response, while for the pitch response, the maximum RAO is 0.54 deg/m at 0.075 Hz.

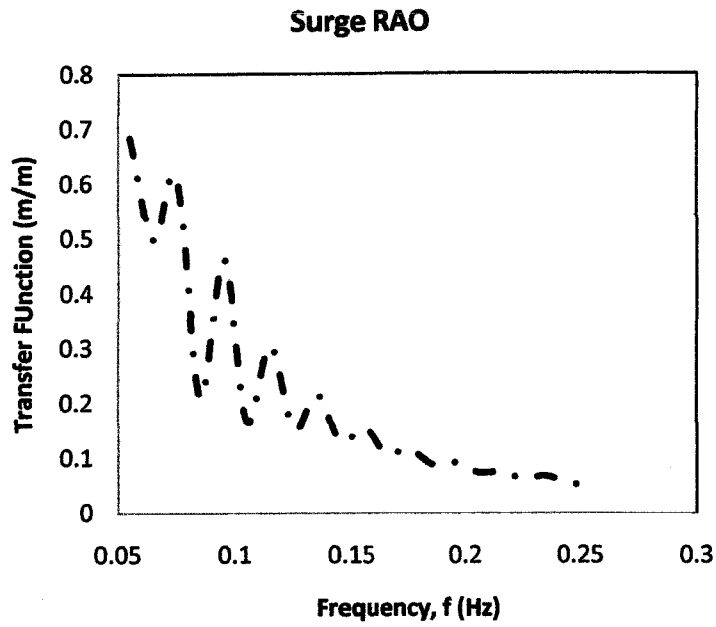


Figure 4.19: FD Analysis – Classic Spar Surge Response

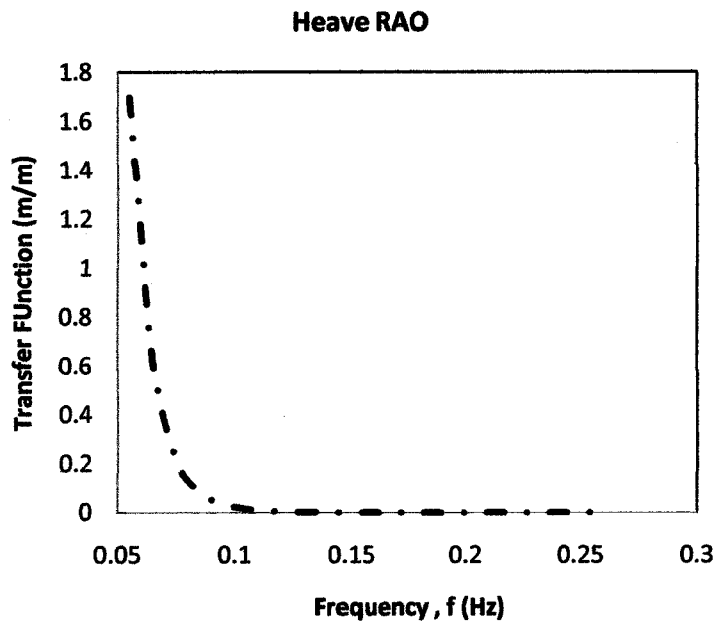


Figure 4.20: FD Analysis – Classic Spar Heave Response

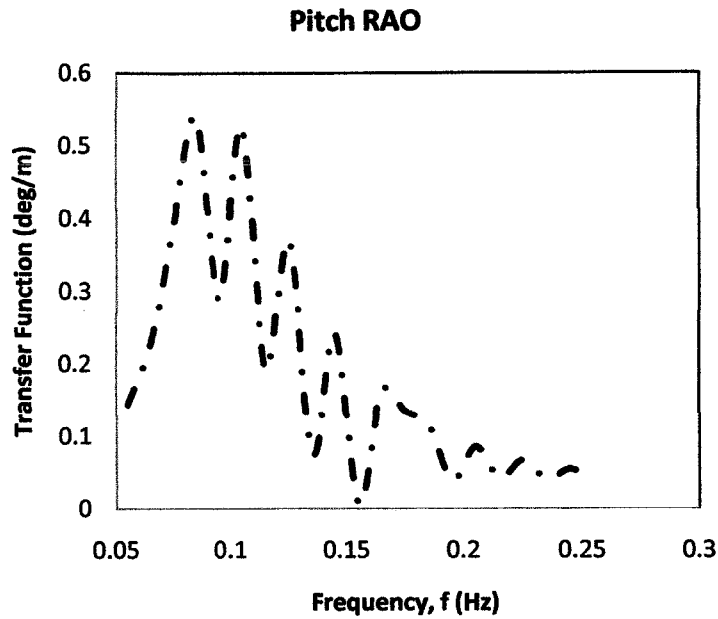


Figure 4.21: FD Analysis – Classic Spar Pitch Response

#### 4.3.1.2 Truss Spar Prototype

The surge, heave and pitch responses for classic spar are shown in Figures 4.22 to 4.24. The maximum RAOs were found to be at 0.055 Hz for both surge and heave responses where 0.64 m/m for surge response and 0.92 m/m for heave response, while for the pitch response, the maximum RAO is 1.06 deg/m at 0.085 Hz.

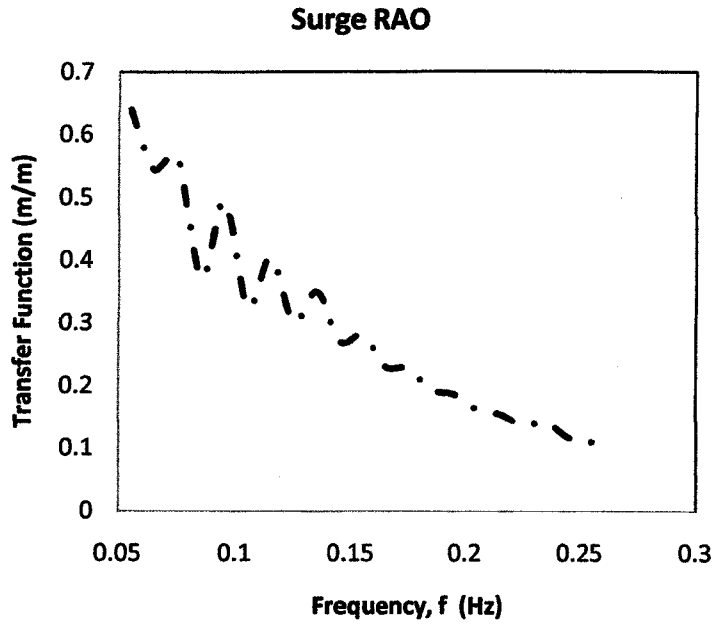


Figure 4.22: FD Analysis – Truss Spar Surge Response

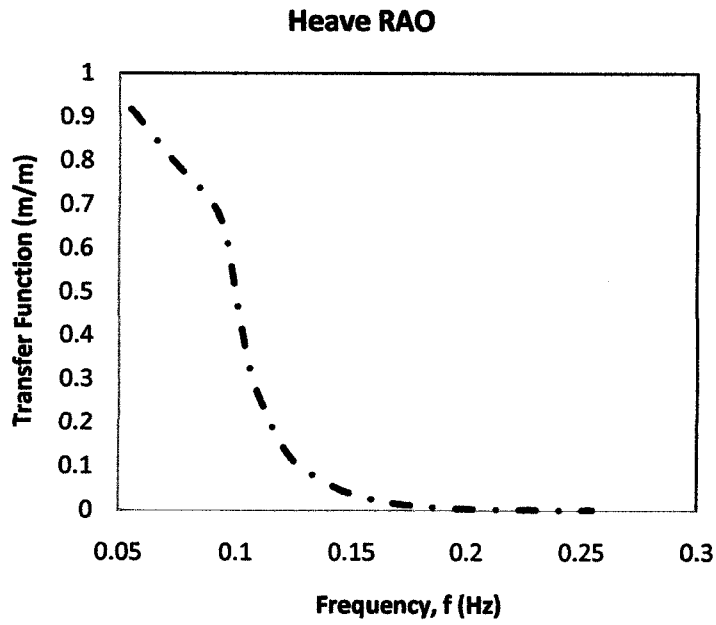


Figure 4.23: FD Analysis – Truss Spar Heave Response

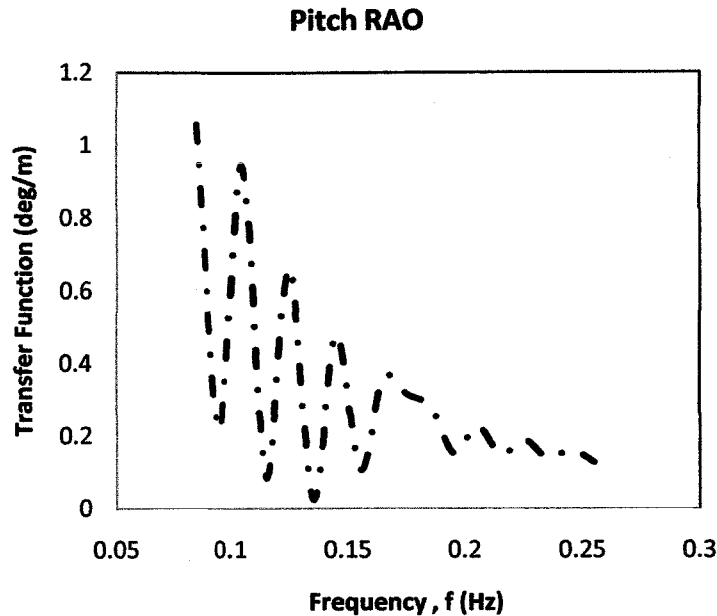


Figure 4.24: FD Analysis – Truss Spar Pitch Response

#### 4.3.2 Time Domain (TD) Analysis Results for Prototypes

The time domain analysis was done by solving the equation of motion using the Newmark Beta integration method. A MATLAB code developed was modified in the case of currents. The results were directly obtained at the output of the analysis. The responses of the structures are presented below.

##### 4.3.2.1 Classic Spar Prototype

The surge, heave and pitch responses for classic spar are shown in Fig 4.25 to 4.27. The maximum RAOs were found to be at 0.065 Hz where 0.41 m/m for surge response, 0.32 m/m for heave response, and 0.71 deg/m for pitch response.

##### 4.3.2.2 Truss Spar Prototype

The surge, heave and pitch responses for truss spar are shown in Figures 4.28 to 4.30. The maximum RAOs were found to be at 0.055 Hz where 0.84 m/m for surge response, 0.43 m/m for heave response, and 0.33 deg/m for pitch response.

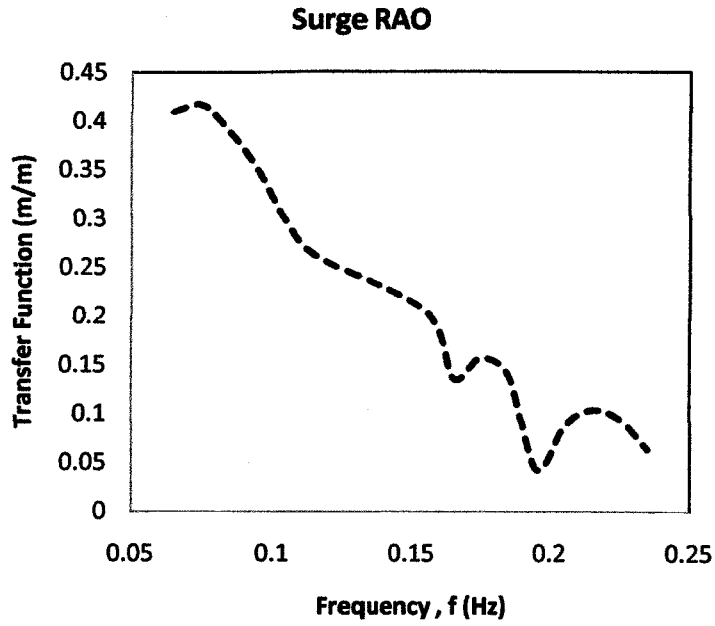


Figure 4.25: TD Analysis – Classic Spar Surge Response

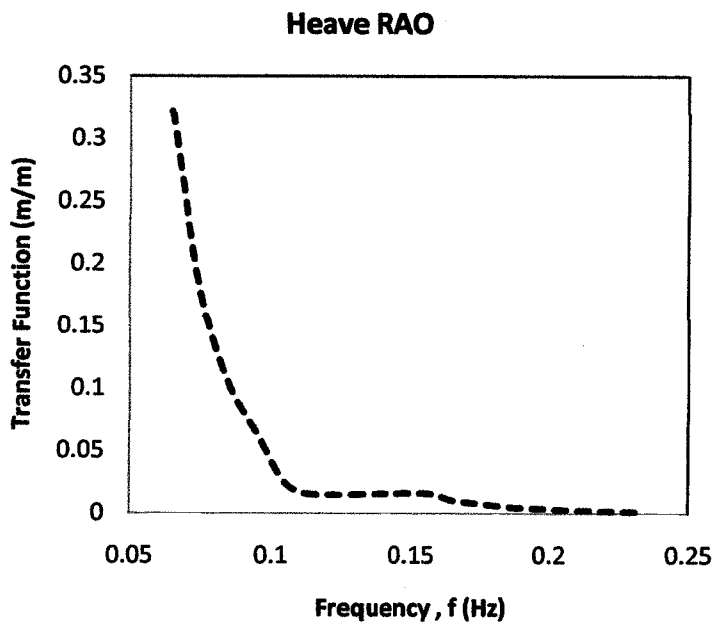


Figure 4.26: TD Analysis – Classic Spar Heave Response

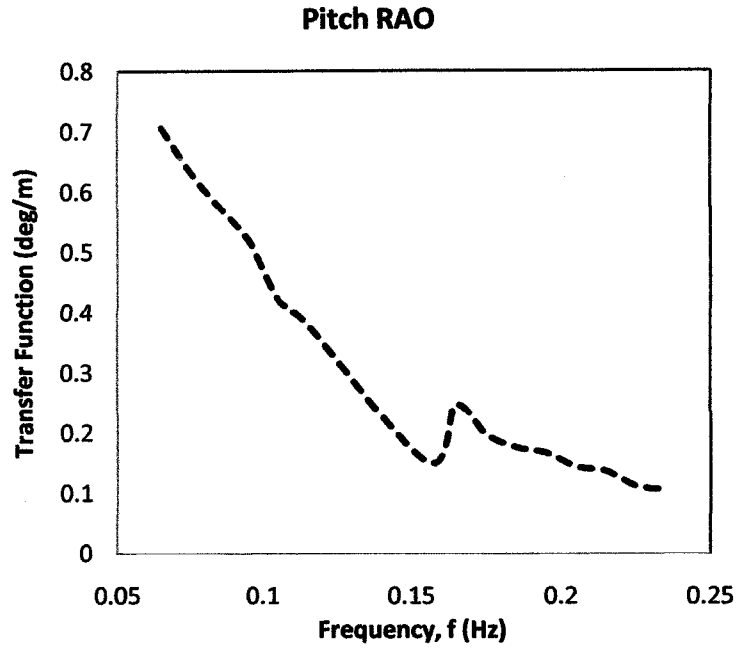


Figure 4.27: TD Analysis – Classic Spar Pitch Response

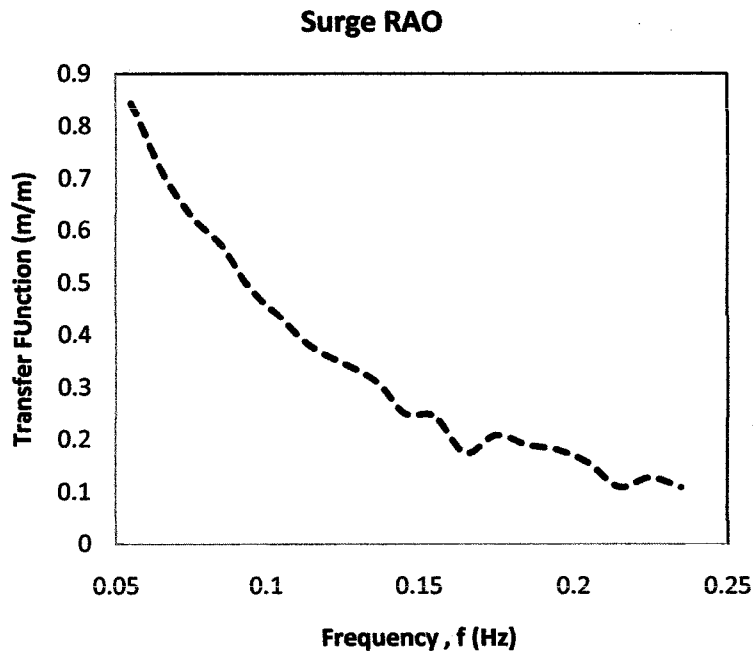


Figure 4.28: TD Analysis – Truss Spar Surge Response

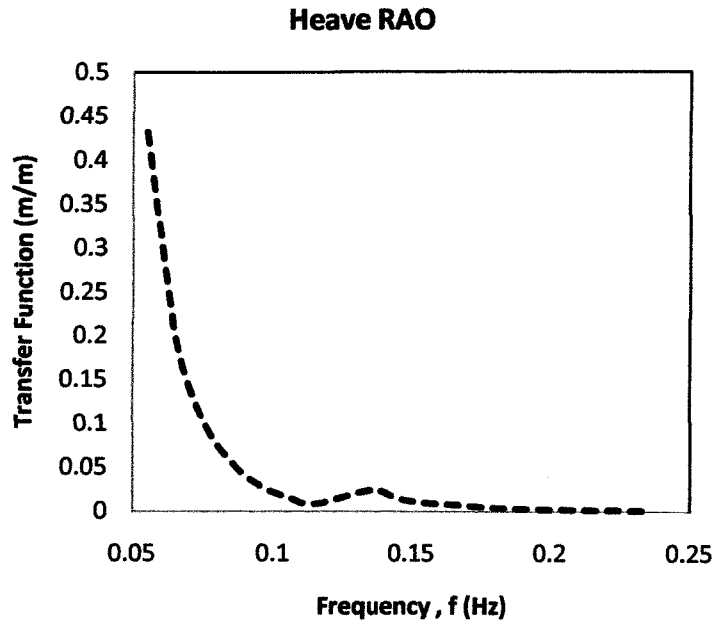


Figure 4.29: TD Analysis – Truss Spar Heave Response

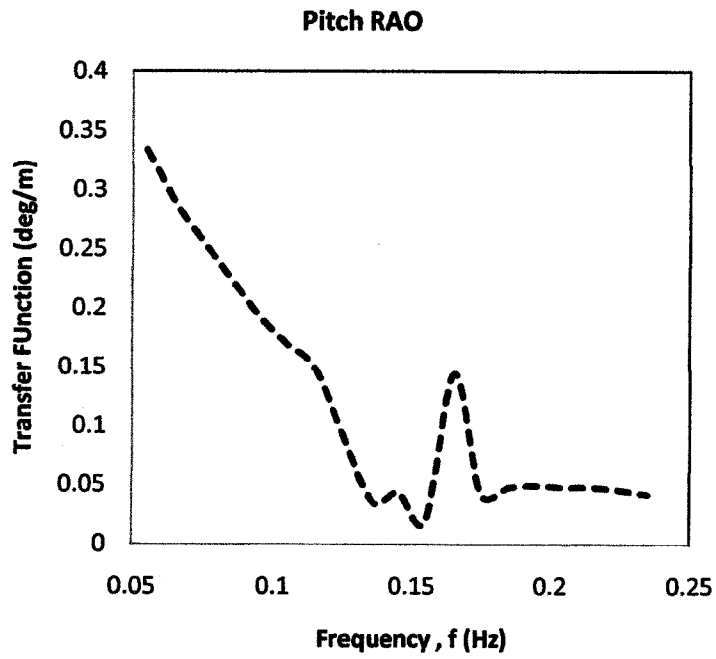


Figure 4.30: TD Analysis – Truss Spar Pitch Response

### 4.3.3 Spar Model Test Results

The wave tank tests were performed for both classic and truss spar models. For accuracy, the test was done for two times. The results show a very small difference and nearly the same. The results are presented below.

#### 4.3.3.1 Classic Spar Model Results

The surge, heave and pitch responses for classic spar are shown in Figures 4.31 to 4.33. The maximum RAOs were found to be at 0.055 Hz where 0.55 m/m for surge response, 2.85 m/m for heave response, and 0.86 deg/m for pitch response.

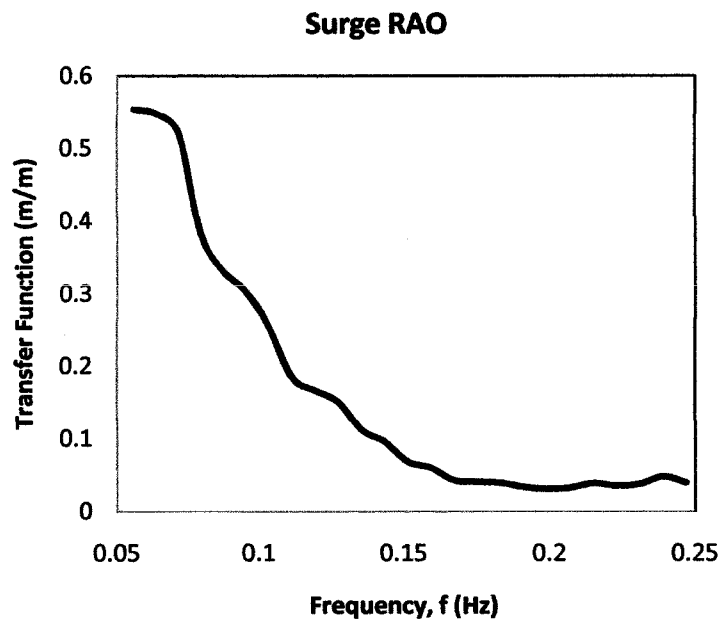


Figure 4.31: Model Test – Classic Spar Surge Response

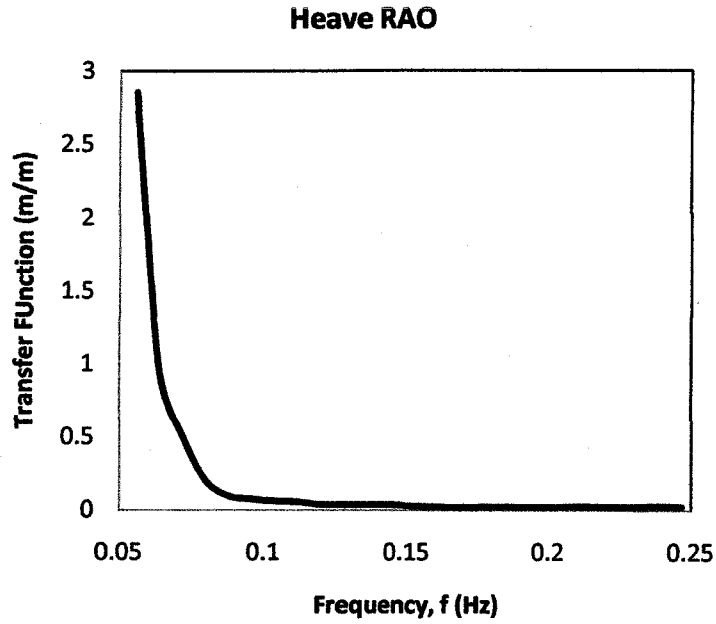


Figure 4.32: Model Test – Classic Spar Heave Response

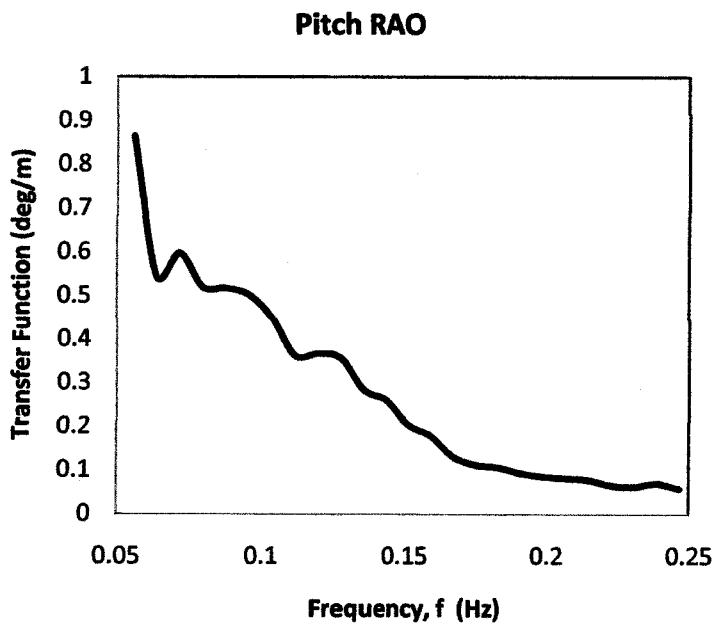


Figure 4.33: Model Test – Classic Spar Pitch Response

#### 4.3.3.2 Truss Spar Model Results

The surge, heave and pitch responses for truss spar are shown in Figures 4.34 to 4.36. The maximum RAOs were found to be at 0.055 Hz where 0.75 m/m for surge response, 1.79 m/m for heave response, and 0.92 deg/m for pitch response.

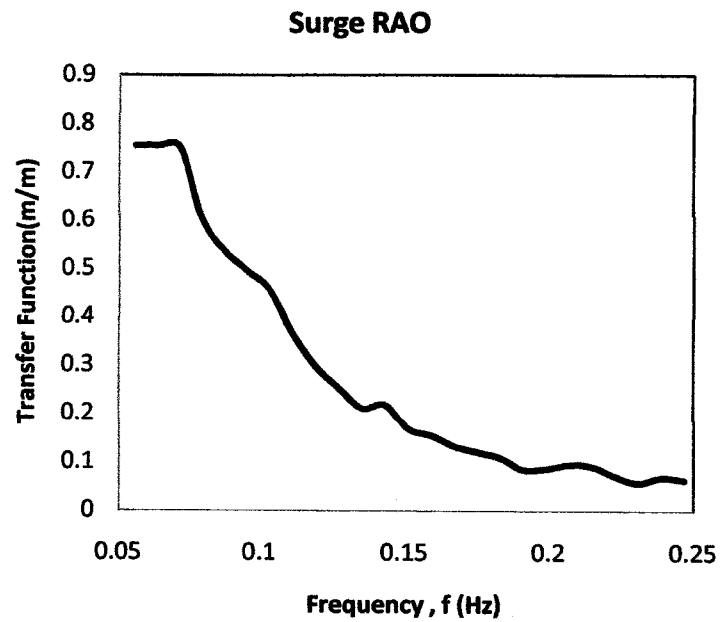


Figure 4.34: Model Test – Truss Spar Surge Response

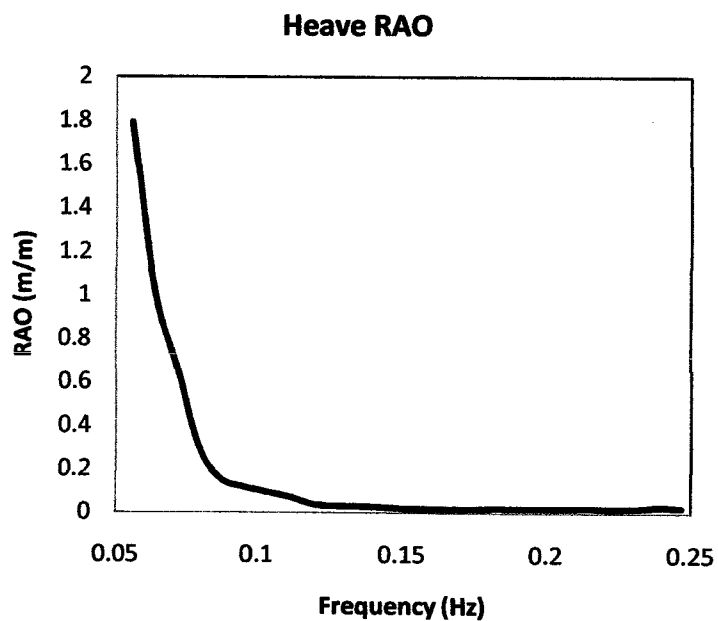


Figure 4.35: Model Test – Truss Spar Heave Response

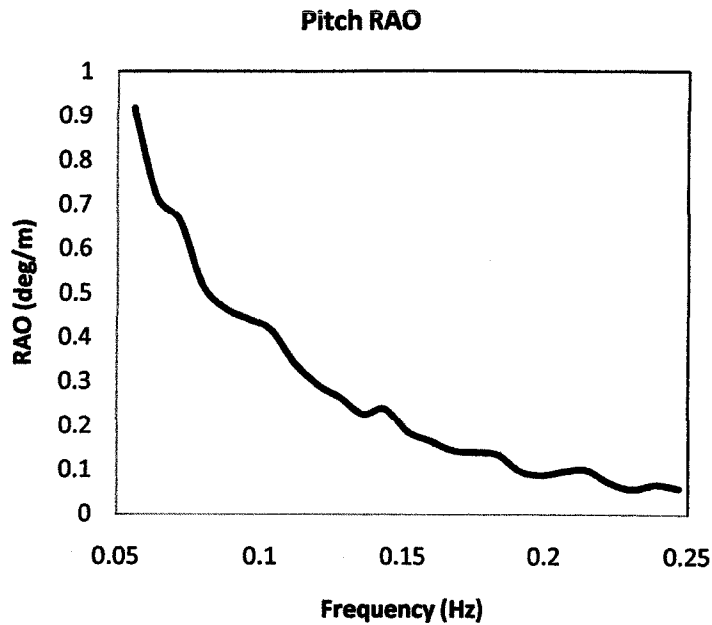


Figure 4.36: Model Test – Truss Spar Pitch Response

#### 4.3.4 Linear Wave Diffraction Analysis (LWD) using SACS Simulation Software

The simulation analysis of linear wave diffraction was done for both classic and truss spars. The responses of the classic and truss spars for surge, heave and pitch are presented below. The results were directly obtained in the output of the analysis.

##### 4.3.4.1 Classic Spar Prototype

The surge, heave and pitch responses for classic spar are shown in Figures 4.37 to 4.39. The maximum RAOs were found to be at 0.055 Hz where 1.02 m/m for surge response, 0.33 m/m for heave response, and 0.40 deg/m for pitch response

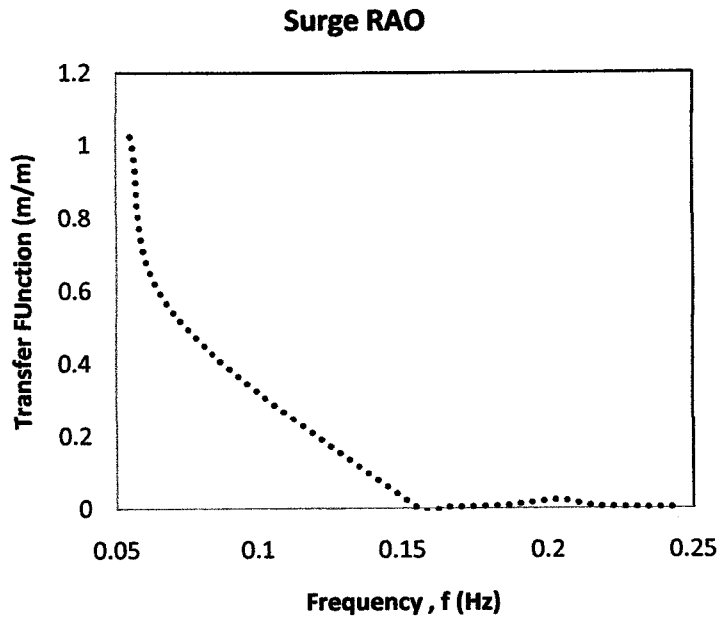


Figure 4.37: LWD Analysis – Classic Spar Surge Response

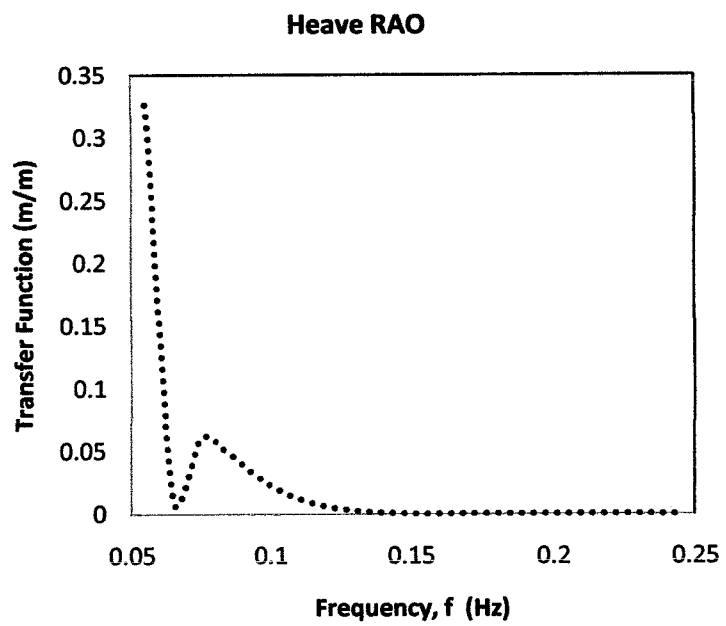


Figure 4.38: LWD Analysis – Classic Spar Heave Response

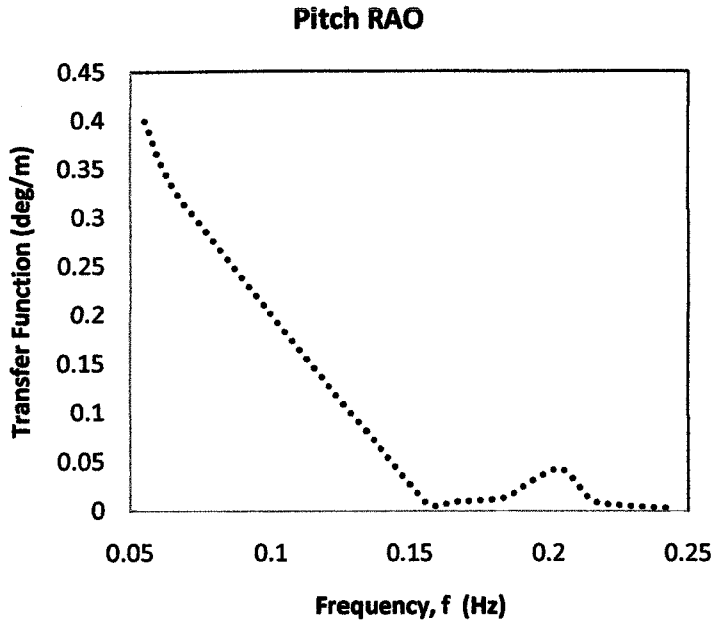


Figure 4.39: LWD Analysis – Classic Spar Pitch Response

#### 4.3.4.2 Truss Spar Prototype

The surge, heave and pitch responses for classic spar are shown in Figures 4.40 to 4.42. The maximum RAOs were found to be at 0.055 Hz where 0.50 m/m for surge response, 0.35 m/m for heave response, and 0.38 deg/m for pitch response.

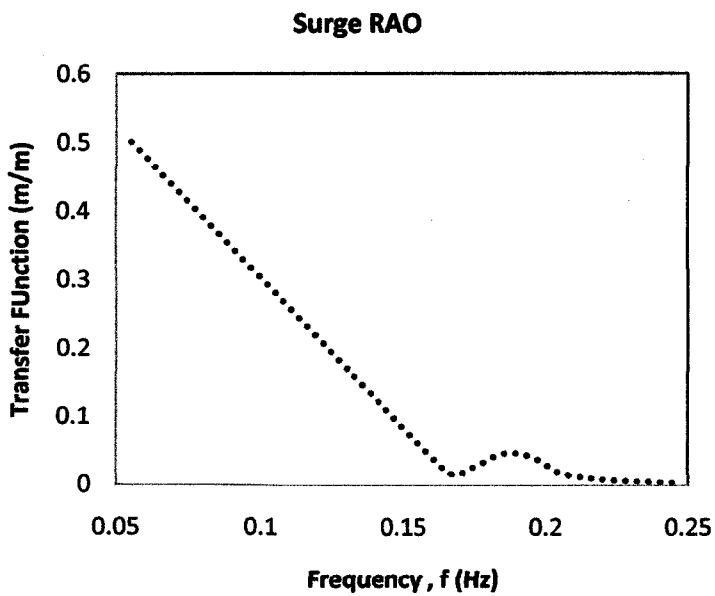


Figure 4.40: LWD Analysis – Truss Spar Surge Response

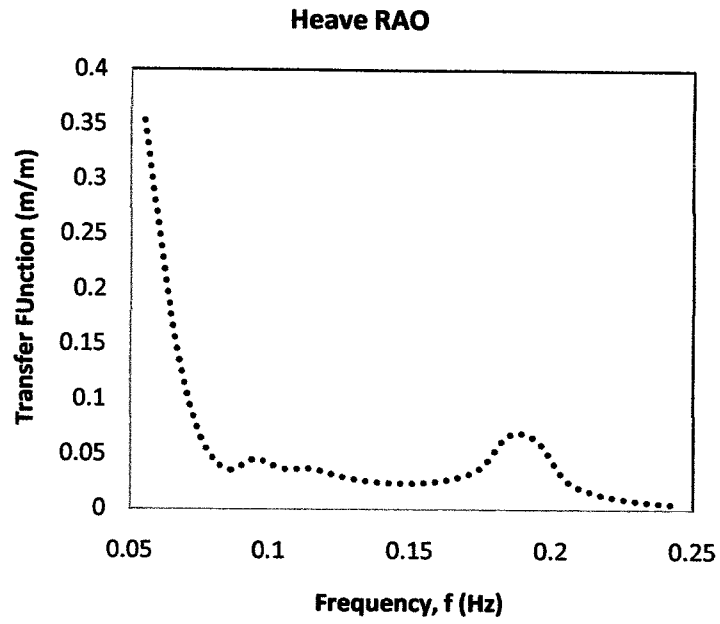


Figure 4.41: LWD Analysis – Truss Spar Heave Response

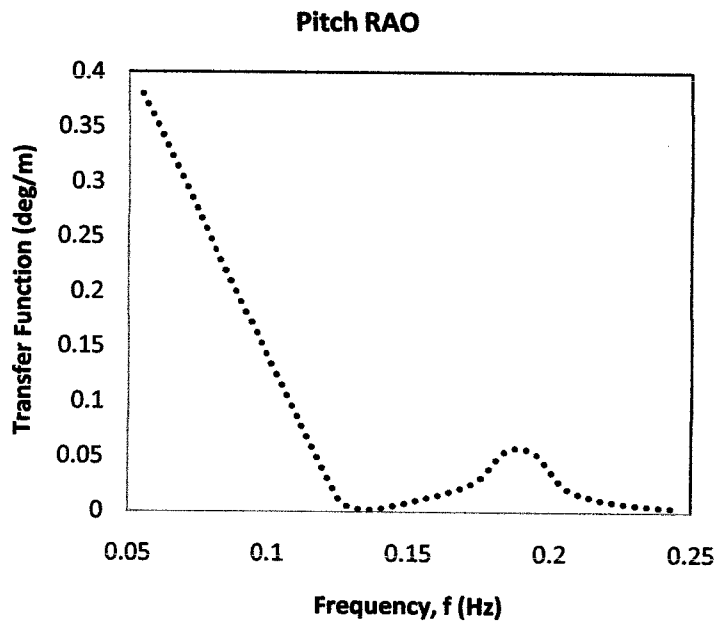


Figure 4.42: LWD Analysis – Truss Spar Pitch Response

### **4.3.5 Comparison of Results**

#### *4.3.5.1 Frequency Domain (FD) Analysis & Model Test Results*

The responses of the classic and truss spars physical model were determined numerically by using the model dimensions, properties, draft and the generated wave characteristics as inputs. Some of the results are presented. The results are compared with the corresponding model test results.

##### **4.3.5.1.1 Classic Spar-Comparison of Results**

The classic spar RAOs for surge, heave, and pitch of the model test processed results are compared to the FD analysis for random wave (RD3) combined with current (C1) in Figures 4.43, 4.44, and 4.45 respectively. For the surge RAO, although the trends of surge RAO were same, the value of surge RAO computed by FD analysis shows some variation when compared to the model test. The FD analysis results were higher in magnitude compared with the model test results for frequency above 0.1 Hz. For the heave RAO, it could be observed that both methods are in excellent agreement. For higher frequencies, the trends agreed with some differences in magnitude. For the pitch RAO, the comparison shows distinct differences between these two methods in terms of magnitude of RAO. The comparison between simplified FD analysis and model test marked significant difference at frequency 0.05 Hz. However, the trend of the model test results agreed with the numerical results of FD analysis for all frequencies above 0.085 Hz. The FD analysis results were lower compared to the model test results especially at the low frequency region. These discrepancies were due to the limitations such as neglect of diffraction effects as well as that could not be included in the analysis thereby underestimating the responses. However, the results of FD analysis can still be used during the preliminary design stage.

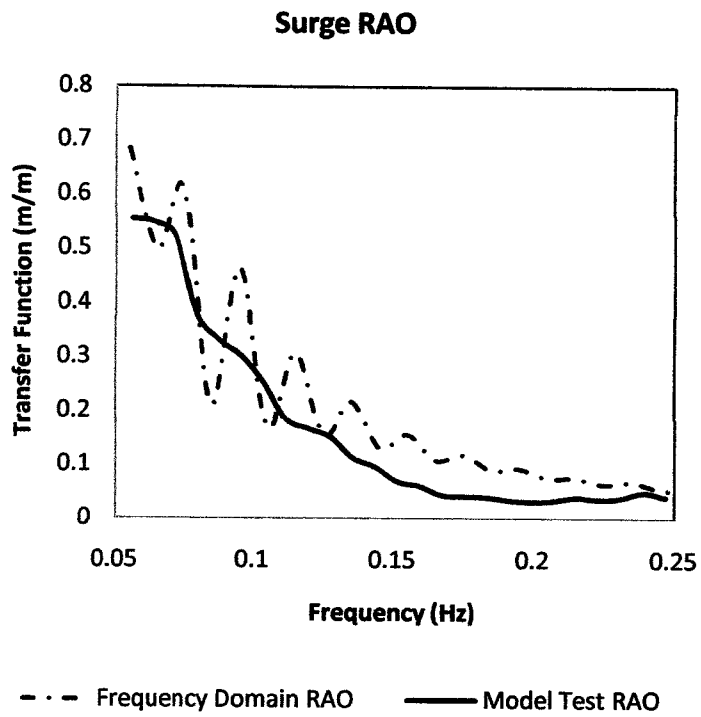


Figure 4.43: Surge RAO Comparison for Classic Spar Subjected to Random Wave (RD3) and Current (C1)

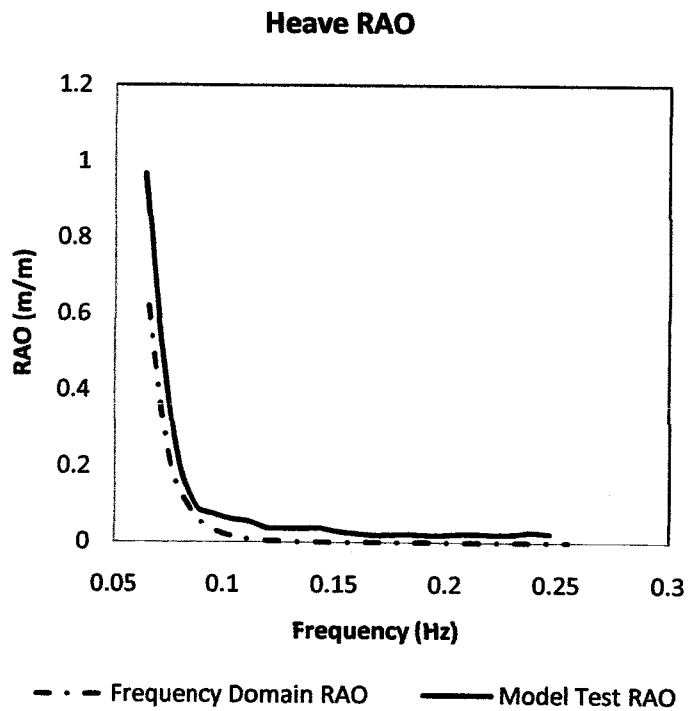


Figure 4.44: Heave RAO Comparison for Classic Spar Subjected to Random Wave (RD3) and Current (C1)

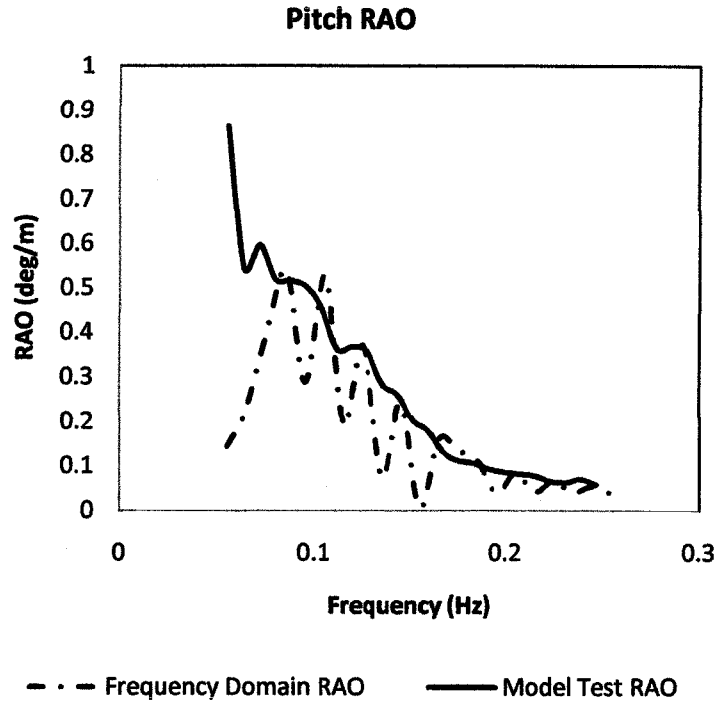


Figure 4.45: Pitch RAO Comparison for Classic Spar Subjected to Random Wave (RD3) and Current (C1)

#### 4.3.5.1.2 Truss Spar-Comparison of Results

Figures 4.46 to 4.48 show the comparison of the truss spar RAOs for surge, heave, and pitch between the experimental model test processed results and the FD analysis for random wave (RD3) combined with current (C1) in respectively. For the surge RAO, the trend of the experimental results agreed by the numerical results of FD analysis for all frequencies. The FD domain analysis results were higher compared to the experimental results for frequency above 0.11 Hz. For the heave RAO, all methods resulted in almost similar results for the frequency above 0.15 Hz. The trends of the numerical results for FD analysis agreed with the experimental results for higher frequencies. The model test RAO and FD analysis RAO showed some variations in the frequency range 0.07 – 0.14 Hz. This discrepancy was probably due to optical camera resolution, thus underestimating the structural responses. For the pitch RAO, although the trends of pitch RAO were same, the value of pitch RAO computed by FD analysis shows some variation when compared with model test results. This might be because the FD analysis did not consider the nonlinearities in the analysis. However, the results of FD analysis can still be used during the

preliminary design stage. Due to the limitations of the aforementioned methods, for the comparison hereafter, only the time domain (TD) analysis and model test results are compared with the corresponding linear wave diffraction (LWD) simulation analysis using SACS results for validation.

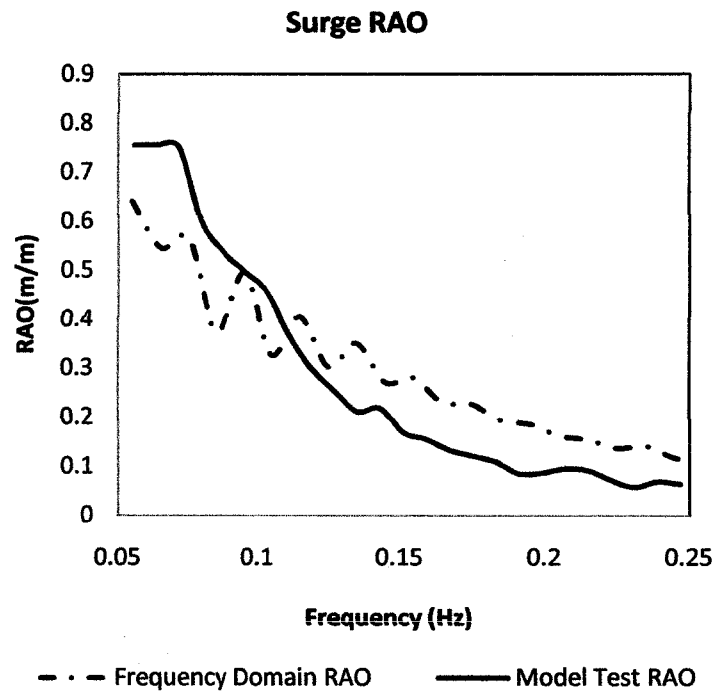


Figure 4.46: Surge RAO Comparison for Truss Spar Subjected to Random Wave (RD3) and Current (C1)

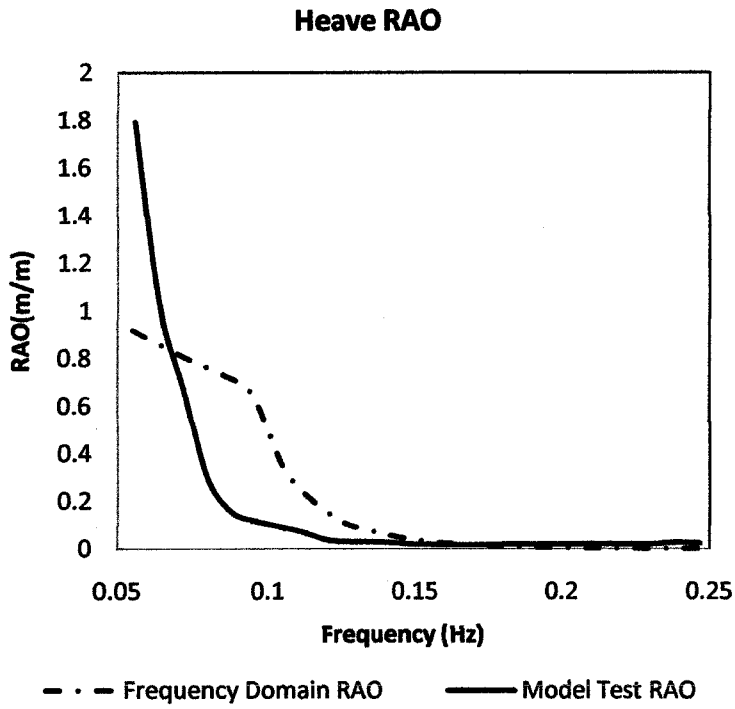


Figure 4.47: Heave RAO Comparison for Truss Spar Subjected to Random Wave (RD3) and Current (C1)

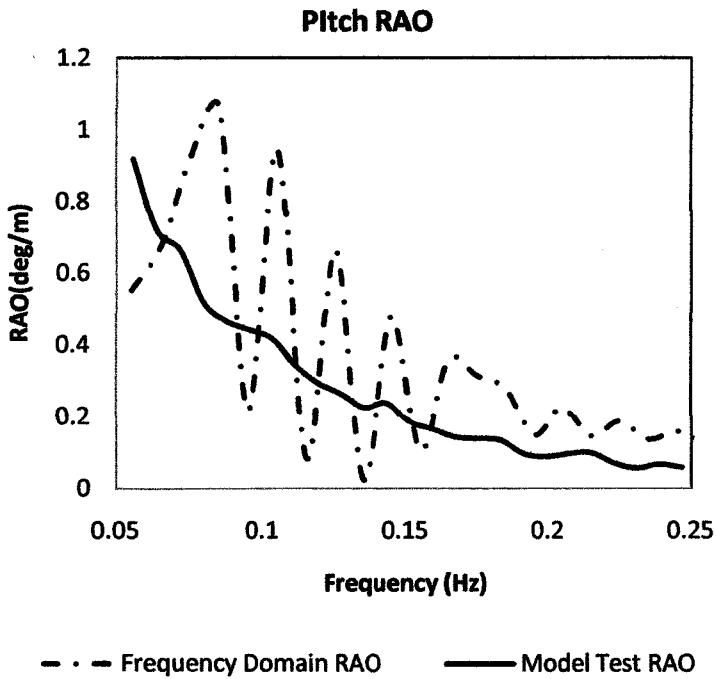


Figure 4.48: Pitch RAO Comparison for Truss Spar Subjected to Random Wave (RD3) and Current (C1)

#### *4.3.5.2 Time Domain (TD) Analysis, Model Test, & Linear Wave Diffraction (LWD) Analysis Results*

The RAO for three degrees of freedom obtained from TD analysis and model tests were compared with the LWD analysis using SACS software for validation. These comparisons for classic and truss spar subjected to random wave (RD3) and current (C1) are discussed in this section.

##### *4.3.5.2.1 Classic Spar-Comparison of Results*

The surge RAO for the classic spar subjected to random wave (RD3) combined with current (C1) is shown in Figure 4.49. From the graph, it could be observed that the trend of the model tests and TD results are in excellent agreement with the simulation results. The TD analysis results were higher compared with the other analysis results for frequency above 0.105 Hz. A wide variation between TD results and LWD results showed at low frequency. However, in this study the low frequency was not included in the analysis. Figure 4.50 shows the heave RAO for the classic spar subjected to random wave (RD3) combined with current (C1). From the graph, the trend of the LWD results agreed by the model test and TD results for the frequencies above 0.075 Hz. At lower frequencies, the model test response was higher than both responses by TD analysis and LWD results. This discrepancy was due to the limitations during the model tests such as the reflected wave coming from the wall of the wave tank and the wave absorber had increased the structural responses, thus overestimating the response. The pitch RAO for the classic spar subjected to random wave (RD3) combined with current (C1) is shown in Figure 4.51. It can be observed that the pitch RAO obtained by LWD analysis using SACS follows the same trend with the TD analysis and model test responses but with lower magnitude for all frequencies. The difference in pitch response obtained from the LWD analysis is smaller than the pitch response obtained from the other methods for all frequencies while the pitch RAO for model test are in a good agreement with pitch responses calculated using TD analysis.

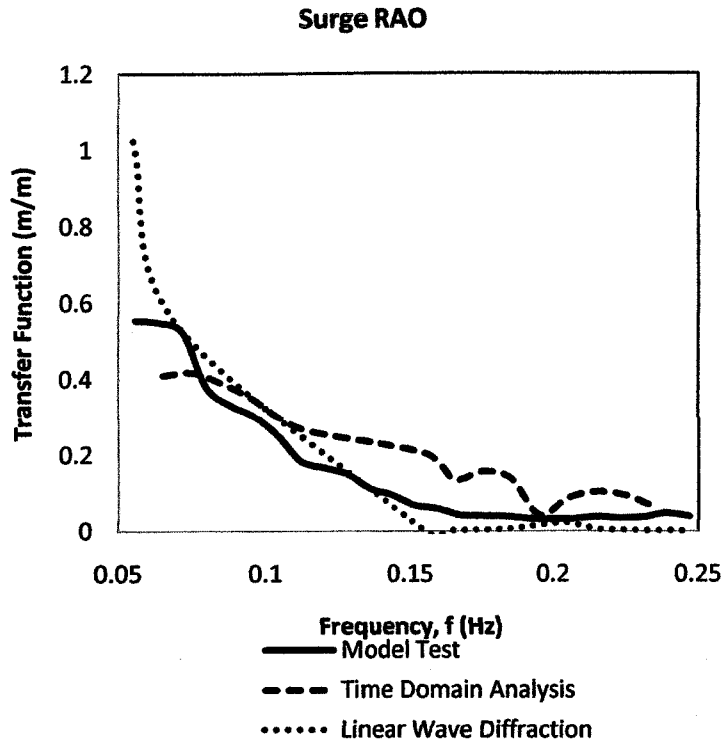


Figure 4.49: Surge RAO Comparison for Classic Spar Subjected to Random Wave (RD3) and Current (C1) for Different Methods

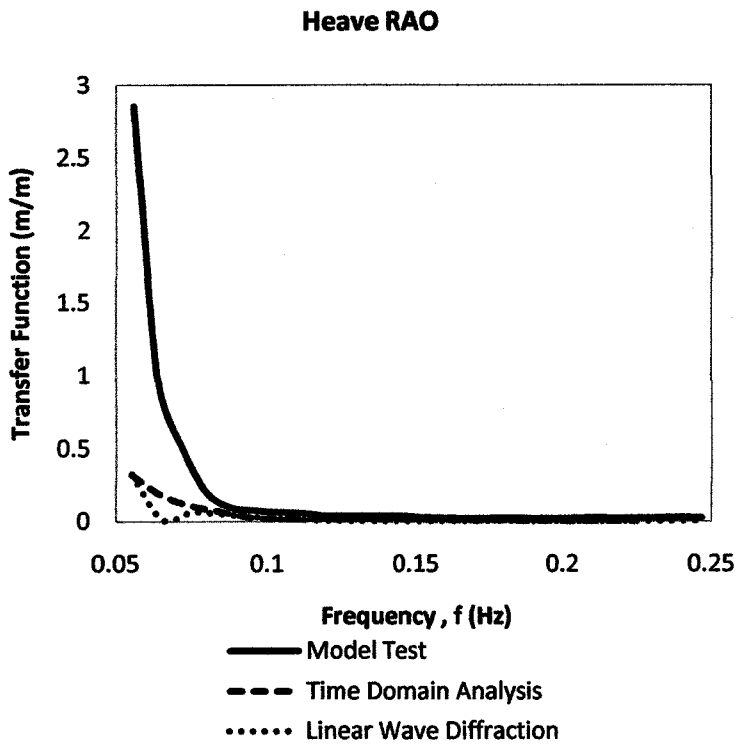


Figure 4.50: Heave RAO Comparison for Classic Spar Subjected to Random Wave (RD3) and Current (C1) for Different Methods

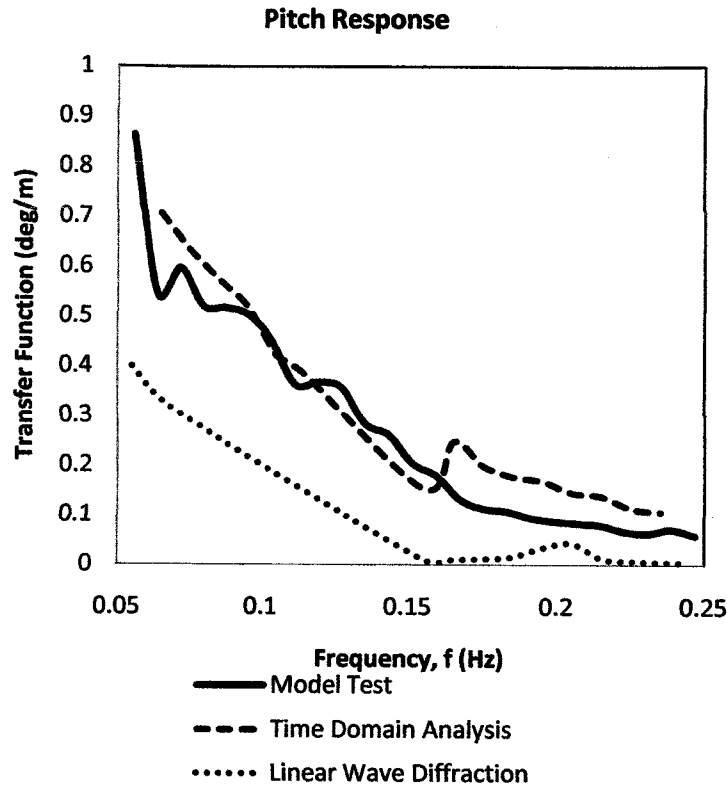


Figure 4.51: Pitch RAO Comparison for Classic Spar Subjected to Random Wave (RD3) and Current (C1) for Different Methods

#### 4.3.5.2.2 Truss Spar-Comparison of Results

The surge RAO for the truss spar subjected to random wave (RD3) combined with current (C1) is shown in Figure 4.52. It can be observed that the surge RAO obtained by LWD analysis using SACS follows the same trend with the TD analysis and model test responses but with lower magnitude for all frequencies. The difference in surge response obtained from the LWD analysis is smaller than the surge response obtained from the other methods by 15% for all frequencies while the surge RAO for model test are in a good agreement with surge responses calculated using TD analysis. Figure 4.53 shows the heave RAO for the truss spar subjected to random wave (RD3) combined with current (C1). From the graph, the trend of the LWD results agreed with the model test and TD results for the frequencies above 0.13 Hz. At lower frequencies, the model test response was higher than both responses by TD analysis and LWD results. The pitch RAO for the truss spar subjected to random wave (RD3) combined with current (C1) is shown in Figure 4.54. From the graph, the trend of the LWD results agreed with the TD results for all frequencies. The difference in pitch

response obtained from the model test is higher compared to the pitch responses obtained from the other methods for all frequencies while the pitch RAO for LWD analysis are in a good agreement with pitch responses calculated using TD analysis. The same trend showed by the heave response. This might be because of the limitations during the model tests such as the reflected wave coming from the wall of the wave tank and the wave absorber had increased the structural responses, thus overestimating the responses.

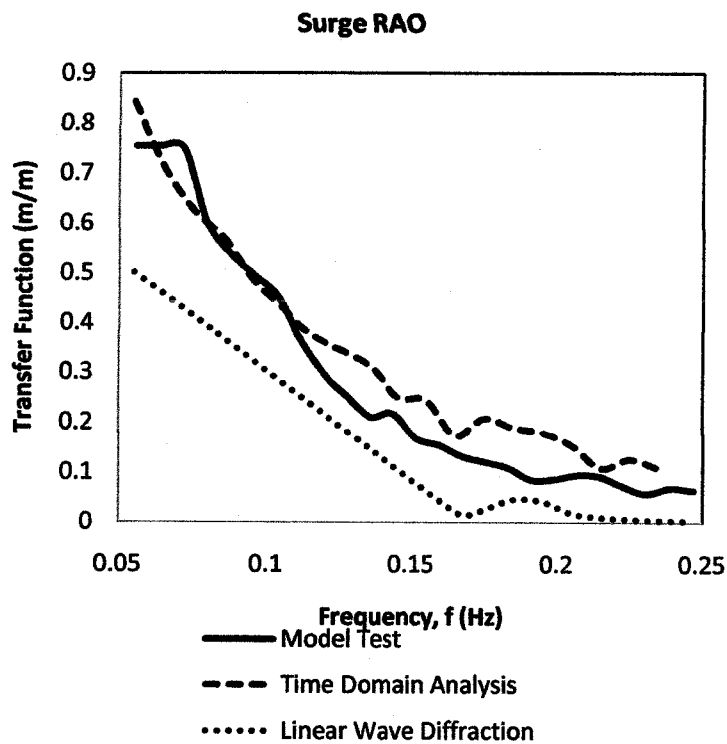


Figure 4.52: Surge RAO Comparison for Truss Spar Subjected to Random Wave (RD3) and Current (C1) for Different Methods

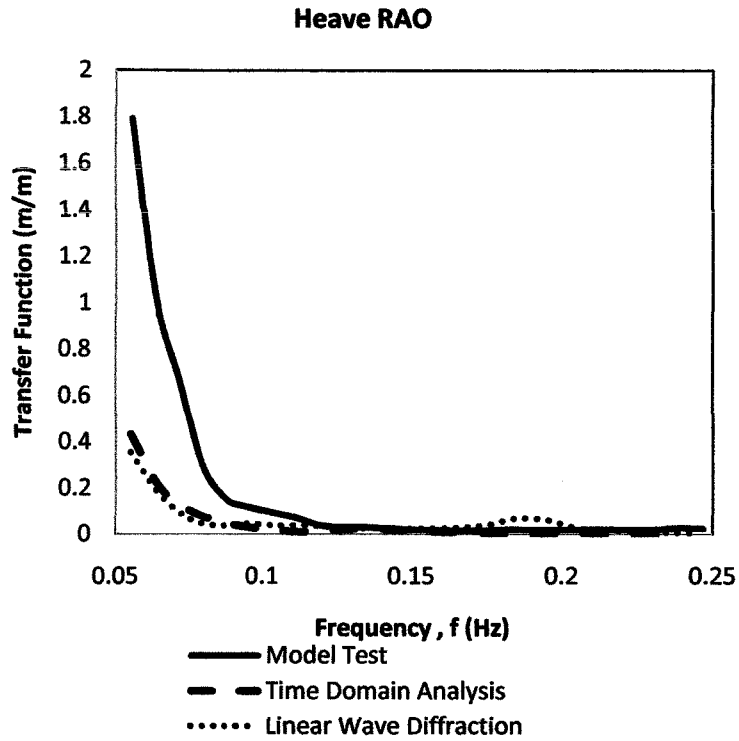


Figure 4.53: Heave RAO Comparison for Truss Spar Subjected to Random Wave (RD3) and Current (C1) for Different Methods

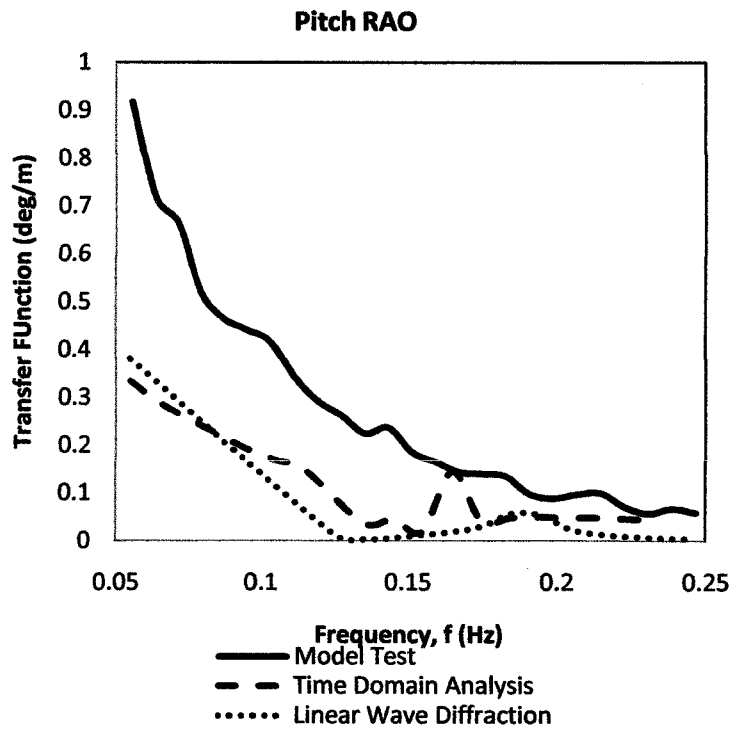


Figure 4.54: Pitch RAO Comparison for Truss Spar Subjected to Random Wave (RD3) and Current (C1) for Different Methods

## **4.4 Parametric Study**

The experimental parametric study is done in order to determine the effect of important parameter which is the current velocities and the type of the structures. The results are summarized below.

### **4.4.1 Current Velocities**

Figures 4.55, 4.56, and 4.57 show the comparison of surge, heave, and pitch RAO for different currents respectively. The graphs present the comparison between a set of currents which are C2, C3, and C5 and the currents were having velocities of 1.29 m/s, 1.05 m/s, and 0.086 m/s respectively. From all figures, the results found the RAO value for C2 was the highest compared to the other currents, C3 and C5. This showed the highest current gave the highest response. This might be because the existence of current had given an additional lateral force in the water body which increased the surge and pitch structure resonance. As a result, while the current velocities were increasing, the responses of the structure responses were increasing. For all comparisons, the RAO values were same in trend and near in values. Since the result shows the presence of current in the water body has given a significant influence to the structure response, thus the inclusion of the current in the structural response analysis is very essential.

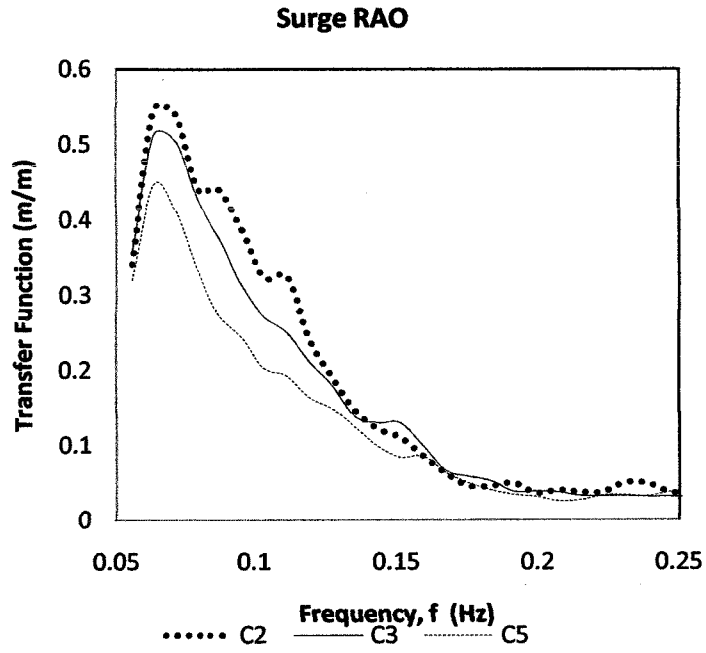


Figure 4.55: Surge RAO Comparison for Different Currents

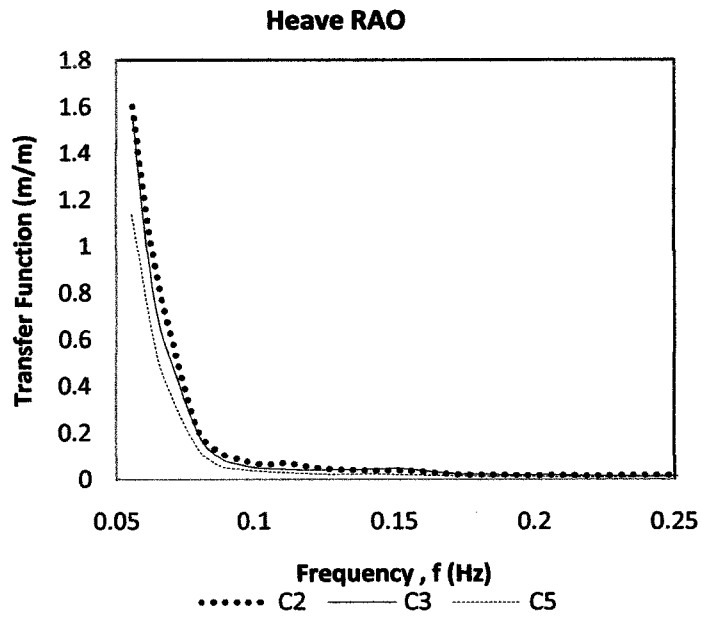


Figure 4.56: Heave RAO Comparison for Different Currents

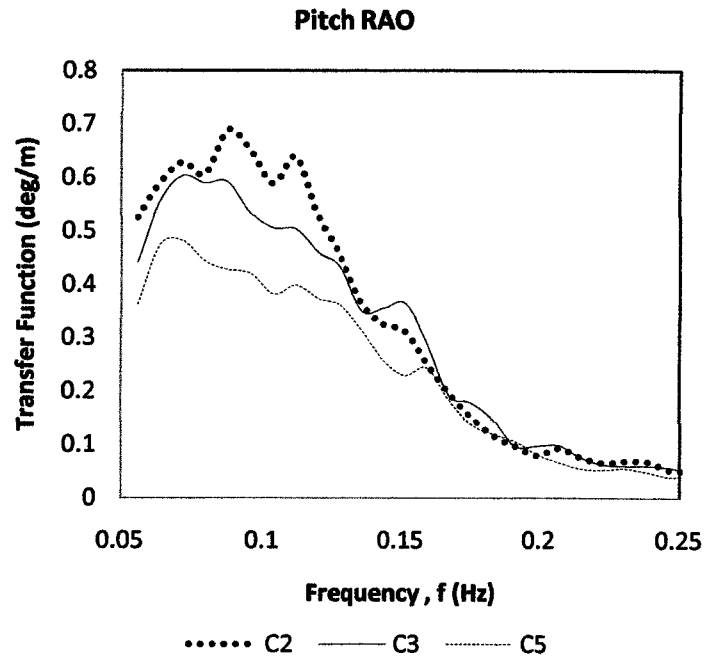


Figure 4.57: Pitch RAO Comparison for Different Currents

#### 4.4.2 Type of Spars

Figures 4.58, 4.59, and 4.60 present the comparison of structure responses in surge, heave, and pitch between two types of spars which are classic and truss spars. From all figures, the results found the surge and heave RAO values for classic spar was higher compared to the truss spar. This might be because the stability of the truss spar had reduced the structure responses. For pitch response, the RAO values for both spar were found to have a small difference in magnitude and nearly the same. As a conclusion, the truss spar had lower responses compared to the classic spar, thus, the truss spar was the most preferable structure to be installed in the Malaysian offshore regions.

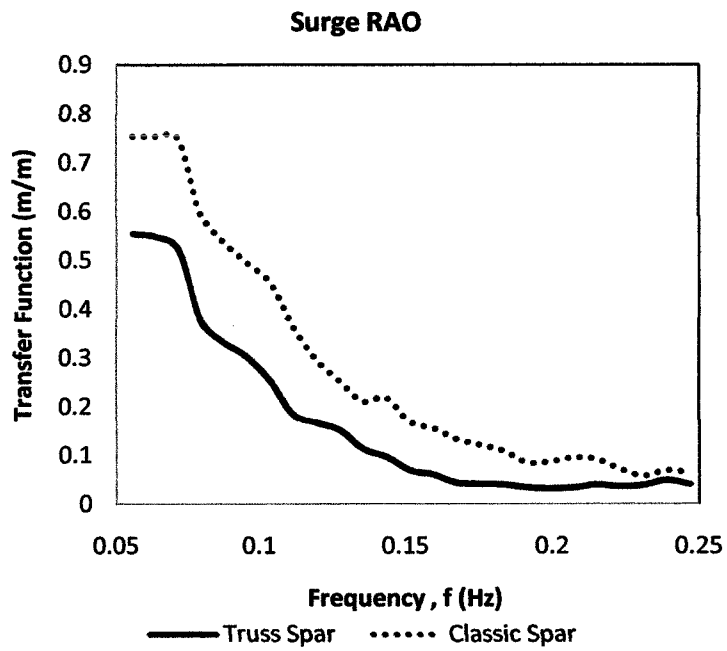


Figure 4.58: Surge RAO Comparison for Different Spars

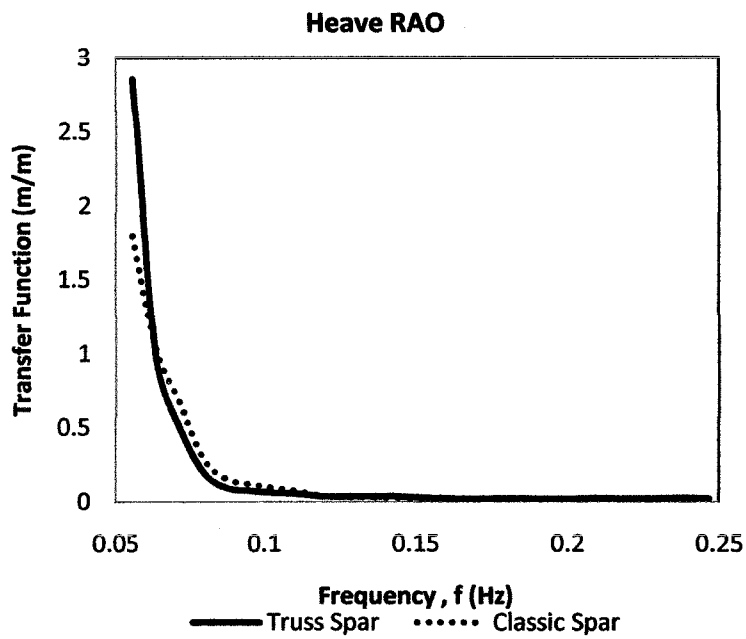


Figure 4.59: Heave RAO Comparison for Different Spars

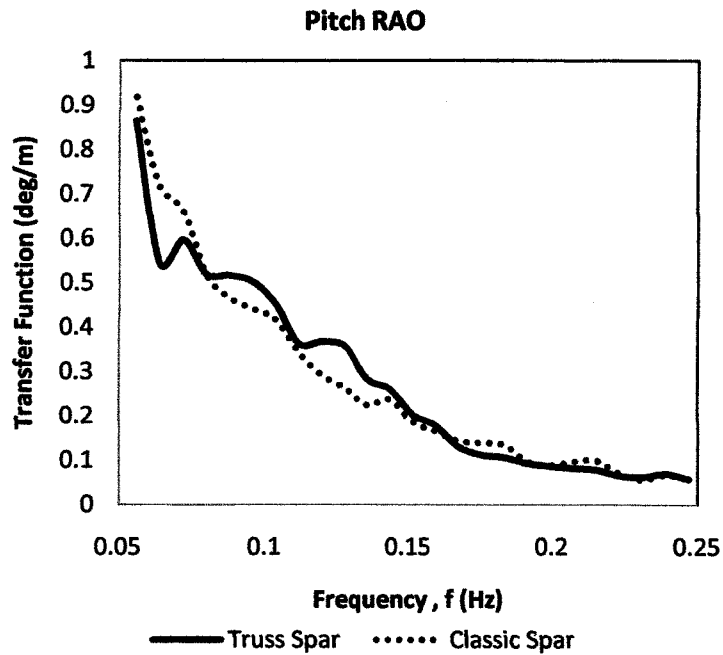


Figure 4.60: Pitch RAO Comparison for Different Spars

#### 4.5 Chapter Summary

This chapter presented the typical responses obtained from the numerical analysis which include frequency and time domain analysis, the model tests, and also the simulation analysis using SACS software. Also, the comparison of the RAO between those methods were presented and discussed. For validation, the RAO values from the numerical analysis and model tests were compared to the simulation analysis. In addition, a parametric study was done to determine the effect of important parameter which are the current velocities and the type of structures.

## CHAPTER 5

### CONCLUSIONS AND FURTHER STUDIES

#### **5.1 Chapter Overview**

In this study, the response of the spar platforms subjected to both wave and current were determined. The combination of these two loadings results in significant response on the structure. As discussed in Chapter 3, the frequency and time domain analyses were conducted in order to study the response behavior of the structures when subjected to the wave and current loads. Model tests were done in the UTP laboratory for both classic and truss spar as well. A simulation work was done in linear diffraction analysis by using commercial software called SACS. In Chapter 4, the results from each analysis were compared for validation. Also, a parametric study of different current velocities and types of the spars were also conducted. This chapter summarizes and concludes the results obtained in this study. Some suggestions for further studies are explained at the end of this chapter.

#### **5.2 Conclusions**

Based upon the studies described earlier, the following conclusions were derived.

1. Dynamic frequency domain analysis was successfully completed for various wave and current combinations. The response in terms of RAOs for surge, heave, and pitch were obtained for regular and random waves added to current and plotted. This analysis used simplifying assumptions to make it linear. Dynamic time domain analysis was successfully completed using the Newmark Beta Method. The time series, spectra, and RAOs were obtained for various wave and current combinations. As was discussed in Chapter 4, time domain analysis proved to be more accurate compared to frequency domain analysis.

2. Experimental model tests were conducted for various wave and current combinations selected for the study based on the Metocean data and laboratory limitations. The results were analyzed and the RAOs were plotted. Linear Wave Diffraction Analysis was conducted using the SACS commercial software. The RAOs were directly obtained. The time domain analysis RAOs were compared with model test results and simulation results for surge, heave, and pitch for both types of spars. The trend of the results agreed well for surge and heave for both types of spars, except for a small range in the low frequency. This is because the time domain analysis did not consider the low frequency forces. For pitch response, the simulation result was lower compared to the other two results in the case of classic spar. For truss spar pitch response, both the time domain and simulation results were lower compared to the model tests. This proved that pitch response is not well predicted by both time domain and simulation. It could also be found that there was some experimental error in the pitch response measurement.
  
3. The parametric study for varying current velocities has clearly shown that the highest current velocity gave highest response. This might be because the existence of current had given additional lateral forces in the water body which increased structure resonance. Hence, it is necessary to include wave added to current in the analysis of spars for all the Malaysia offshore regions. Besides, another parametric study was done for two types of structures which are classic and truss spars. The results shows that the truss spar was having lower response compared to the classic spar in heave and pitch. This shows that truss spar was having higher stability compared to the classic spar. Hence, the truss spar is more preferable in the design of offshore structures.

### **5.3 Future Studies**

From this study, there are some recommendations for future studies.

#### **1. Model Test**

- a. **Current velocity** – a series of current velocities with large interval should be generated to see a clear effect of the current in the water body.
- b. **Current direction** – a series of current with an opposing direction with the wave should be generated in order to see the changing behavior of the wave and the response of the structure.
- c. **Wave direction** - instead of uni-directional wave, the bi-directional and multi directional waves combined with current should be generated in order to see the response of the structure.
- d. **Water depth** – a wave tank test in a deeper water depth should be done in order to fit the right scale.
- e. **Platform model** – another type of floating structures such as semi-submersible should be used for the model test in order to see the effect of the wave-current interaction on the structure.

#### **2. Software Simulation**

- a. Another commercial software such as FINEMARINE and SESAM can be used for validation.

## REFERENCES

- [1] M. Olabarrieta, R. Medina, & S. Castanedo. (2010). Effects of Wave-Current Interaction on the Current Profile. *Journal of Coastal Engineering* , 643-654.
- [2] M. Popescu, & A. Simbotin. (2002). Hydrodynamic Loads on Offshore Platform Structures. *Ovidius University Annals of Construction* (pp. 433-438). Romania: Ovidius University Press.
- [3] M. Isaacson, & K. F. Cheung. (1993). Time Domain Solution for Wave-Current Interactions with a Two Dimensional Body. *Applied Ocean Research* , 39-52.
- [4] C. H. Wang, W. H. Wai, Y. S. Li, & Y. Chen. (2006). Modelling of the Wave-Current Interaction in the Pearl River Estuary. *Conference of Global Chinese Scholars on Hydrodynamics*, (pp. 159-165). Hong Kong, China.
- [5] S. K. Chakrabarti. (1994). *Hydrodynamics of Offshore Structures*. USA: WIT Press.
- [6] V. J. Kurian, M. A. Gasim, & S. P. Narayanan. (2009). Frequency and Time Domain Analyses for TLP Responses. *7th Asia Pacific Structural Engineering & Construction Conference 2009*, (pp. 555-560). Pulau Langkawi.
- [7] N. Roitman, R. F. Andrade, & R. C. Batista. (1992). Dynamic Responses Analysis of a Small-Scale Model Tension Leg Platform. *Marine Structures* , 491-513.
- [8] I. Anam, J. M. Roesset, & J. M. Niedzwecki. (2003). Time Domain and Frequency Domain Analysis of Spar Platform. *The Thirteenth International Offshore and Polar Engineering Conference*, (pp. 240-247). Honolulu, Hawaii, USA.
- [9] V. J. Kurian, B. S. Wong, & O. A. A. Montasir. (2008). Frequency Domain Analysis of Truss Spar Platform. *International Conference of Construction and Building Technology*, (pp. 235-244). Kuala Lumpur.

- [10] O. A. Montasir, V. J. Kurian, N. & Shafiq. (2009). Numerical and Model Test Results for Truss Spar Platform Subjected to Random Waves. 2nd International Conference on Engineering Technology, (pp. 1-6). Kuala Lumpur.
- [11] J. Wolf, & D. Prandle. (1999). Some Observation of Wave-Current Interaction. *Coastal Engineering* , 471-485.
- [12] M.A. Tayfun, R. A. Dalrymple, & C. Y. Yang. (1976). Random Wave-Current Interactions in Water of Varying Depth. *Ocean Engineering* , 3, 403-420.
- [13] O. T. Gudmestad, & D. Karunakaran. (1990). Wave Current Interaction. *Environmental Forces on Offshore Structures and Their Prediction*, (pp. 81-110). Netherlands.
- [14] Z. Liu, B. Teng, D. Ning, & Y. Gou, (2009). Wave-Current Interactions with Three-Dimensional Floating Bodies. *Journal of Hydrodynamics* , 229-240.
- [15] J. F. Wilson. (2002). Dynamics of Offshore Structures. USA: John Wiley & Sons, Inc., Hoboken, New Jersey.
- [16] A. B. Saiful Islam, M. Jameel, M. Z. Jumaat, & S. M. Shirazi. (2011). Spar Platform at Deep Water Region in Malaysian Sea. *International Journal of the Physical Sciences* , 6872-6881.
- [17] Welton, G. C., & Guez, D. a. (2003). *Spar Overview*. Technip-Coflexip. Available: <http://phx.corporate-ir.net>
- [18] Halkyard, J. (2001). Spar Global Response. The Coflexip Stena Offshore Group. Available:  
<http://info.ogp.org.uk/metocean/FloatingSystems/presentations/Halkyard.pdf>
- [19] Barton, C. M. *An Overview of Offshore Concept*. FloaTEC. Available: [http://www.thepaltforma.org/files/Offshore\\_Concepts.pdf](http://www.thepaltforma.org/files/Offshore_Concepts.pdf)

- [20] M. Y. Luo, J. J. Wang, & R. R. Lu. (2003). Spar Topsides-to-Hull Connection Fatigue – Time Domain vs. Frequency Domain. International Offshore and Polar Engineering Conference (pp. 280-284). Hawaii, USA: The International Society of Offshore and Polar Engineers.
- [21] B. B. Mekha, D. C. Weggel, C. P. Johnson, & J. M. Roesset. (1996). Effects of second Order Diffraction Forces on the Global Response of Spars. International Offshore and Polar Engineering Conference (pp. 273-280). Los Angeles: The International Society of Offshore and Polar Engineers.
- [22] *Review of Deepwater Floating Structures and Dry Tree Semi Developments*. (2006, November). Retrieved February 23, 2012, from [http://www.floatec.com/images/pr\\_content/DOT-2006-Presentation.pdf](http://www.floatec.com/images/pr_content/DOT-2006-Presentation.pdf)
- [23] *Kikeh - Malaysia First Deepwater Project*. (n.d.). Retrieved May 30, 2012, from Murphy Oil Corporation: <http://www.murphyoil.com>
- [24] DNV. (2010, October). *Global Performance Analysis of Deepwater Floating Structures*. Retrieved October 2012, from Det Norske Veritas: Available: <http://exchange.dnv.com/publishing/Codes/download.asp?url=2009-04/rp-f205.pdf>
- [25] N. Haritos. (2007). Introduction to the Analysis and Design of Offshore Structures - An Overview. *Loading on Structures* , 55-65.
- [26] K. Merz. (2010). *A Review of the Morrison Equation for Calculating Hydrodynamic Loads on Vertically-Oriented Cylinder*. Norway: NTNU. Available: [http://www.sintef.no/project/Nowitech/Wind\\_presentations/Merz,%20K.O.,%20NTNU.pdf](http://www.sintef.no/project/Nowitech/Wind_presentations/Merz,%20K.O.,%20NTNU.pdf)

- [27] P. M. Aagaard, & R. G. Dean. (1969). Wave Forces: Data Analysis and Engineering Calculation Method. Offshore Technologies Conference, (pp. 95-102). Dallas, Texas.
- [28] E. L. Wilson. (2002). Three-Dimensional Static and Dynamic Analysis of Structures. California: Computers and Structures. Inc.
- [29] Dynamic Analysis by Numerical Integration. In *Static and Dynamic Analysis* (pp. 1-111). Available: <http://www.csiberkeley.com/system/files/technical-papers/20.pdf>
- [30] G. B. Burke, & J. Y. Tighe. (1972). A Time Series Model for Dynamic Behavior of Offshore Structures. *Society of Petroleum Engineers Journal* , 156-170.
- [31] E. Huse. (1996). *Workshop on Model Testing of Deepsea Offshore Structures*. ITTC. Available: <http://itc.sname.org/proc21/Model%20Testing%20of%20Deep%20Sea%20Offshore%20Structures.pdf>
- [32] K. Hebblewhite, P. K. Sahoo, & L. J. Doctors. (2007). A Case Theoretical and Experimental Analysis of Motion Characteristics of a Trimaran Hull Form. *Ships and Offshore Structures* , 149-156.
- [33] F. Zhang, J. Yang, R. Li, & G. Chen. (2008). Coupling Effects for Cell-Truss Spar Platform: Comparison of Frequency- and Time-Domain Analysis with Model Tests. *Journal of Hydrodynamics* , 424-432.
- [34] Q. W. Ma, & M. H. Patel. (2001). On the Non-Linear Forces Acting on a Floating Spar Platform in Ocean Waves. *Applied Ocean Research* , 29-40.
- [35] V. J. Kurian, O. A. A. Montasir, & S. P. Narayanan. (2009). Numerical and Model Test Results for Truss Spar Platform. *International Society of Offshore and Polar Engineers* , 1-9.

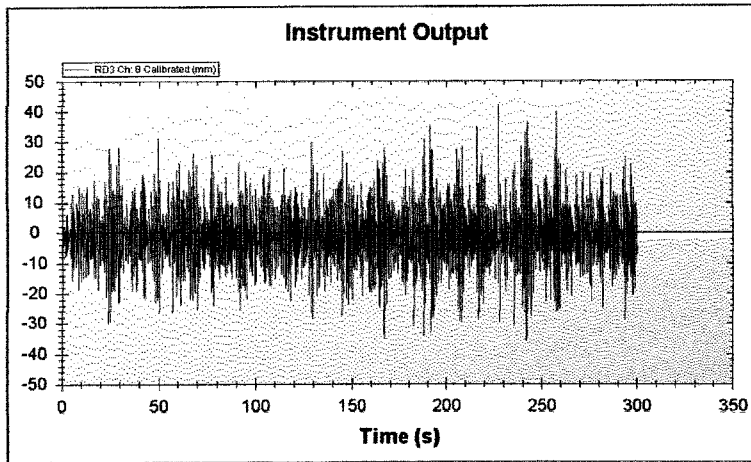
- [36] B. B. Li, J. P. Ou, & B. Teng. (2011). Numerical Investigation of Damping Effects on Coupled Heave and Pitch Motion of an Innovative Deep Draft Multi-Spar. *Journal of Marine Science and Technology* , 231-244.
- [37] V. J. Kurian, B. S. Wong, & O. A. A. Montasir. (2008). Frequency Domain Analysis of Truss Spar Platform. International Conference on Construction and Building Technology, (pp. 235-244).
- [38] B.B. Mekha, C. P. Johnson, & J. M. Roesset. (1995). Nonlinear Response of a Spar in Deep Water: Different Hydrodynamic and Structural Models. International Offshore and Polar Engineering Conference (pp. 462-469). The Netherlands: The International Society of Offshore and Polar Engineers.
- [39] Y. Wang, J. Yang, Z. Hu, & L. Xiao. (2008). Theoretical Research on Hydrodynamics of a Geometric Spar in Frequency- and Time-Domains. *Journal of Hydrodynamics* , 30-38.
- [40] I. Datta, I. Prislina, J. E. Halkyard, W. L. Greiner, et. all (1999). Comparison of Truss Spar Model Test Results with Numerical Predictions. International Conference on Offshore Mechanics and Arctic Engineering (pp. 535-548). Newfoundland, Canada: ASME.
- [41] A. K. Agarwal, & A. K. Jain. (2003). Dynamic Behavior of Offshore Spar Platforms under Regular Sea Waves. *Ocean Engineering* , 487-516.
- [42] W. Ye, I. Anam, & J. Zhang. (1998). Effects of Wave Directivity on Wave Loads and Dynamic Responses of a Spar. International Conference on Offshore Mechanics and Arctic Engineering (pp. 1-6). ASME.
- [43] F. Zhang, J. Yang, R. Li, & G. Chen. (2007). Numerical Investigation of the Hydrodynamic Performance of a New Spar Concept. *Journal of Hydrodynamics* , 473-481.

- [44] *Hydrodynamics*. (2010, February). Retrieved February 2012, from USFOS:  
Available:  
[http://www.usfos.no/manuals/usfos/theory/documents/Usfos\\_Hydrodynamics.pdf](http://www.usfos.no/manuals/usfos/theory/documents/Usfos_Hydrodynamics.pdf)
- [45] J. M. Journee, & W. W. Massie. (2001). *Offshore Hydromechanics* (First ed.).  
Delft University of Technology.
- [46] M. C. Lin, & S. S. Hsiao. (1994). Boundary Element Analysis of Wave-Current  
Interaction Around A Large Structure. *Engineering Analysis with Boundary  
Elements* , 14, 325-334.
- [47] J. Noorzaei, S. I. Bahrom, M. S. Jaafar, W. A. Thanoon, & S. Mohammad. (2005).  
Simulation of Wave and Current Forces on Template Offshore Structures.  
*Suranaree J. Sci. Technol.* , 193-210.
- [48] B. D. Chandler, & J. B. Hinwood. (1982). Combined Wave-Current Forces on  
Horizontal Cylinders. *Coastal Engineering* , 2171-2188.
- [49] F. Arena, & A. Romolo. (2005). Random Forces on a Slender Vertical Cylinder  
Given by High Sea Waves Interacting with a Current. *International Journal of  
Offshore and Polar Engineering* , 21-27.
- [50] R. Zhao, & O. M. Faltinsen. *Wave-Current Interaction Effects on Large Volume  
Structure*. Norway: Norwegian Institute of Technology, Norway.
- [51] T. Taniguchi, & K. Kawano. (2001). Current Effects on Extreme Response Value  
Statistics of Offshore Structures Subjected to Wave and Current. *International  
Offshore and Polar Engineering Conference* (pp. 347-353). Norway: The  
International Society of Offshore and Polar Engineers.
- [52] N. E. Huang, D. T. Chen, & C. Tung. (1972). Interactions Between Steady Non-  
Uniform Currents and Gravity Waves with Application for Current Measurements.  
*Journal of Physical Oceanography* , 420-431.

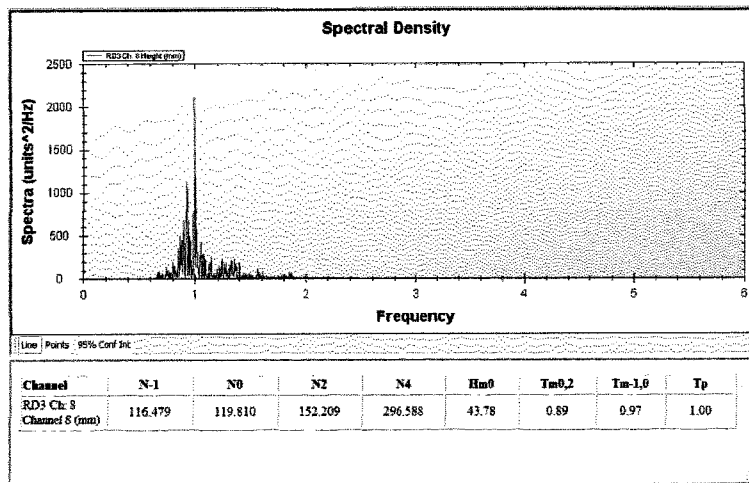
- [53] T. S. Hedges, K. Anastasiou, & D. Gabriel. (1985). Interactions of Random Wave and Current. *Journal of Waterway, Port, Coastal and Ocean Engineering* , 275-288.
- [54] H. Margaretha. (2005). *Mathematical Modelling of Wave-Current Interaction in a Hydrodynamic Laboratory Basin*. The Netherlands: Phd Thesis, Universiteit Twente.
- [55] P. Osuna, & J. Monbaliu. (2004). Wave-Current Interaction in the Southern North Sea. *Journal of Marine Systems* , 52, 65-87.
- [56] H. K. Johnson, T. V. Karambas, I. Avgeris, & et. al. (2005). Modelling of Waves and Currents around Submerged Breakwaters. *Ocean Engineering* , 949-969.
- [57] G. Moe. Linear Wave Theory. NTNU, Trondheim, Norway. Available: [http://www.ieawind.org/AnnexXXIII/Secure/Meeting8/GeirMoe\\_Chap6-6\\_LinearWaveTheory.pdf](http://www.ieawind.org/AnnexXXIII/Secure/Meeting8/GeirMoe_Chap6-6_LinearWaveTheory.pdf)
- [58] A. H. Techet. (2004). *Morrison's Equation*. Available: <http://web.mit.edu/13.42/www/handouts/reading-morrison.pdf>
- [59] H. Y. Jan, H. H. Chen, & J. F. Conlon. (1982). Dynamic Response of Offshore Structures. Offshore South East Asia Conference (pp. 1-14). Singapore: Marine Construction.
- [60] PTS, "PETRONAS Technical Standard," ed. Malaysia: PETRONAS, 2010.

**APPENDIX A**

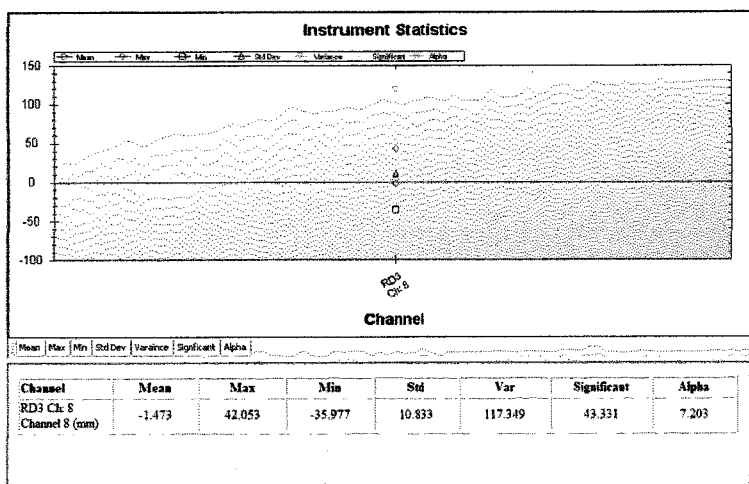
**MODEL TEST DATA**



(a)

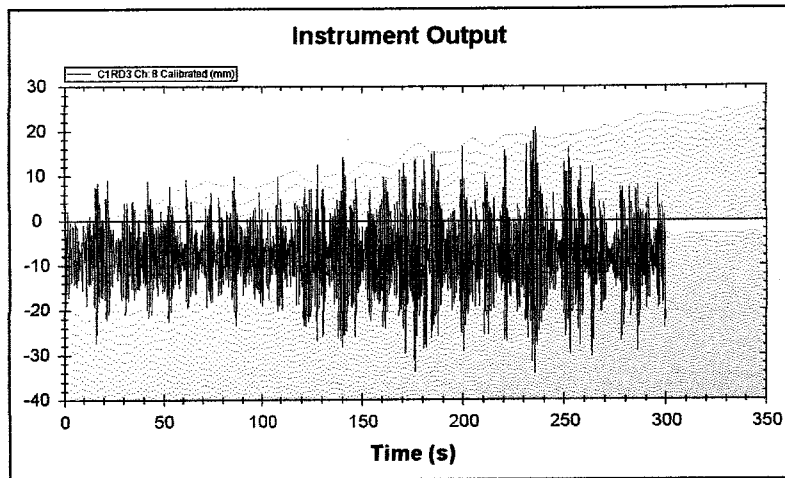


(b)

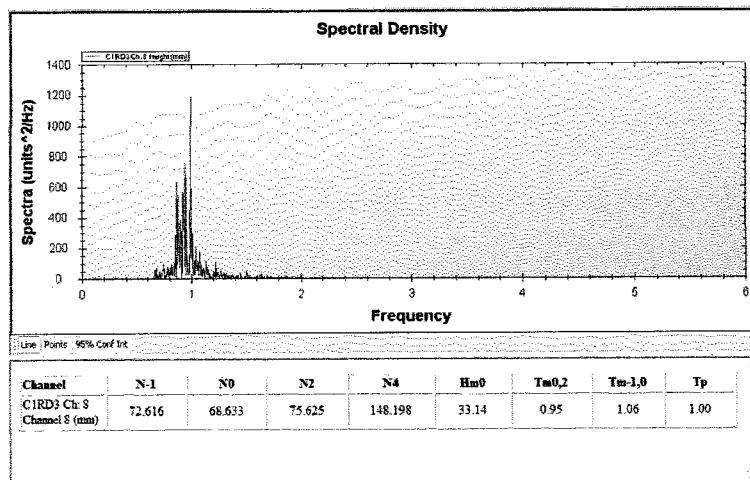


(c)

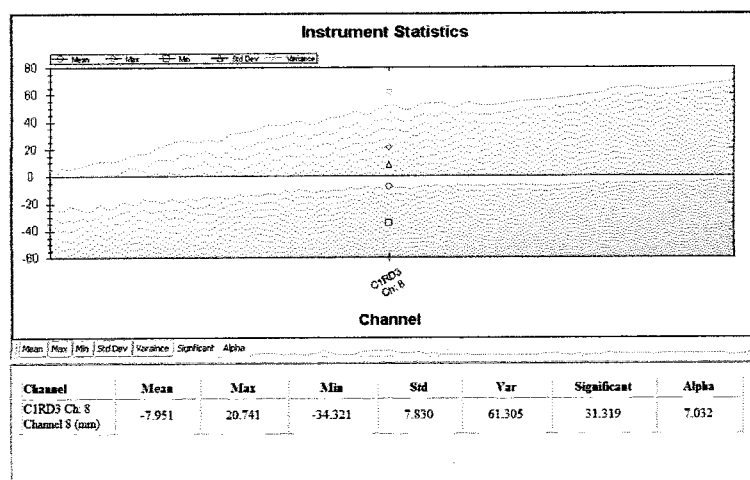
Figure A-1: Wave Probe RD3, (a) time series (b) density spectrum (c) wave statistics



(a)

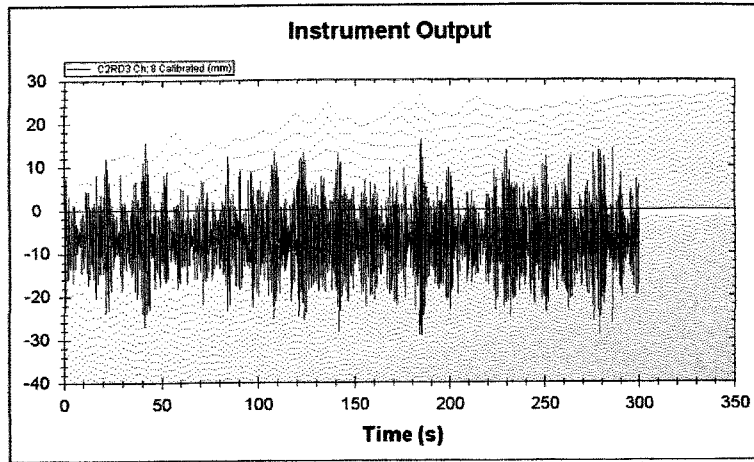


(b)

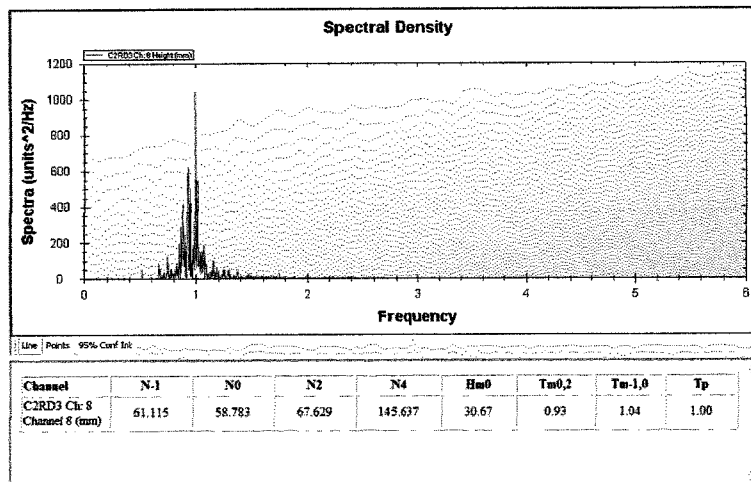


(c)

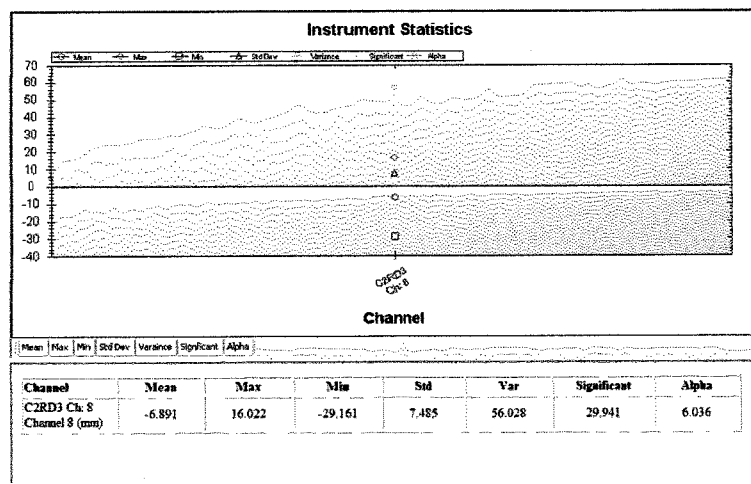
Figure A-2: Wave Probe RD3+C1, (a) time series (b) density spectrum (c) wave statistics



(a)

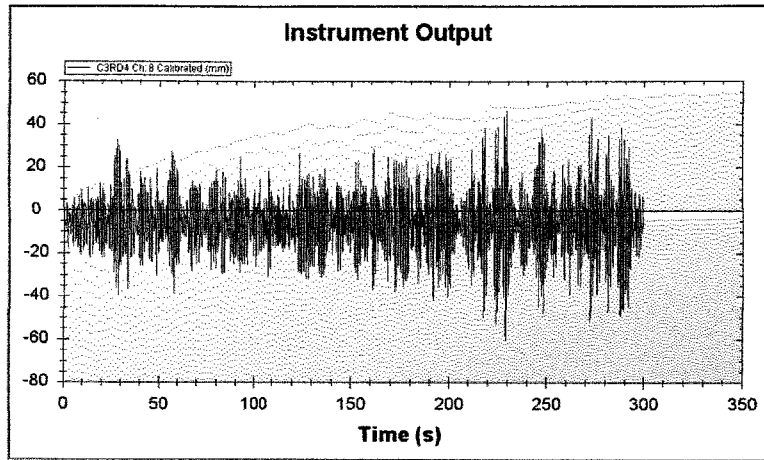


(b)

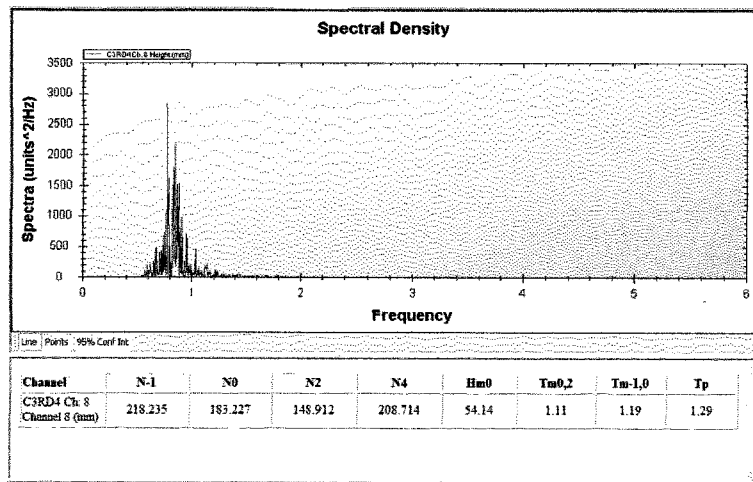


(c)

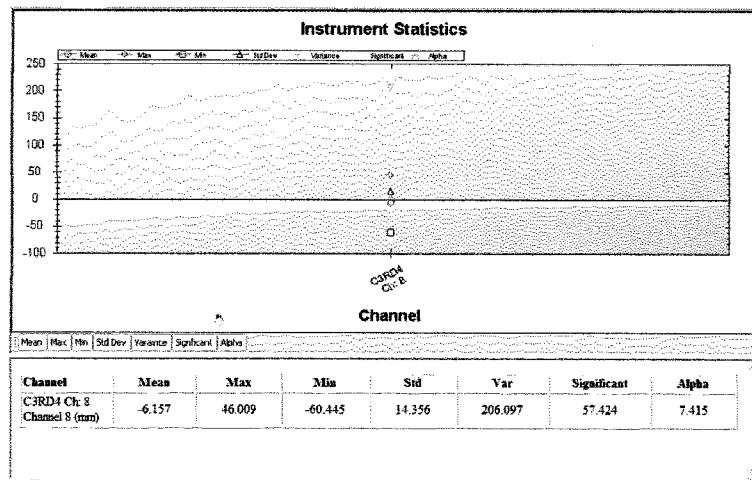
Figure A-3: Wave Probe RD3+C2, (a) time series (b) density spectrum (c) wave statistics



(a)

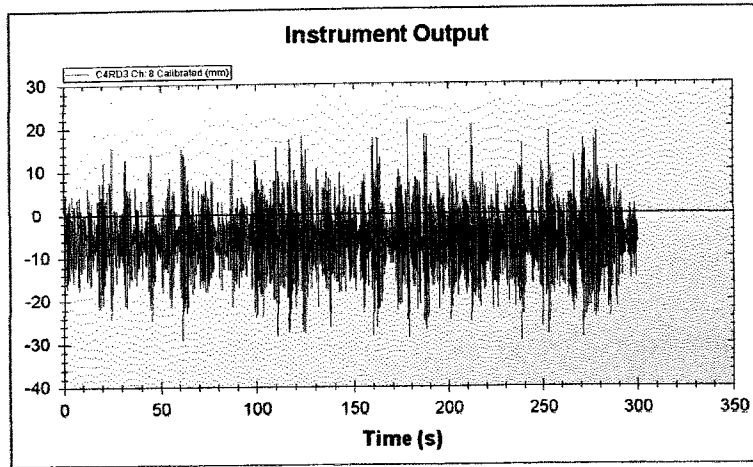


(b)

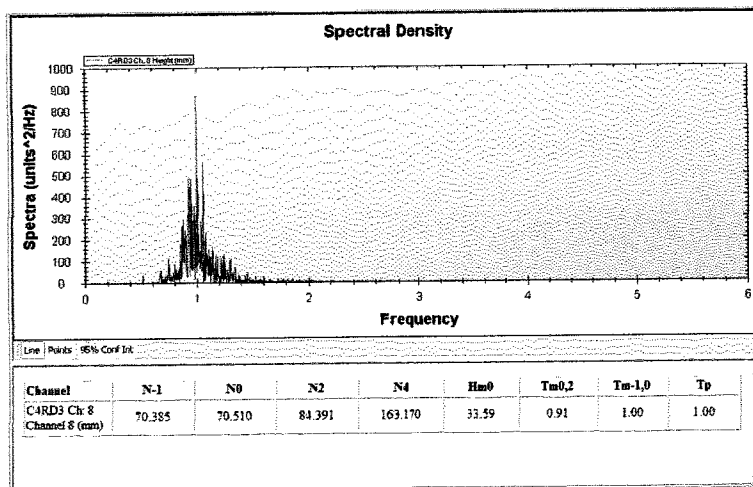


(c)

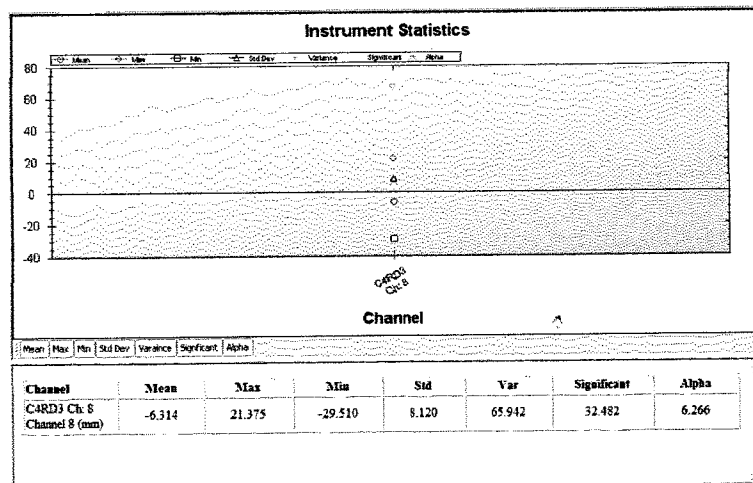
Figure A-4: Wave Probe RD3+C3, (a) time series (b) density spectrum (c) wave statistics



(a)

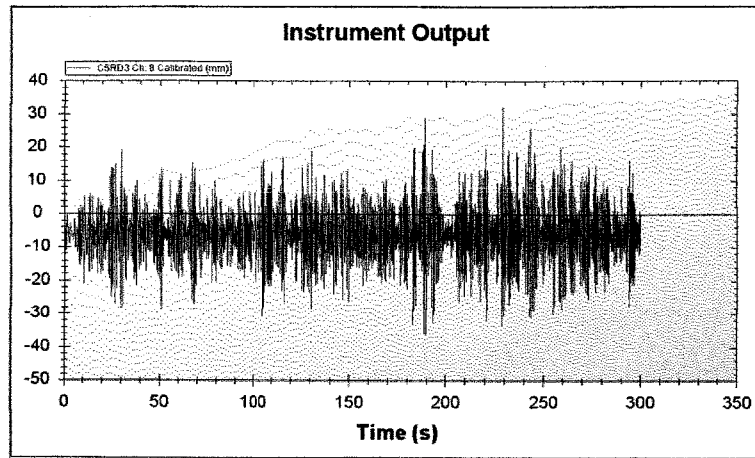


(b)

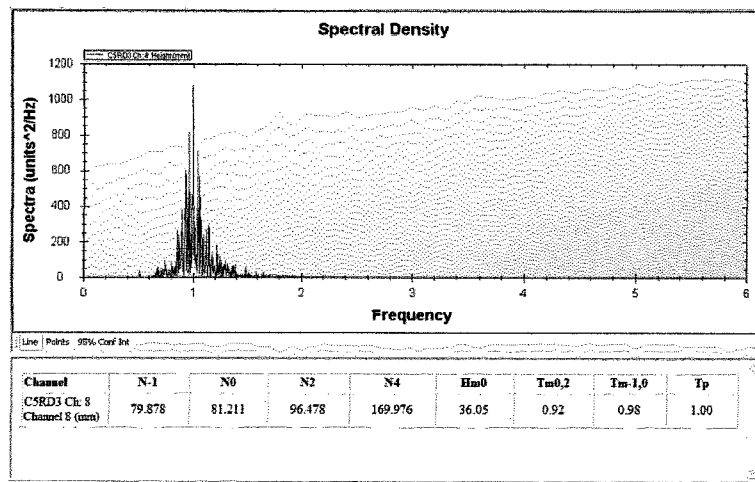


(c)

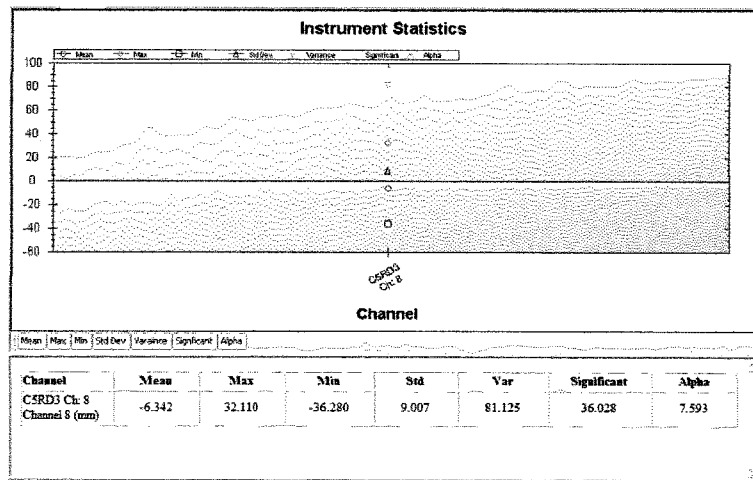
Figure A-5: Wave Probe RD3+C4, (a) time series (b) density spectrum (c) wave statistics



(a)

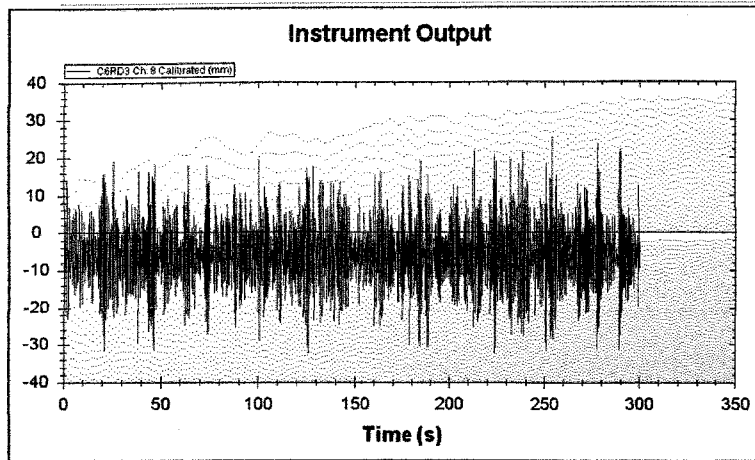


(b)

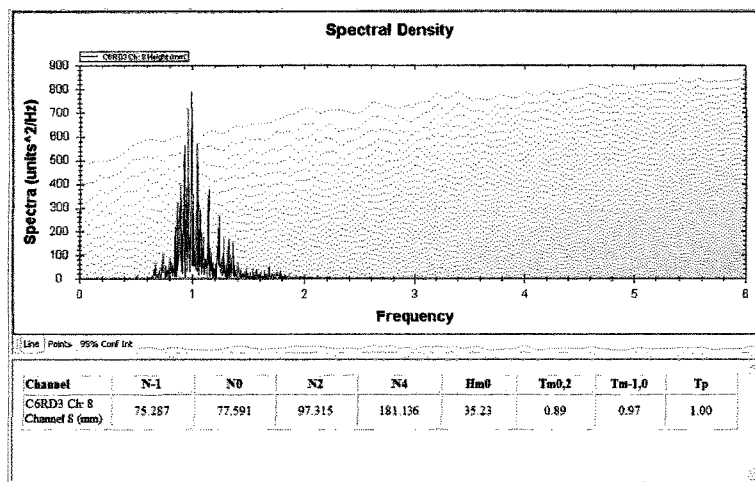


(c)

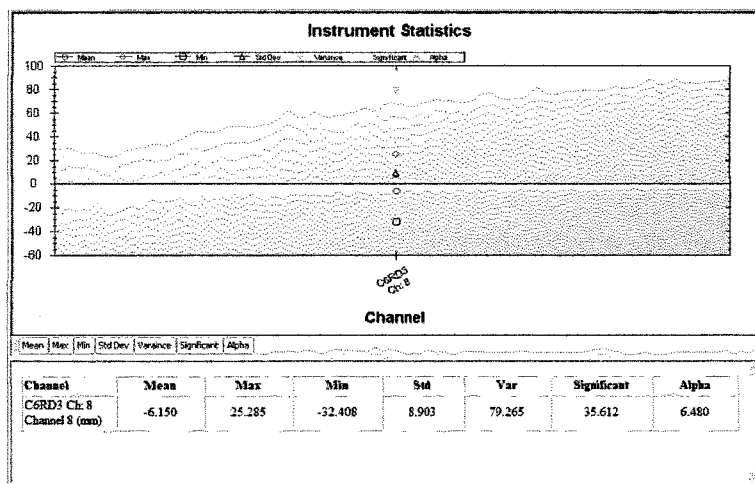
Figure A-6: Wave Probe RD3+C5, (a) time series (b) density spectrum (c) wave statistics



(a)

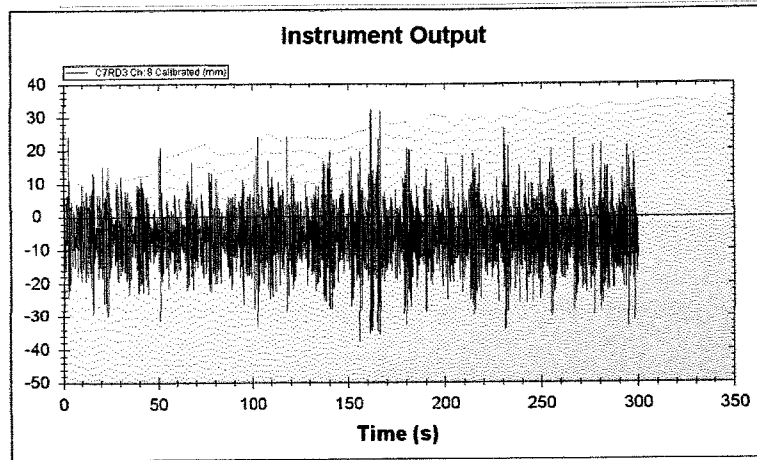


(b)

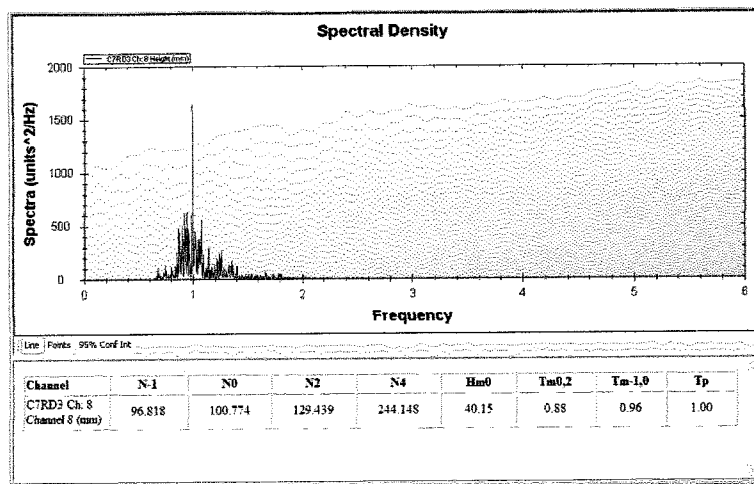


(c)

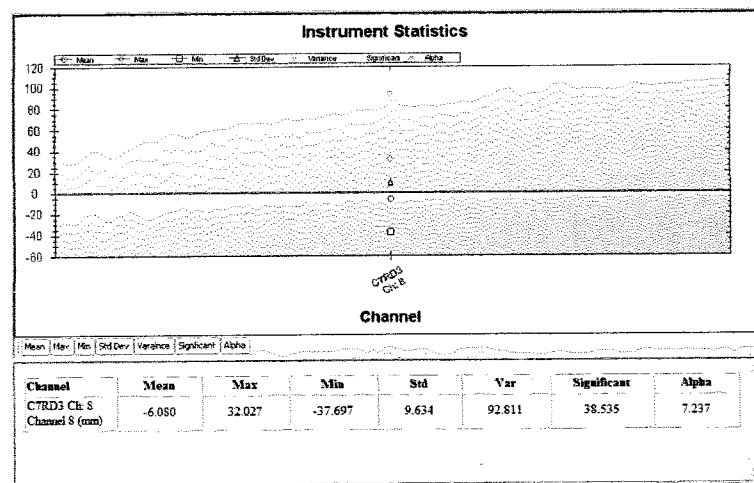
Figure A-7: Wave Probe RD3+C6, (a) time series (b) density spectrum (c) wave statistics



(a)

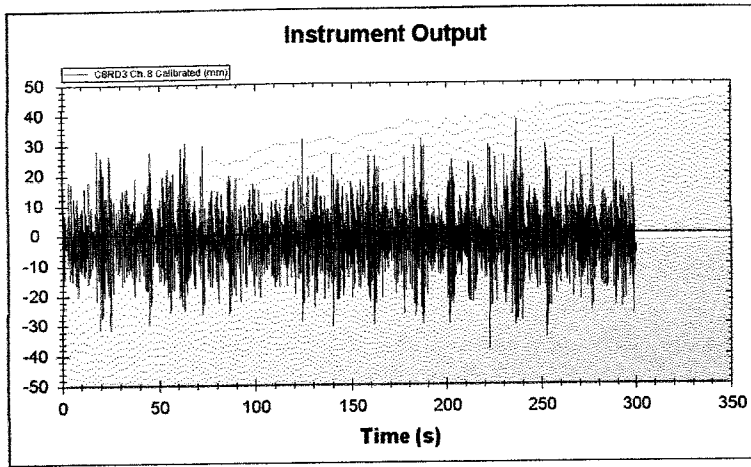


(b)

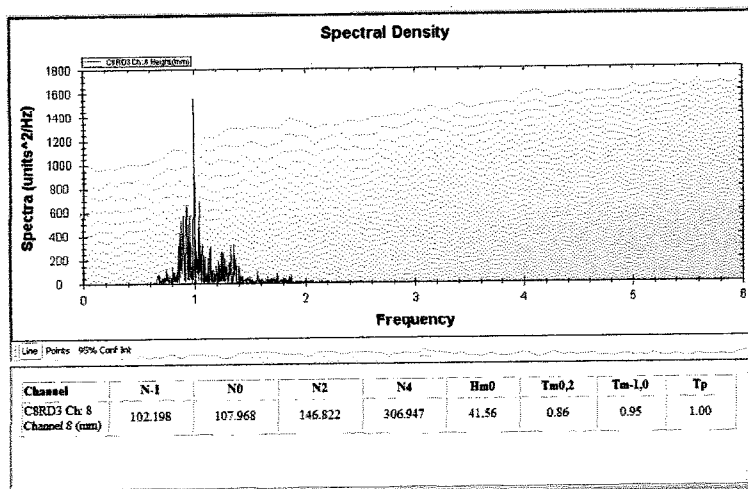


(c)

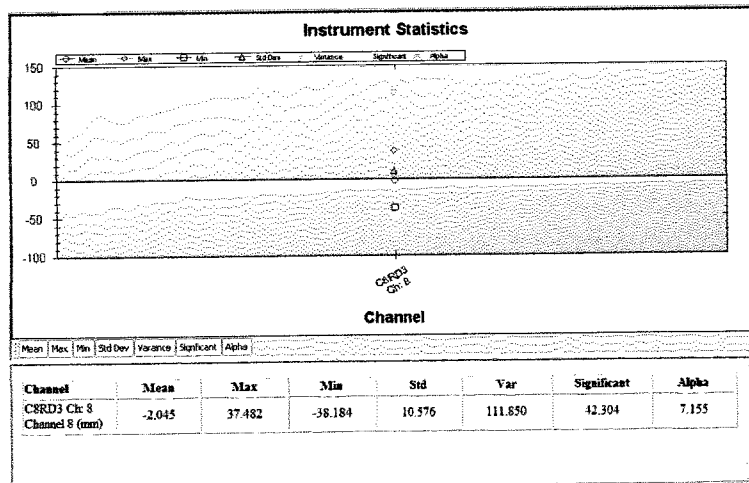
Figure A-8: Wave Probe RD3+C7, (a) time series (b) density spectrum (c) wave statistics



(a)



(b)



(c)

Figure A-9: Wave Probe RD3+C8, (a) time series (b) density spectrum (c) wave statistics

**APPENDIX B**

**FREE DECAY TEST**

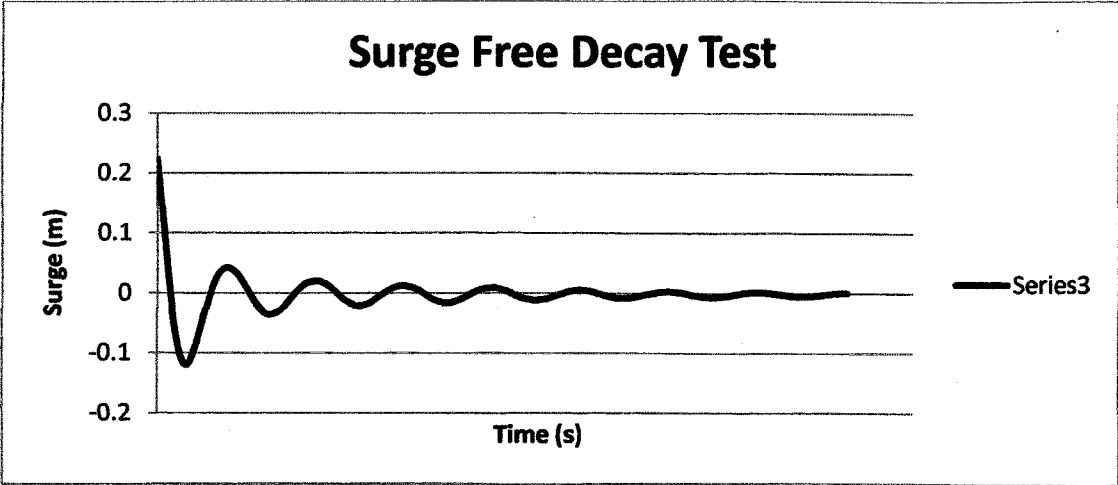


Figure B-1:: Surge Free Decay Test For Truss Spar

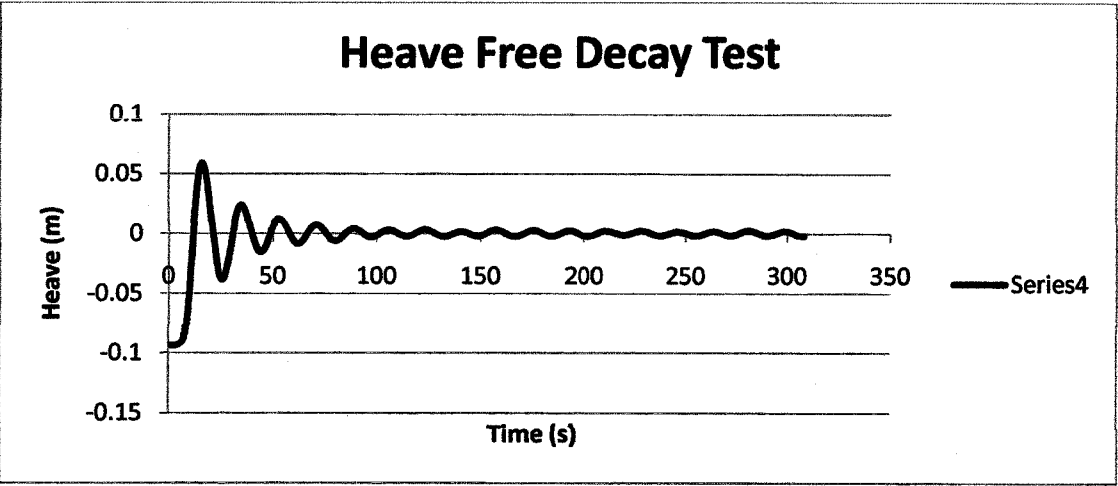


Figure B-2:: Heave Free Decay Test For Truss Spar

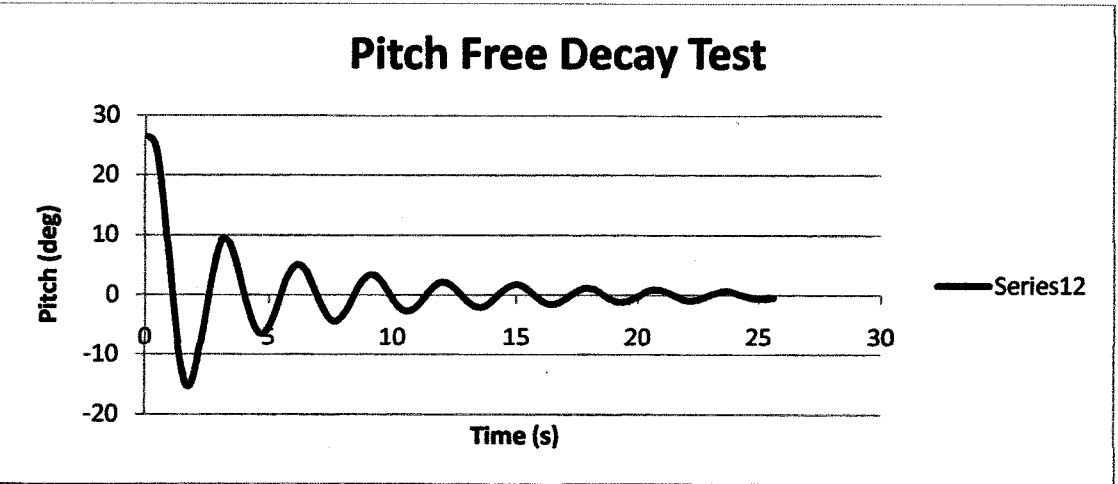


Figure B-3:: Pitch Free Decay Test For Truss Spar



